AN ASSESSMENT OF RENEWABLE ENERGY IN SOUTHERN AFRICA:

WIND, SOLAR, HYDRO

By Charles William Fant IV

B.S., Clemson University, 2006

M.S., University of Colorado, 2008

A dissertation submitted to the

Faculty of the Graduate School of the

University of Colorado in partial fulfillment

of the requirement for the degree of

Doctor of Philosophy

Department of Civil, Environmental, and Architectural Engineering

2013

This dissertation entitled:

An Assessment of Renewable Energy in Southern Africa: Wind, Solar, Hydro

written by Charles William Fant IV

has been approved for the Department of Civil, Environmental, and Architectural Engineering

Kenneth Strzepek, PhD

Paul Chinowsky, PhD

C. Adam Schlosser, PhD

Channing Arndt, PhD

Ross Corotis, PhD

*Date*_____

The final copy of this dissertation has been examined by the signatories, and we Find that both the content and the form meet acceptable presentation standards Of scholarly work in the above mentioned discipline

Fant, Charles William (Ph.D., Civil, Environmental, and Architectural Engineering)
An Assessment of Renewable Energy in Southern Africa: Wind, Solar, Hydro
Thesis directed by Kenneth Strzepek and Paul Chinowski

Abstract

While electricity demand is rising quickly in the Southern African Power Pool (SAPP), the nations involved struggle to build the necessary infrastructure to meet the demand. In addition, the principal member—the Republic of South Africa—has made ambitious targets to reduce emissions via renewable energy technology. In this dissertation, three stand-alone studies on this subject are presented that address the future reliability of renewable energy in southern Africa, considering climate variability as well as long-term trends caused by climate change. In the first study, a suite of models are used to assess the vulnerability of the countries dependent on resources from the Zambezi River Basin to changes in climate. The study finds that the sectors most vulnerable to climate change are: hydropower in Zambia, irrigation in Zimbabwe and Mozambique, and flooding in Mozambique. In the second study, hourly reanalysis data is used to characterize wind power intermittency and assess the value of interconnection in southern Africa. The study finds that wind potential is high in Kenya, central Tanzania, and southern South Africa. With a closer look, wind power resource in South Africa is unreliable (i.e. intermittent) and is weak when power demand is highest on all relevant time-scales. In the third study, presented in Chapter 4, we develop a risk profile for changes in the long-term mean of wind and solar power sources. To do this, we use a statistical relationship between global mean temperature and each local gridded wind speed and solar radiation from the GCMs. We find that only small changes in wind speed and solar radiation are predicted in the median of the distributions projected to 2050. Furthermore, at the extremes of the distribution, relatively significant changes are

predicted in some parts of southern Africa, and are associated with low probability. Finally, in the conclusion chapter, limitations and assumptions are listed for each of the three studies, South Africa's options for reducing emissions are revisited, power trade and interconnection are discussed broadly, and future research is suggested.

Acknowledgments

I would like to express my deep appreciation and gratitude to Dr. Kenneth Strzepek, for his patience, wisdom, and experience. His hard work has inspired me to work hard; his inspiration has kept me inspired; his hope in this research has given me hope. I hope I have gained as much of his personality, work ethic, excitement, and humor in the past five years that we have been working together. He believed in me even when I didn't believe in myself.

I also want to thank the rest of my committee, starting with Dr. Paul Chinowsky, who always seems to know the simplest and most effective answers to my questions. This dissertation would not be possible without his organization and management of our team. I want to thank Channing Arndt, who has set up much of the vision for this research and who has and will be able to get these research findings into the right hands, so that this work will have real-world impacts. I also want to thank Adam Schlosser, who has provided much of the insight and ingenious ideas on the climate science front. He is always such a pleasure to work with. And finally, I would like to thank Dr. Ross Corotis, who brought a unique perspective of which this work has truly benefited. His insight into the engineering side of wind energy was not only valuable but fascinating, and, although I have not known him long, I have found his truly impressive attention to detail inspiring.

There have been many others who have contributed significantly to this work, all who have given great advice and were able to explain complicated things in the simple terms that I needed. Bhaskar Gunturu who helped on the wind power intermittency work, Yohannes Gebretsadik who was always willing to talk through any technical or intellectual difficulties I have had, Alyssa McCluskey who helped with the water resources modeling on the Zambezi Basin work, and Kevin Ummel who helped on the wind and solar modeling aspect.

This research was funded by United Nations University - World Institute for Development Economic Research (UNU-WIDER). I gratefully acknowledge this as well as additional financial support for this work provided by the MIT Joint Program on the Science and Policy of Global Change through a consortium of industrial sponsors and Federal grants.

I would also like to thank my parents, Charles and Jill Fant, as well as my sister, Bethany Moore, who have been incredibly supportive and encouraging through the entire process. I couldn't ask for a better family growing up.

Finally, I would like to thank the most important person to me, Amy Fant, the love of my life. She has endured quite a bit, from doing much more than her share while I was busy, to giving me time and space to work on this degree for weeks at a time. She also proofread and edited my entire dissertation more than once. She is brilliant, beautiful, caring, and my best friend in the world. I don't deserve her but I wouldn't give her up for anything.

Table of Contents

List of Tables

List of Figures

CHAPTER 1

INTRODUCTION

As the threat of climate change builds, there is a push towards lower emissions. Ironically, the energy sources available with no emissions are usually climate dependent, which is especially the case for wind, solar, and hydro resources. Even with our advances in the fields of climate measurement and modeling, much of our past climate variability remains mysterious. Furthermore, as future climates begin to behave less like past climates, modeled predictions of changes in the long-term future state are attractive for national energy investment planning. These undertakings are complicated for wealthy countries with excess funds for research, development and measurement, as well as a reliable base of existing infrastructure. For developing countries, on the other hand, planning of this nature poses a different set of obstacles—funds are limited and infrastructure is sparse or nonexistent, so minimizing costs and maximizing benefits, as well as avoiding investment risk, are paramount. Methods of original policy development geared toward the needs of these nations need to be developed that consider the full academic spectrum—namely climate science, engineering, and economics.

Access to modern energy is one of the basic preconditions of development and poverty reduction. Many developing countries have the potential to produce substantial amounts of renewable energy. In fact, the majority of these countries could produce much more electricity than they currently use, or will need in the near future, from accessible renewable sources—specifically hydro, wind, solar, and biomass. Furthermore, once the infrastructure needed to tap into these sources has been built, these countries would no longer be reliant on foreign oil and natural gas, making them less vulnerable to global price variability. However, taking advantage of these renewable sources requires significant up-

front cost and careful planning. Also, investing in these resources means taking on the risks of technologies that are not well tested on a large scale, which is especially the case with harvesting solar and wind power, or causing adverse effects to the natural ecosystem, as is often the case with hydropower. In addition, the climate is unpredictable and climate dependent resources do not always produce electricity when households or industries wish to use it, which can result in unexpected blackouts and the need to build expensive quick-start units such as gas-fired plants. Herein lies the tension. Is it cost-effective for developing countries to invest in climate dependent renewable resources? What are the risks and what are the hidden costs? The beginning of answering these questions lies in understanding the local climate behavior from a renewable energy planning perspective. Southern Africa, in particular, provides a unique and diverse region for unpacking these issues, as well as the beginning of uncovering viable solutions.

In the following chapters, future reliability of the major climate-dependent renewable resources for southern Africa is assessed, considering state-of-the-art science and engineering in three separate but related studies, which are described in Chapters 2-4 of this manuscript. In Chapter 1, the dissertation is introduced, providing general motivation as well as the current and potential state of hydro, solar, and wind resources in southern Africa. The first study, which is contained in Chapter 2, evaluates the impact of climate change on the Zambezi Basin, with emphasis on future hydropower reliability. The second study is presented in Chapter 3, where the goal is to characterize wind intermittency in southern Africa and evaluate the possibility of interconnecting wind farms as a way to mitigate intermittency. The third study attempts to evaluate the risk of climate change on wind and solar resources in southern Africa, and is presented in Chapter 4. And finally, in Chapter 5, I summarize and conclude the three studies as well as suggest a way forward.

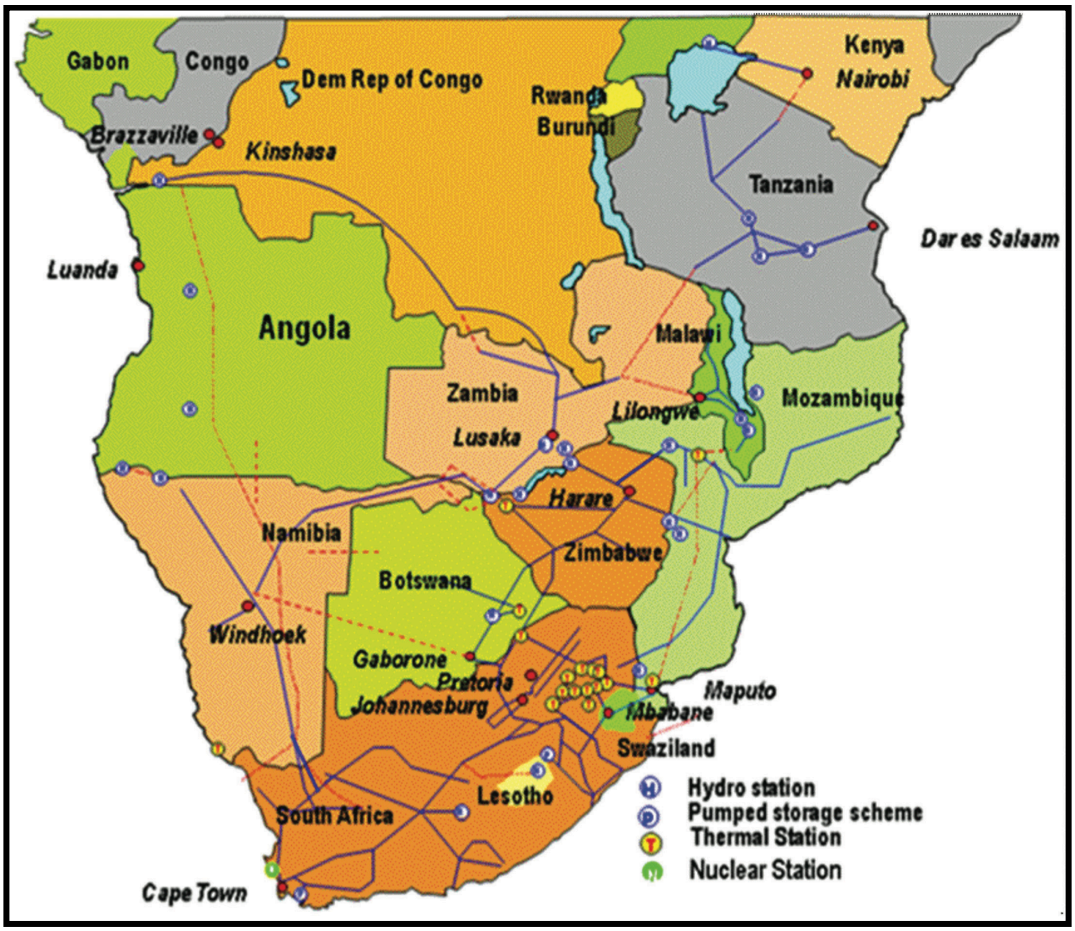

Figure 1: Map of the Southern African Power Pool (SAPP 2012)

Current state of the power sector in southern Africa

In sub-Saharan Africa, renewable energy, specifically hydropower, plays a unique role. As shown, many of the nations rely almost entirely on a few large hydropower plants for energy production. The continent is divided into either three or four power pools: West African Power Pool, East African Power Pool, Southern African Power Pool (SAPP), and Central African Power Pool (CAPP, often combined with SAPP). This study focuses on the Southern Africa Development Community (SADC) because this list of countries has been well established. The SADC includes all of the countries part of the SAPP at the time this manuscript was written. Table 1 shows the generation mix for the major utility companies in

this region that reported data to the SAPP for the most recent annual report. There are four utilities not shown in this table, two of which only produce power through hydro, and one of which is a transmission-only utility. As shown in Table 1, all but three of these utilities rely on hydropower for the majority of their power generation. However, Eskom, the state-owned power company in South Africa, produces the majority of electricity in this region using coal-fired plants. Eskom produces 45% of the electricity used in Africa as a whole (Ekom 2013), and close to 80% of the electricity used in southern Africa (SADC 2012).

Table 1: SAPP Utility Generation Mix for hydro and coal, installed capacity, and peak demand in 2011

Utility	**Country**	**Installed Capacity (MW)**	**Base Load Hydro**	**Coal**	**Peak Demand in 2011 (MW)**
BPC	Botswana	202	0%	65%	542
EDM	Mozambique*	233	91%	0%	616
ENE	Angola	1,508	64%	22%	870
ESCOM	Malawi	287	100%	0%	277
Eskom	South Africa	44,170	5%	86%	36,664
LEC	Lesotho	72	100%	0%	125
NamPower	Namibia	393	61%	34%	611
SEC	Swaziland	70	88%	13%	200
SNEL	DRC	2,442	100%	0%	1,050
TANESCO	Tanzania	1,008	50%	0%	890
ZESA	Zimbabwe	2,045	37%	63%	2,029
ZESCO	Zambia**	1,812	99%	0%	1,562

This shows the utility generation mix of hydro and coal, the remainder includes nuclear, CCGT (combined cycle gas turbine), or distillate (oil). Data is for 2011 / 12 based on data reported in SAPP (2012).

* Data for HCB (with installed capacity of 2,075 MW) or MATRACO, both in Mozambique, are not included in these values

** Data for the Copperbelt Energy Coorporation (ITC) or Lunsemfwa Hydro Power Company (LHPC), both in Zambia, are not included in these values

The countries in southern Africa will need to invest about 2-3% of GDP annually at least through 2015 to meet the growing power demand (Rosnes and Vennemo 2008). Understandably, power reliability is a constant struggle in southern Africa. Most of the people in these countries who are connected to the electric grid frequently experience blackouts due to a limited or unreliable electricity supply. Even the wealthiest country in the

region, South Africa, struggles to meet demands. In fact, South Africa has a long history of rolling blackouts (i.e. load shedding), the most recent of which occurred in 2007 and 2008 and was attributed to a lack of funds and poor planning. In spite of these shortcomings in South Africa, the Department of Energy has adopted aggressive national renewable energy targets. These aspirations are particularly noteworthy given that the country is heavily reliant on energy-intensive industry and coal-fired electricity. Of course, these plans are likely politically motivated, where the hope is to give South Africa a reputation as an environmentally friendly nation. One can certainly imagine the benefits of such a reputation. However, investments in national renewable energy infrastructure are not likely cost-effective, and the true cost of such a massive revamping of the energy sector is highly uncertain.

With 80% of the electricity capacity of the Southern Africa Power Pool (SAPP 2012), South Africa is one of the most carbon-intensive countries in the world (DEA 2011). Economic growth has been driven largely by the abundance of local coal resources, which currently satisfies about 77% of South Africa's primary energy needs (DOE 2011). The accessibility of coal has resulted in a dependence on low-cost coal-fired electricity, energy intensive mining, and heavy industry (Alton et al. 2012). Regardless, the South African government aims to reduce greenhouse gas emissions significantly, hoping to cut down on emissions by 42% by 2025 compared to a business-as-usual scenario (RSA 2010), and the Department of Energy in South Africa plans to achieve 30% clean energy by 2025 (DOE 2011). In order to satisfy these goals, enormous changes in infrastructure must take place. One essential change in infrastructure is a move from coal-fired electricity to electricity generated from renewable sources—namely biofuels, wind, solar, and imported hydropower. The major players in the electricity sector of South Africa are Eskom and the Department of

Energy. Eskom generates approximately 95% of the electricity used in South Africa and 45% of the electricity used in Africa, and was converted from private to public in 2002 (Eskom 2012). With stakes in the Cohora Bassa hydroelectric scheme in Mozambique, South Africa can import 1,400MW firm energy plus an additional 300MW non-firm energy (Wilson and Adams 2006). Although renewable sources are occasionally used for rural areas that cannot feasibly connect to the national grid, commercially viable renewable energy capacity is not yet exploited on a large scale. Domestic hydropower capacity is small compared to other sources—less than 2% of current energy production—and has been almost fully developed (DEA 2011).

Renewable energy potential in southern Africa

Renewable energy potential in southern Africa is abundant. The area can be split into two regions. In the "hydro northern network," including both the Congo and Zambezi basins, potential is primarily in hydropower. In the "thermal southern network," which includes Botswana, Namibia, South Africa, Lesotho, and Swaziland, power potential lies in the vast coal reserves in South Africa, as well as the promising solar energy potential in the area around the Kalahari Desert (SAPP 2013). Of course, wind power potential is not included in this regionalization, which exists mostly in South Africa and in the East in Tanzania and Kenya.

Hydropower potential: Of the estimated 1.16 Million GWh/yr technically feasible hydropower potential in Africa, only about 0.10 Million GWh/yr are utilized (intpow 2010). The Zambezi has an estimated potential of 13,000 MW of hydropower generation capacity, with almost 5,000 MW installed. A total of 53 projects have been proposed which would increase installed capacity by 7,300 MW for a potential production of firm power from

22,776 to 43,000 GWh/year, and increase average energy production from 30,000 to 60,000 GWh/year (World Bank 2010). In the Congo basins, there are currently about 40 hydropower plants constructed, the majority of which are small (Showers 2009). The largest single untapped resource is the Inga, located near the mouth of the Congo River in the Democratic Republic of the Congo. The Inga includes 4 dams, 2 existing and 2 planned, which together make the largest single resource of hydropower in the world. The Grand Inga, the largest of the 4, is estimated to have 324,900 GWh of gross energy capacity, when constructed (Tshome and Ferreira 2007).

Wind Power Potential: In this region, only small, experimental wind farms have been constructed. Most of these are in South Africa where there are currently 3 that are operational, although there are a few large-scale wind farms in planning. The largest of which is the Sere Wind Farm, which is proposed to be built near the city of Vredendal in the Western Cape (Savannah Environmental 2007). Based on mean wind speed calculated from the MERRA data, shown in Figure 2, wind resource potential is highest in Kenya, central Tanzania, and southern South Africa, with scattered moderate potential throughout Namibia, Botswana, Zambia, Zimbabwe and Mozambique. Angola and the DRC, as well as the countries in the northwest of the map, have low wind power potential.

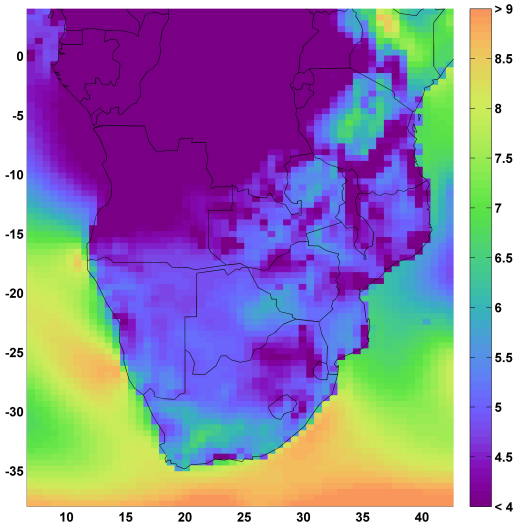

Figure 2: Mean wind speed for southern Africa, calculated from the MERRA data

Solar Power Potential: Also using the MERRA data, the mean of near-surface solar radiation was calculated for this region and is shown in Figure 3. This value is often used to demonstrate solar resource potential. As shown, there are basically two areas of high potential: one in the northeast of the map, including mostly Tanzania and Kenya; and one in the southwest of the map, including mostly Namibia, Botswana, and Zimbabwe, with the edges of the region stretching to Angola and South Africa. Again, South Africa has shown the most interest in investing in solar power infrastructure. Eskom has recently invested in planning a 100 MW CSP plant in the Northern Cape near the city of Upington (Eskom 2012), and the South African government is promoting a 5,000 MW solar park, also to be built in the Northern Cape (Zawilska et al. 2012).

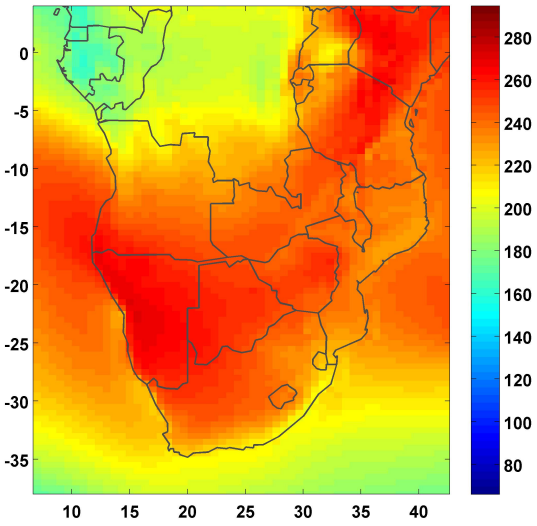

Figure 3: Geographic variation of mean incident solar radiation (W/m^2) over southern Africa

CHAPTER 2

IMPACT OF CLIMATE CHANGE ON CROPS, IRRIGATION AND HYDROPOWER IN THE ZAMBEZI BASIN

Abstract: Reliance on observed weather patterns for future investment in basic infrastructure planning (e.g. irrigation schemes, hydropower plants, roads, etc.) has been questioned considerably in recent years. For this reason, efforts to study the impacts of a changing future climate based on climate projections from Global Circulation Models (GCMs) has been popular, where the Coupled Model Intercomparison Project (CMIP) models, used in the Intergovernmental Panel for Climate Change (IPCC) Assessment Reports, are typically used. Studies tend to focus either on climate sensitivity, ignoring specific GCM predictions, or an effort is made to select a set of GCMs for use in an impact study. Here, we present a method for quantifying the impacts on biophysical measures—surface water supply, crop production, flooding events, and hydropower generation—of the Zambezi Basin countries using a large pool (6,800) of climate projections, which are based on the full set of the CMIP-3 GCMs and projected to 2050. This study estimates that, due primarily to increases in near-surface temperatures and reductions in precipitation, the Zambezi Basin will experience risks associated with drought. Surface water availability will reduce, rainfed crop yields will decrease, irrigation demand will increase, damaging floods will happen more often, and hydropower generation will decrease basin-wide–although these results vary considerably both spatially and throughout the distribution of future climates. Studies like this can help decision makers develop an informed risk-based strategy for national policy decisions and help to direct further studies where local detail is considered.

Introduction

There has been a growing interest in better understanding the economic impacts of climate change on future investment in areas with a large potential for basic infrastructure growth. Due to the lack of existing development in these areas, options for planning are numerous and the present decisions are principal to future economic progress. Also, these areas tend to have a limited set of historical records both spatially and temporally, which presents problems. Past studies have typically involved one of two approaches: (1) a climate sensitivity analysis on existing or planned infrastructure using a wide, unguided range of future climate possibilities (e.g., Kurukulasuriya 2006, Wilks 1992); or (2) use of select Global Circulation Models (GCMs) from the Coupled Model Intercomparison Project (CMIP) used in the Intergovernmental Panel for Climate Change (IPCC) fourth Assessment Reports applied directly to assess the impacts of climate change resulting in a limited set of future scenarios (e.g., Liu et. al 2013, Arndt et. al 2010, World Bank 2009, Immerzeel 2008).

In this study, we present a method for quantifying the impacts on biophysical measures (surface water supply, crop production, flooding events, and hydropower generation) of the Zambezi Basin countries using a large pool (6,800) of climate projections, which are based on the full set of the IPCC AR4 GCMs. The Zambezi River Basin in southern Africa provides a problem area suitable for this type of study both because of the hydrologic and agricultural importance for the people who live in the basin and due to previous studies concluding that the impact of climate change will be economically significant (World Bank 2010).

This study is divided into four interdependent efforts: climate scenario analysis, surface water modeling, crop modeling, and water resource modeling. This division is used in the following sections: materials and methods in section 2, results and discussion in section 3, and the conclusion in section 4.

Spatial scale of the analysis

The majority of the basin is contained in four countries: Malawi, Mozambique, Zambia, and Zimbabwe. Regionalization, spatial resolution and aggregation are adapted separately to meet two different sub-goals of this study. The first, water resource modeling, splits the Zambezi Basin into 29 hydrologically significant sub-basins as shown in Figure 4. The second regionalizes the study area using politically and economically significant boundaries (primarily by country borders, and secondarily splitting each country into regions), as shown in Figure 5.

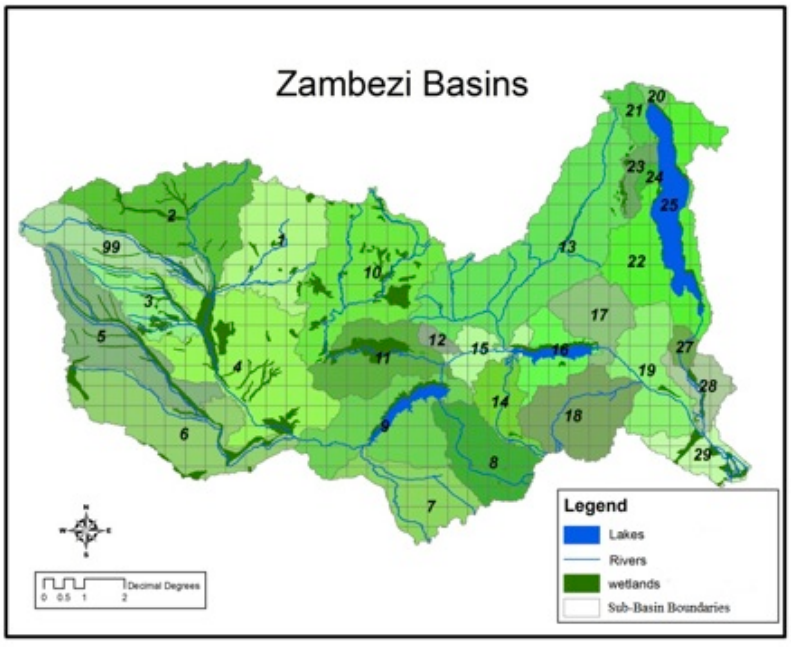

Figure 4: Sub-basin division of Zambezi River basin with superimposed half-degree grids

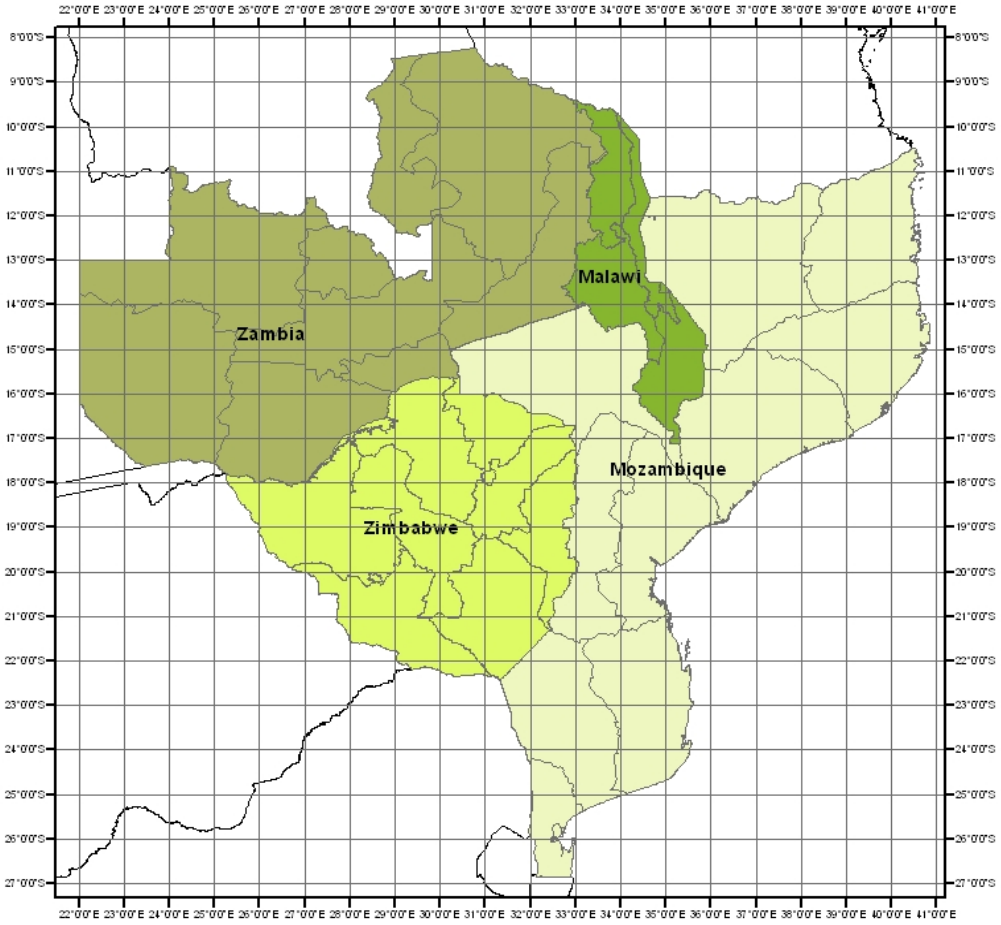

Figure 5: Political division of Zambezi river basin by country boundaries and sub-regions with a superimposed 1-degree square grid

Climatology overview

The Zambezi is a large, multi-country basin that spans portions of southern Africa and is characterized by great seasonal climatic swings, from rainy to dry, which are highly variable from year to year. The climate in these four countries varies from hyper-arid in western Zambia to semi-humid in Malawi and northern Mozambique. This region experienced food shortages caused primarily by drought in the 1980s and 1990s, which stressed the importance of research

and planning in the area of food and water security. Mean annual precipitation ranges from about 500 to over 1,200 mm/year, with an average for the basin of about 925 mm/year. The larger amounts of rainfall occur around Lake Malawi in Tanzania, while the west of the basin near Botswana and Namibia is drier (FAO 2011). The seasonality in the basin is characterized by a strong, 4 to 6-month rainy season when the Inter Tropical Convergence Zone moves over the basin from the north around October and continues through the valley until around March (Beilfus and dos Santos 2001).

Biophysical background

Agriculture is essential for most of these economies and accounts for a significant portion of GDP, including about 50% in Zimbabwe and 20% in Mozambique. 85% of the 5.2 million ha of cultivated land in the Zambezi Basin is contained in Malawi, Zambia, and Zimbabwe– only about 180,000 ha of which are equipped for irrigation (World Bank 2010).

Agriculturally, the year is split into two productive seasons—a wet summer season and a dry winter season. The average cereal yield is about 1 tonne per hectare basin-wide, while some estimate a potential irrigated yield of 5 to 8 tonnes per hectare (World Bank 2010). Over 100 irrigation projects have been proposed in the basin, which would, in total, increase the equipped irrigated area by 366,000 ha., effectively tripling the irrigated area. Still, irrigated agriculture in the basin would remain far short of the total potential, which FAO estimates to be more than 3 million ha (Tilmant et al. 2010). Given the importance of agriculture to local economies, the need for food security, current dependence on subsidence agriculture, and the irrigation potential in the basin, investment in irrigation infrastructure will be an important issue in future planning.

Hydropower is another greatly untapped resource in the basin. Currently there is nearly 5,000 MW of installed hydropower generation capacity in the region, while the potential is estimated to be about 13,000 MW (World Bank 2010). Although hydropower has many advantages compared to other energy sources, there are many challenges as well: environmental sensitivity, complications related to reservoir filling, dependence on an uncertain climate, high capital costs of the infrastructure, and losses through evaporation, which are estimated by Beck and Bernauer (2011) to be as large as 10 percent of total potential basin flow, relative to a river with no manmade reservoirs). Given the high demands for electricity, a total of 53 projects have been proposed which would increase installed capacity by 7,300 MW for a potential production of firm power from 22,776 to 43,000 GWh/year, and increase average energy production from 30,000 to 60,000 GWh/year (World Bank 2010).

Material and methods

Climate scenarios

Monthly near-surface temperature and precipitation data at a half-degree by half-degree spatial scale were obtained from the Climatic Research Unit (CRU) of East Anglia (Mitchell and Jones 2005). The data are available for 1901-2002, but only the data from 1951 to 1990 were used in this study. Daily climate data, required for the crop modeling, were sourced from the Land Surface Hydrology Research Group at Princeton University (Sheffield et al. 2006) in August 2011. These data are at a scale of 1-degree by 1-degree and are corrected to match the CRU mean monthly data.

The future climate scenarios used in this study are based on GCM ensemble results from the CMIP-3, but are expanded to represent a larger range of possible outcomes following that of previous work (Schlosser et al. 2011). The MIT Integrated Global Systems Model (IGSM; Reilly et al. 2012) developed near-surface temperature and precipitation projections to 2050 at the zonal spatial scale. A Taylor expansion technique, described by Schlosser et al. (2011), was used to expand from the zonal level of detail in the longitudinal direction. This transformation requires the construction of climate-change pattern kernels, which vary through time as global temperature changes. The full ensemble of climate change projections is produced through a numerical hybridization of the IGSM zonal trends with pattern kernels of regional climate change from the IPCC AR4 models. This ensemble of future climate projections is called "hybrid frequency distributions" (HFDs). Using this framework, 6,800 climate projections are produced for each of the five CO_2 emissions policy scenarios, although only the "unconstrained CO_2 emissions" scenario is used in this analysis. In order to reach a reasonable computation time for all subsequent modeling, the number of projections was reduced using the methods described in Arndt et al. (2012), which reduced the climate projection pool to 421 statistically significant scenarios. The changes in climate were calculated as changes in precipitation and near-surface temperature, and were then applied to the historical data on a monthly basis. This technique maintains the daily distribution of precipitation by adding the changes proportionally by daily intensities. In this study, future climate changes from 2011 to 2050 are used in the modeling efforts described in the remainder of this section. Although climate change is predicted to be more drastic after 2050, a 40-year planning horizon is apt for investment decisions.

Runoff model

Runoff modelling converts the climate changes into changes in surface water availability important for the water resource modelling endeavour. Surface water runoff was modeled with the rainfall-runoff model CLIRUN-II, the latest available model in a family of hydrologic models developed specifically for the analysis of the impact of climate change on runoff, first proposed by Kaczmarek (1993). CLIRUN-II models runoff with a lumped watershed defined by climate inputs and soil characteristics averaged over the entire watershed, simulating runoff at a gauged location at the mouth of the catchment. For this analysis, a monthly time step is used to simulate the runoff from provided weather variables.

CLIRUN-II has adopted a two-layer approach following the framework of the SIXPAR hydrologic model (Gupta and Sorooshian 1983, 1985). Although CLIRUN-II can model headwater catchments or interflow catchments, interflow catchments were modeled in this study for the sake of accuracy in the calibration process. In the observed runoff data, many of the interflow basins had negative flows over long periods likely caused by the many wetlands in the Zambezi Basin. Negative flows cannot be modeled in CLIRUN-II. An extension to CLIRUN-II, "CLIRUN-II-WET", was developed to better model the losses caused by the wetland areas. The model simulates wetland hydrology based on the work of Sutcliffe and Park (1987) for the White Nile Sudd wetland, Yates and Strzepek (1998) for the White Nile wetlands generally, and Kashaigili et al. (2006) for the Usangu Plains wetlands in Tanzania. The wetland area is modeled in each catchment using a reservoir-based hydrologic response, where the estimated ET and runoff at the catchment is used to simulate the water balance, including inflow, outflow and storage.

A unique conditional calibration procedure was used to determine the coefficient values that characterize each of the 29 catchments. This procedure optimizes via a pattern search algorithm developed by MATLAB minimizing the sum of square errors of the simulated and observed runoff. This parameter estimation requires observed runoff at each catchment outflow. The observed runoff was provided by Charly Cadou through personal communication.

Crop model

The purpose of the following analysis is to assess the changes in crop yields (to be used in economic models in subsequent work to assess investment opportunity), and to estimate changes in irrigation demands to feed into the water resource model. Nine crops were chosen to represent the agriculture sector across all four countries. The 9 crops are maize, wheat (used to represent other cereals), cassava (used to represent root crops), horticulture (i.e. a generic vegetable crop), tobacco, cotton, sugarcane, and tea (used to represent other export crops). A variation of the CliCrop model (Fant et al. 2012) was used to estimate the variability of the impact on crop water requirement and rainfed crop yields caused by the range of climate projections present in the HFDs.

The CliCrop model is an attempt to balance accuracy and simplicity with an emphasis on estimating the effects of the changing climate on irrigation demand and rainfed crop yield. CliCrop is a generic crop water deficit model. The version of CliCrop used in this study uses the soil properties and precipitation amount to calculate the infiltration using a version of the USDA Curve Number method (USBR 1993). The model then calculates the soil moisture in each soil

layer, calculates the amount of moisture allowed to percolate into the deep soil layers, and calculates a yield coefficient at the end of the growing season.

The effects of climate on crop production are modeled by estimating water stress on crops. Water stress is related to the estimate of evapotranspiration (ET), and more specifically, the extent by which the actual ET (AET) falls short of the crop demand ET (DET). In CliCrop, a yield ratio (Y) is reported as a measure of water stress. Y is calculated from a set of yield ratios (y) representing the ratio of actual yield to a theoretical maximum yield, and is based on the ratio of AET to PET. The theoretical maximum yield is the yield obtained in the complete absence of water stress. Four yield ratios are calculated, one for each of the four development stages (d): initial, crop development, mid-season, and late season (Allen, et al. 1998). y is weighted using a yield response factor (K), as follows:

$$y_d = 1 - K_d \left(1 - \frac{AET_d}{DET_d}\right) \quad \text{(EQ-1)}$$

The final reported yield ratio (Y) is calculated using the multiplicative model proposed by Rao et al (1988).

$$Y = \prod y_d \quad \text{(EQ-2)}$$

Here, Y represents the ratio of actual yield to the theoretical maximum yield due to water stress, and therefore, is unitless. This value is reported for each year of the simulation.

Actual ET is calculated as a function of precipitation, temperature, PET, soil moisture, root depth, crop type, and atmospheric CO_2 concentration. This calculation is done each day, for each soil layer. The model uses a daily form of the Modified Hargreaves equation to calculate PET (Farmer et al. 2011). Soil moisture is calculated using a bucket-type scheme similar to the

method used in the SWAT model (Neitsch et al. 2005), details are given in Fant et al. (2012). Crop specific parameters similar to the ones used in CROPWAT (Allen et al. 1998) are used in this calculation, as well as in the calculation of the daily ET crop demand. The atmospheric CO2 concentration affects the daily ET crop demand, which follows the methods explained in Rosenzweig and Iglesias (1998). The crop parameters are adjusted from year to year using methods developed by Allen et al. (1998)–adjusting crop ET demand–and Wahaj et al. (2007)–adjusting crop stage durations, which estimate the local crop's reaction to deviations from "average" climate conditions.

The rainfed yield shocks are used in economic modeling in subsequent studies and the changes in irrigation demand are used in the water resource model, discussed next.

Water resource system model

The water resource modeling in this study attempts to simulate the sequence of existing and planned reservoir activity and demand nodes along the system. The focus of this modeling effort is on three main indicators of future impact: assessing possible changes in flood risks, the operation of major hydropower plants, both existing and planned, and maintaining agricultural production, taking into account changing irrigation demands over time. Three demand types, or nodes, are modeled throughout the system, which are in competition for water dependent on the sequence (upstream/downstream). The node types are municipal and industrial (M&I) water use, hydropower generation, and irrigation withdrawal. M&I demands increase over time, consistent with projections used in the World Bank Economics of Adaptation to Climate Change study (EACC; World Bank 2009). Hydropower production is calculated for existing and planned

projects based on expected investment and construction schedule using the relevant scenario data from the World Bank study (2010). And the existing and planned irrigation infrastructure changes over time are also obtained from World Bank (2010). The analysis projects perturbations, or "shocks," to hydropower production and irrigated crop yield resulting from these conflicts from 2011 to 2050 across the Zambezi Basin using the Water Evaluation And Planning (WEAP) model (Sieber and Purkey 2007), the software for integrated water resources planning. WEAP provides a mathematical representation of the river basins encompassing the configuration of the main rivers and their tributaries, the hydrology of the basin in space and time, existing as well as potential major diversion schemes, and the various demands for water.

Computations are performed on a monthly time scale for 40 years for a base-case scenario (i.e., no climate change) and the HFD climate change scenarios. Each climate change scenario is characterized by unique inflows, evaporation, and irrigation demand. Unmanaged inflows are modeled using CLIRUN-II; the output runoff projections from CLIRUN-II are used as the available runoff in WEAP.

Surface water inflows from CLIRUN-II were used as inflows to an aggregated river in each basin modeled in WEAP. Water supplies and demands are linked between upstream and downstream basins, and reservoirs, irrigation, and municipal and industrial demand locations were sequenced consistent with their actual locations. If hydropower is generated in a basin, the reservoir and turbine characteristics are calibrated to ensure that the power produced is validated with historical values. While the reservoir and aggregate demands are physically located within each basin, they are not located to represent any specific reservoir or demand site. In Section 3.4, the indicator results are discussed from this analysis.

Results and Discussion

Future climate scenarios

Median changes in temperature are fairly uniform across the basin, showing an increase between 1.5 and 2 degrees Celsius by the later half of the 2040s (see Figure 6). The coastal regions tend to show slightly less warming, while the temperature in the western regions is predicted to increase about 0.2 degrees Celsius. The distribution tails generally range from slightly less than 1 degree to about 3 degrees. Alternatively, changes in annual precipitation vary considerably across the basin with a tendency toward a precipitation decrease basin-wide (see Figure 7); although, in northern Malawi and northeastern Zambia, the median precipitation is predicted to be between a 3% and 8% increase. The remaining regions in the basin countries generally show a median reduction in precipitation ranging from almost no change to around 8% less, while the tails of the distribution show an alarming range of about -20% to +20% basin wide.

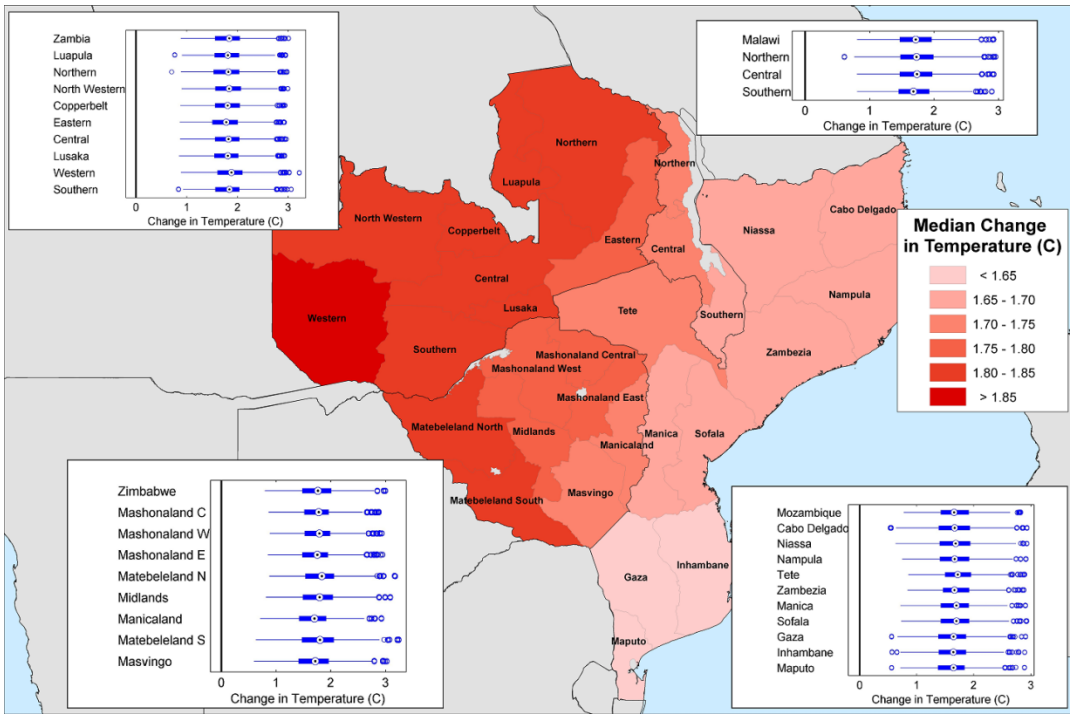

Figure 6: Climate scenario distribution of near-surface temperature (in °C) over the political regions of the four Zambezi Basin countries averaged over the last 5 years simulated, 2046-2050

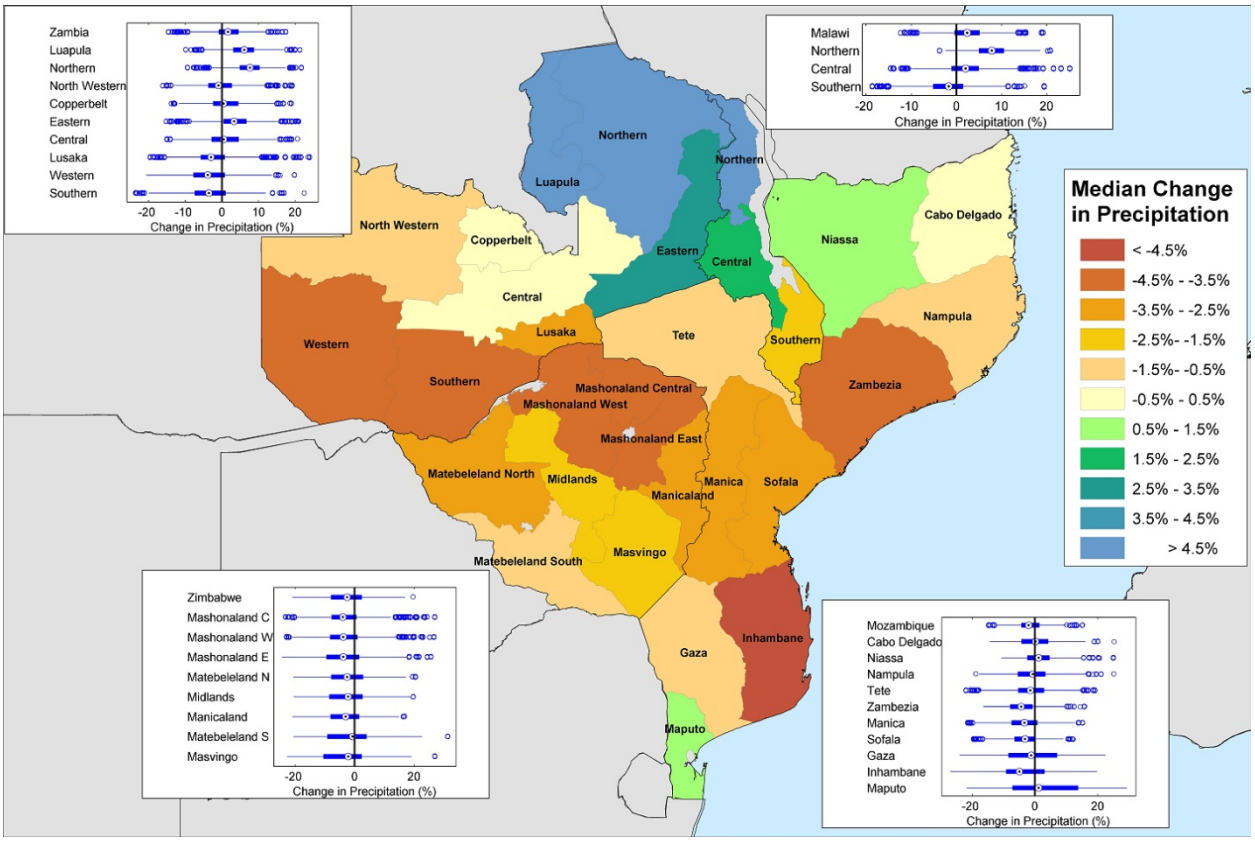

Figure 7: Climate scenario distribution of percent changes in precipitation over the political regions of the four Zambezi Basin countries averaged over the last 5 years simulated, 2046-2050

Changes in Climate Moisture Index (CMI) are shown in Figure 8. The CMI is an indicator of aridity, which depends on average annual precipitation and average annual Potential Evapotranspiration (PET). If PET is greater than precipitation, the climate is considered to be dry, whereas if precipitation is greater than PET, the climate is wet. When PET is greater than precipitation, CMI = (Precip./PET)-1, and when precipitation is greater than PET, CMI = 1-(PET/Precip.). A CMI of –1 is very arid, and a CMI of +1 is very humid. As a ratio of two depth measurements, CMI is dimensionless. As shown in the figure, almost all of the Zambezi country regions are predicted to be drier in more than half of the climate scenarios. Only the three

northernmost regions are predicted to be wetter, while the driest are predicted in the regions around the mouth of the Zambezi River in Mozambique.

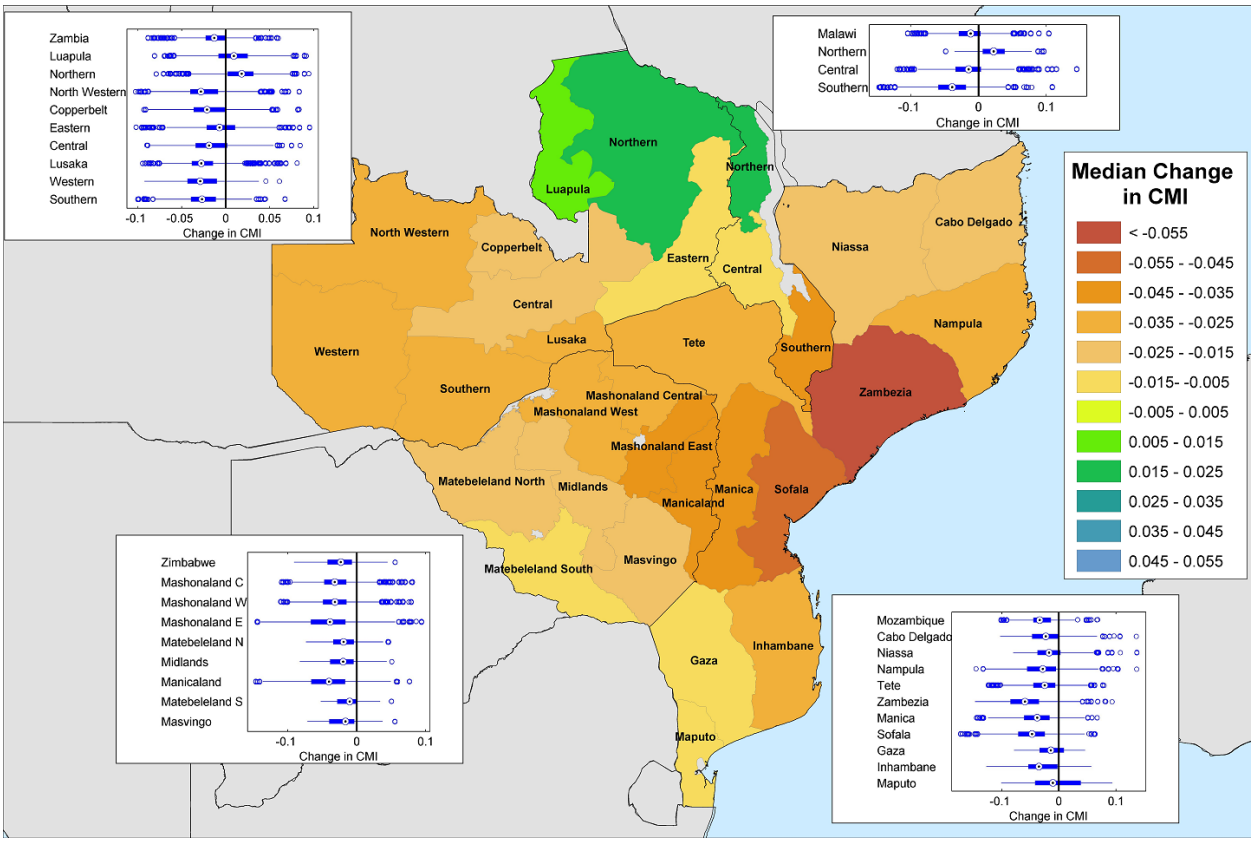

Figure 8: Climate scenario distribution of changes in Climate Moisture Index (CMI) over the political regions of the four Zambezi Basin countries averaged over the last 5 years simulated, 2046-2050

Runoff modeling results

The precipitation and near-surface temperature data described above (the HFD approach), along with potential ET calculated using the Modified Hargreaves equation (Hargreaves et al. 2003) were used to represent the future climate scenarios. The percent change in mean annual runoff, aggregated to 5 major basins, is shown in Figure 9. In this figure, the baseline mean

annual runoff is shown as a proxy for the hydrologic significance of each basin. The majority of the climate scenarios predict an increase in runoff in the Shire River Basin and basically no change in the Zambezi at Cahora Bassa, while the remaining three basins are showing a very likely decrease in runoff. The Upper Zambezi, where almost half of the runoff is generated, is predicted to dry in over 68% of the climate scenarios. Based on this analysis, the flows in the Zambezi Basin as a whole are likely to decrease, suggesting adverse impacts associated with drought. These results will be used in the water resource modeling, discussed in Section 3.4.

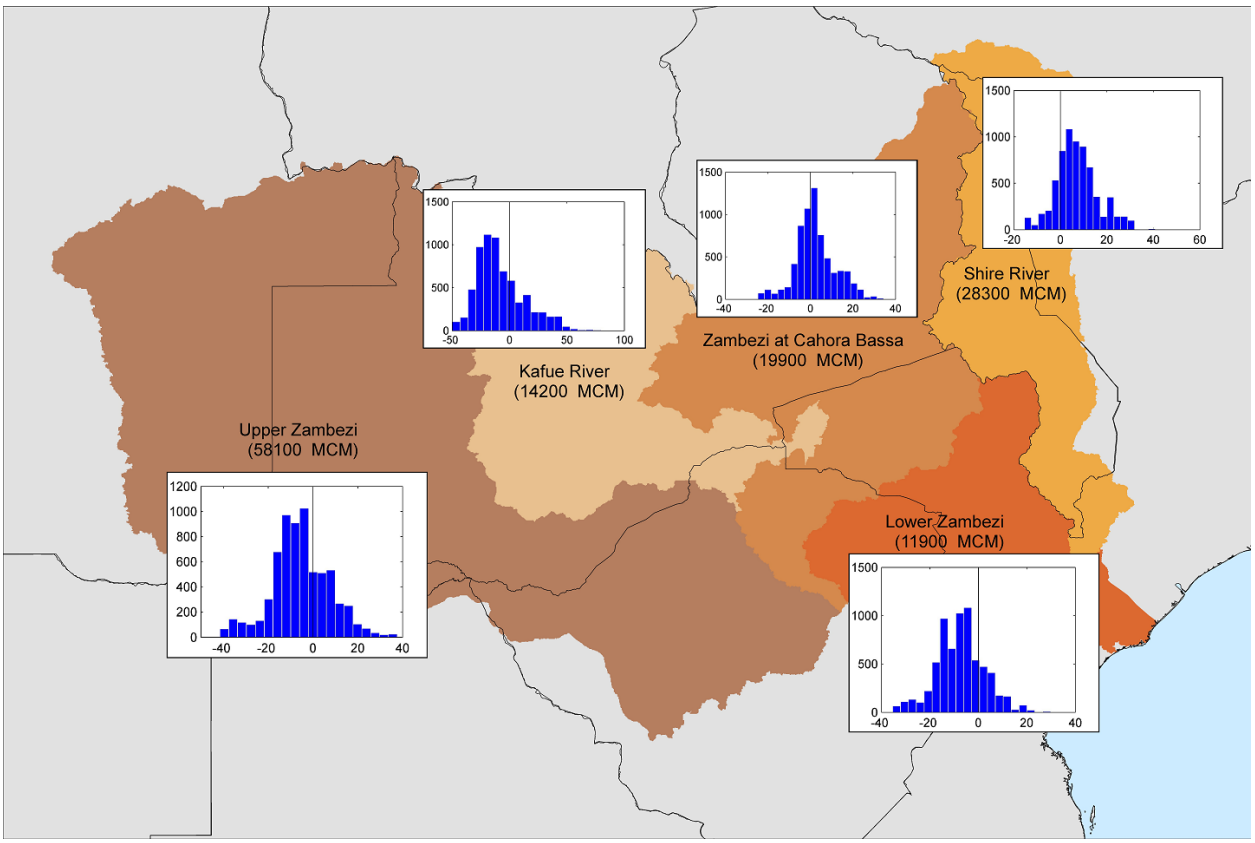

Figure 9: Climate scenario distribution results of the predicted percent change in runoff for the five major sub-basins of the Zambezi Valley averaged over the last 5 years simulated, 2046-2050

Crop modeling results

Using the same baseline scenario (1951-1990) as the runoff analysis, the changes in climate variables were adjusted based on the future projections to produce a range of possible impacts on the agriculture sector. The average predicted changes in the rainfed yield for the Zambezi countries are shown in Figure 10. This study suggests a decrease in rainfed yield for all of the crops in at least 75% of the climate projections. Figure 11 shows the changes in rainfed yield for maize across all of the four countries. Compared to the baseline scenario, rainfed yields are predicted to be worse for Zimbabwe and Mozambique than for Malawi and Zambia, although all countries show a decrease in yield. The range of impacts for Zimbabwe is drastic, from almost -30% to +30%, which makes planning for the future difficult. Figure 12 shows that the irrigation demand is predicted to increase by the 2040s for all of the 9 crops modeled in more than 75% of the climate scenarios. The distribution of the changes in irrigation demand for sugarcane is shown for the four Zambezi counties in Figure 13. There is only a slight difference across the countries where Malawi's irrigation demand is predicted to change the least, and Zimbabwe the most, due to much stronger drying in the southwest than the northeast of the Zambezi Basin.

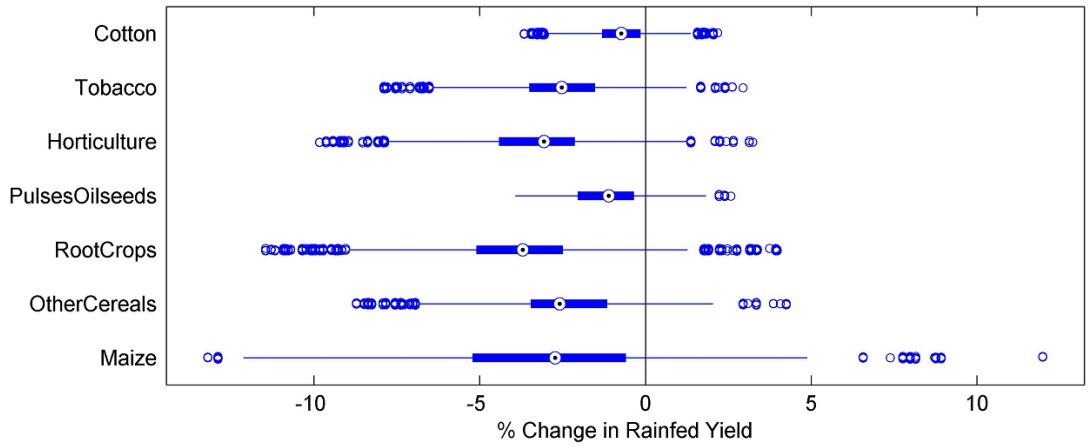

Figure 10: Climate scenario distribution of the four-country mean percent change in the rainfed yield of all Crops for the Zambezi countries averaged over the last 5 years simulated, 2046-2050

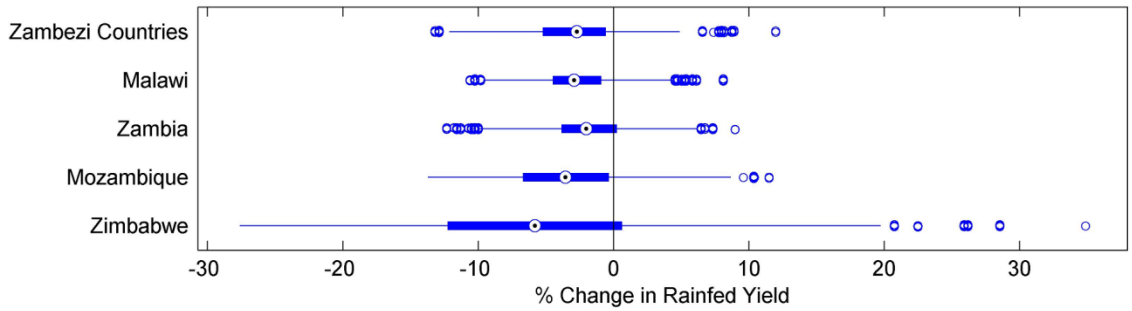

Figure 11: Climate scenario distribution of the country mean percent change in the rainfed yield of Crops for the Zambezi countries averaged over the last 5 years simulated, 2046-2050

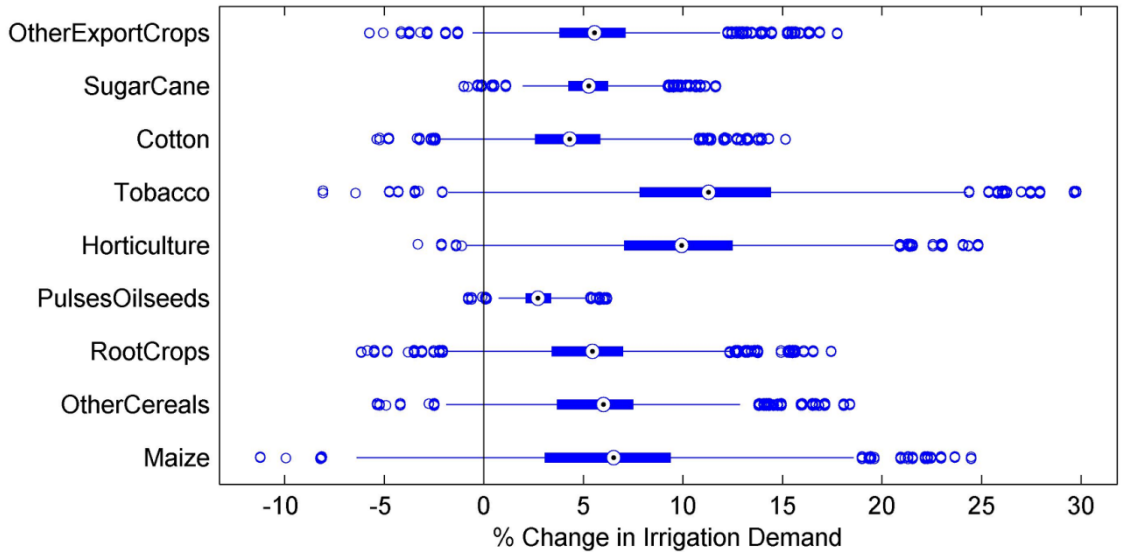

Figure 12: Climate scenario distribution of the four-country mean percent change in the irrigation demand of all Crops for the Zambezi countries averaged over the last 5 years simulated, 2046-2050

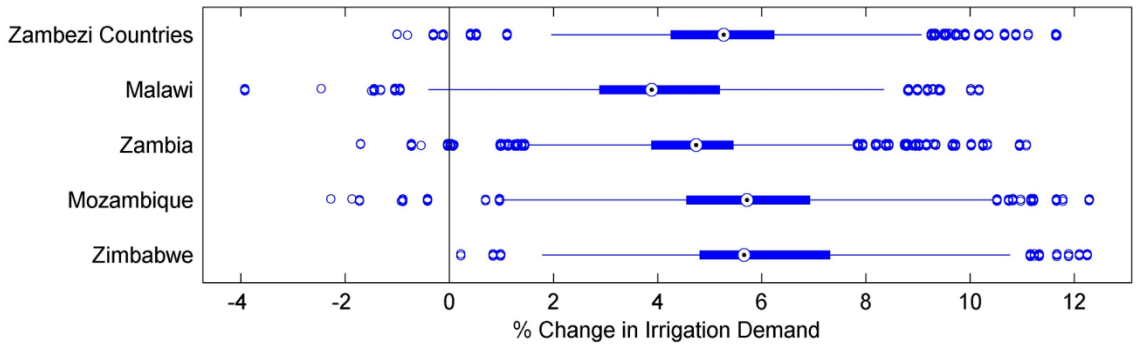

Figure 13: Climate scenario distribution of the country mean percent change in the irrigation demand of all Crops for the Zambezi countries averaged over the last 5 years simulated, 2046-2050

Water resource modeling results

Three measures are used here to present the changes in predicted impacts to the hydrologic system: maximum monthly runoff predictions, used as an indicator for changes in flood risk; hydropower generation changes; and the changes to the unmet irrigation demand. First, percent change in maximum monthly runoff is shown by country mean in Figure 14. Since the nature of the analysis restricts us to monthly changes in runoff, the indicators presented here correspond to large-scale (typically causing river inundation) flooding events rather than local flash flooding events, which occur on a shorter time-scale. As shown, flooding impact is predicted to increase in Malawi for the majority of the climate scenarios with a range from -20% to +40%. In Zimbabwe, flooding is predicted to decrease significantly in most of the climate scenarios, although there is a long, thin tail reaching an alarming 150% increase. Mozambique and Zambia both show a fairly normal distribution somewhat centered on no change, but the range (-20% to +30%) does favor an increase in flooding events. Using a Gumbel distribution fitting, we can make claims on the recurrence of damaging flood events. Figure 15 shows the recurrence of high-damage flood events, greater than the 50-year event intensity, could increase significantly in Mozambique, according to this study. Considering that 1 high-damage flood event occurs in the base scenario, Mozambique is likely to have a significant increase in high-damage flood events in the future with a likelihood of triple the base occurrence, and a tail that suggests there will be between 6 and 8 times more high-damage flood events.

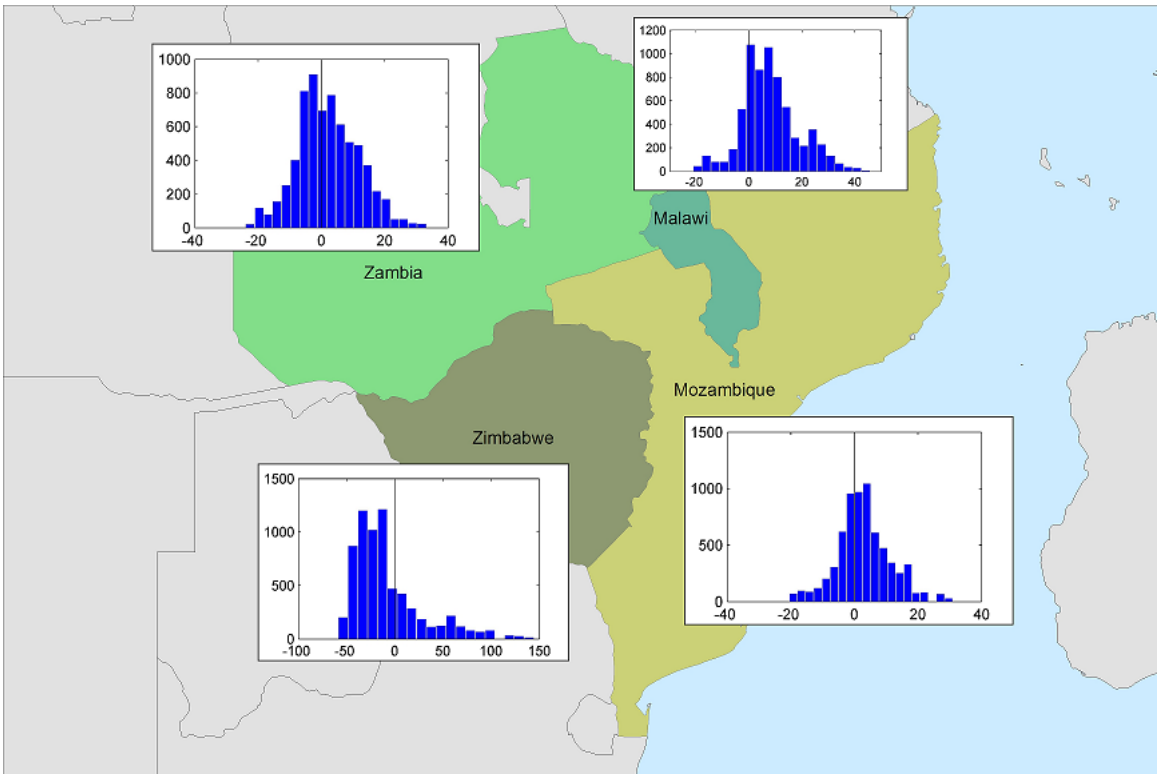

Figure 14: Climate scenario distribution of the percent change in maximum monthly runoff (used as an indicator for changes in flood events) is shown by country mean over the last 5 years simulated, 2046-2050

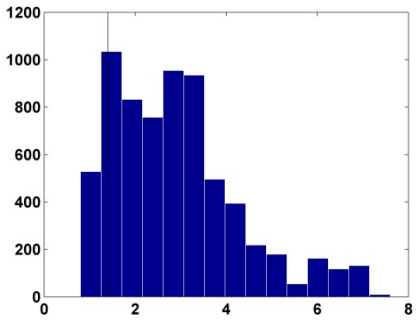

Figure 15: Distribution of flooding events over the 50-year return period intensity in Mozambique normalized by regions. The black line represents the base scenario

The impacts on hydropower generation by country are presented in Figure 16. Malawi is the only country where a positive impact is predicted in the majority of scenarios. Alternatively, in Zambia, hydropower generation is predicted to decrease in most of the future climates. With runoff decreasing in Zambia in the west, upstream of the majority of the hydropower plants, these results are expected. In Zimbabwe, where hydropower is generated downstream of Zambia, hydropower production is predicted to decrease slightly in most of the scenarios, suggesting that no significant impact would be expected. In Mozambique, where there are a few large downstream hydropower plants, there is expected to be no significant change in energy production. The reservoirs behind these hydropower plants are large, with significant storage, and they are downstream of a large portion of the Zambezi Basin dampening the resulting inflow changes. Further, the hydropower demand is small in proportion to the generating capacity. If power trade with neighboring countries were considered, these results might change since Mozambique would likely export excess power when the electricity price is high. With these results, we can see that the upstream hydropower plants located in Zambia and Malawi are much more sensitive to changes in local runoff, while the downstream plants located in Zimbabwe and Mozambique are less sensitive, since they have the luxury of a large contributing area–where a combination of increasing and decreasing runoff is expected.

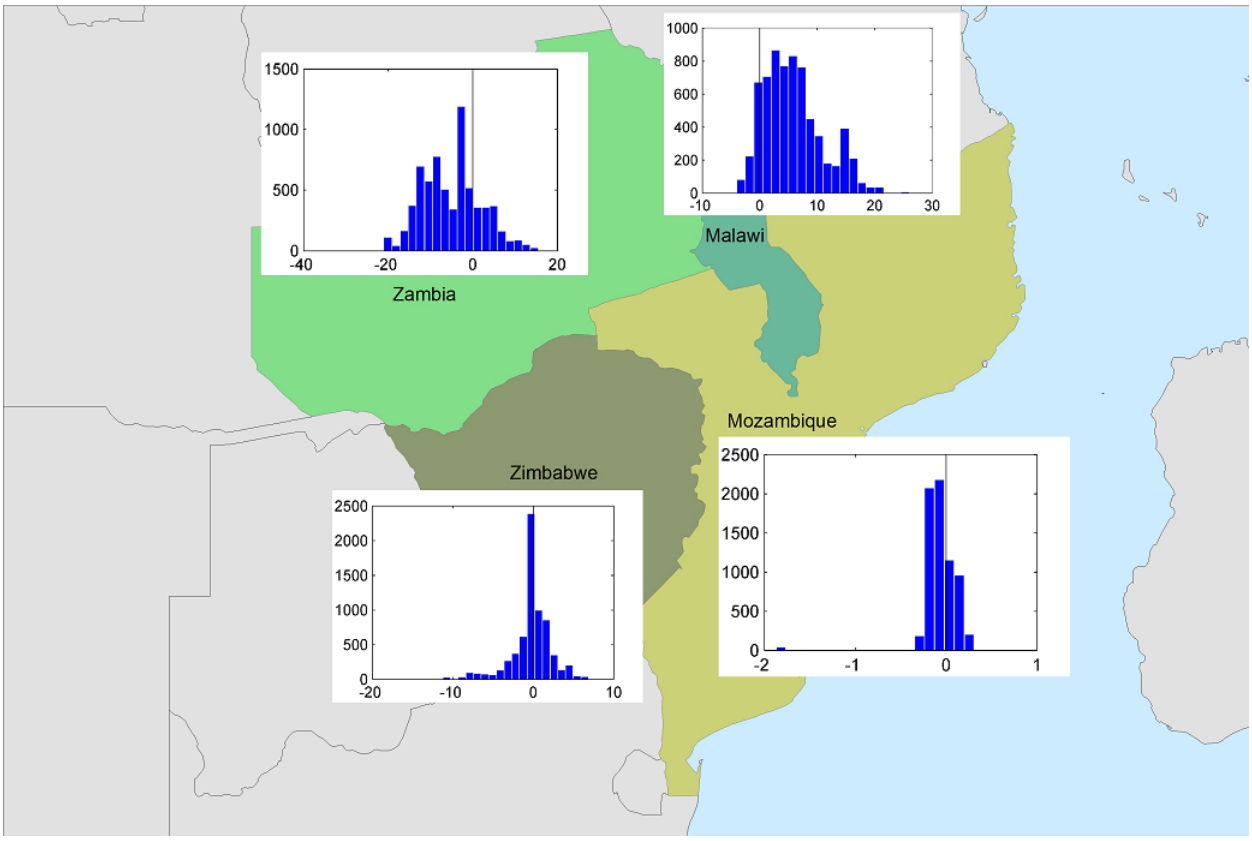

Figure 16: Climate scenario distribution of the percent change in hydropower generation is shown by country mean over the last 5 years simulated, 2046-2050

The impacts on irrigation availability are presented as the changes in shortage volume, where the shortage volume is defined as the volume of water delivered to the irrigation node in the WEAP model subtracted from the volume of water demanded by the particular irrigation node. In the upstream countries, Malawi and Zambia, the irrigation shortage remained insignificant in almost all of the scenarios (i.e., the amount of water delivered equaled the amount of water demanded). Due to mostly increasing predicted runoff in Malawi, and very small irrigation shortages in the base scenario, the impact of climate change on irrigated agriculture is expected to be small. In Zambia, the effect on irrigation demands is also expected

to be small which is mostly attributed to the spatial distribution of irrigation schemes (i.e., areas with more irrigation demands are drying less than areas with more hydropower generation capacity). In contrast, irrigation shortage in Zimbabwe and Mozambique is affected negatively by the predicted drying. Figure 17 shows the distributions for Zimbabwe and Mozambique, where here an increase infers a negative impact. In Zimbabwe, irrigation shortage is predicted to increase about 25% (between 5% and 50%) in most of the scenarios with a full range from a 50% decrease to a 75% increase. For Mozambique, the impacts are predicted to be less severe where, again, the decrease in runoff in the west is balanced in part by the increases in runoff in the north. But the impacts to Mozambique are predicted to be negative in more than 98% of the scenarios with the most common around 15%.

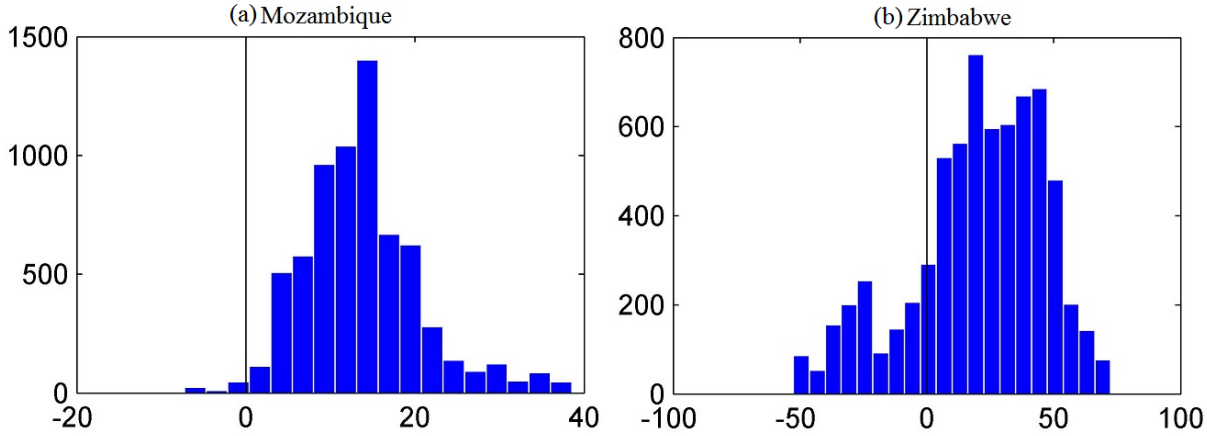

Figure 17: Climate projection distribution of the percent change in irrigation shortage in Mozambique (left) and Zimbabwe (right)

Conclusions

Based on this study of the Zambezi valley system, the future climate is likely to be drier in the basin as a whole, although there is a tendency toward a wetter climate in a small section in the north. Drier climate means more risk related to drought impact. We have quantified how a range of predicted climate (with a tendency toward drying) will likely reduce surface water availability basin-wide, increase irrigation demand, and decrease rainfed crop yields. And finally, using a water resource system model, we have shown a range of possible impacts on economically significant outcomes, namely changes in flood probability, hydropower generation, and unmet irrigation demand. Of the four countries in the region, Malawi is the least sensitive to climate change. Based on the study, the only concern for Malawi is a slight increase in flood risk. Alternatively, Zambia is predicted to experience losses in terms of hydropower generation, caused mostly by expected decreases in runoff in the west, as well as upstream irrigation demands. Also, large increases in flooding risk are not likely but possible for the country as a whole. In Zimbabwe, since hydropower plants are mostly upstream of the irrigation projects, changes in hydropower generation are not likely to be impacted, although there is about an equal chance of increase as decrease. In contrast, the future irrigation investments could be at risk of water shortage. The impacts to Mozambique are likely to be fairly mild because it has the benefit of a large contributing area with varying types of impact (both increases and decreases in surface water availability), but large-scale, high-damage flood events will happen much more often.

As mentioned, climate changes after 2050 are generally predicted to be more drastic. Changes in the latter part of the century, not included in his study, might be useful in future planning. Also, since all of the impacts are discussed here as changes from a baseline scenario,

inter-annual variability, which can be the cause of major impacts, is not considered in this analysis. Regardless, studies like the one presented here can help decision makers develop an informed risk-based strategy for national policy decisions, and help to direct locally detailed studies and designing large projects in the area.

CHAPTER 3

CHARACTERIZING WIND POWER RESOURCE RELIABILITY IN SOUTHERN AFRICA

Abstract: Producing electricity from wind is attractive because it provides a clean, low-maintenance power supply. However, wind resource is intermittent on various timescales, thus introducing variability in power output that is difficult for electric grid planning. In the following study, wind resource is characterized using metrics that highlight these intermittency issues, therefore identifying areas of high and low wind power reliability in southern Africa at different time-scales. After developing a wind speed profile, these metrics are applied at various heights in order to assess the added benefit of raising the wind turbine hub. Furthermore, since the interconnection of wind farms can aid in reducing the overall intermittency, the value of interconnecting near-by sites is mapped using three distinct methods. Of the countries in this region, the Republic of South Africa has shown the most interest in wind power investment. For this reason, we focus parts of the study on wind resource in the country. The study finds that, although Wind Power Density is high in South Africa compared to its neighboring countries, wind power resource tends to be less reliable than in other parts of southern Africa—namely, central Tanzania and parts of Kenya. We also find that South Africa's potential varies over different timescales, with higher potential in the summer than winter, and higher potential during the day than at night. This study is concluded by introducing a variety of methods and measures to characterize the value of interconnection, including the use of principal component analysis to single out areas with a common signal.

Introduction

As the threat of climate change builds, there is a push towards lower emissions. One strategy for reducing emissions is to build away from carbon intensive electricity production and toward clean energy sources like the energy produced from wind and solar. These clean energy resources are dominated by new technologies that are dependent on intermittent, locally unique sources not yet well understood. Understanding past variability of climate in relation to potential renewable resources can steer investment towards beneficial sustainable ventures and avoid poor investment decisions. In the following paper, we present a study of historical wind patterns with the hope that these patters persist in the future. The methods presented here could, for the most part, be applied to solar resource as well.

In the last few decades there has been a growing interest in wind-generated electricity. However, due mostly to the uncertainty caused by the chaotic characteristics of wind near the earth's surface, wind power generation is intermittent on useful operating time scales (hours and days), and likely inconsistent in the long term (years and decades). Southern Africa provides an interesting case study for this analysis, specifically the Southern Africa Development Community (SADC) countries, which include the Democratic Republic of Congo, Tanzania, and all countries south of these two. Energy demand in this region of the world is rising quickly, with an average of 6.5% per year in Mozambique and 9% per year in Angola, for example (SAPP 2012). Of the countries in this region, South Africa has shown the most interest in wind technology investment.

Wind Resource Characterization

Wind resource study is often characterized by a time and spatial scale, which is driven by the overall purpose. Due to the relatively high inertia of wind turbines, changes in wind speed that occur on time scales less than 1 minute (ultra high frequency) are typically considered negligible. This sets the limit on the lower time-scale extremes. Large time scales are limited by the expected life of a wind turbine, which is generally about 20 years. Therefore, useful wind resource assessment falls between a time scale of high frequency (minutes) and inter-annual frequency (years). The relevant spatial scale largely depends on the study objectives. In a project scale, or local scale study (less than 1 km), the effects of trees, buildings, and hills are significant. On larger scales, these effects can be generalized into a roughness length coefficient and aggregated over time to avoid false precision (Peterson et al. 1997).

Typically, for national planning purposes, wind resource is characterized following a few similar steps. First, an annual mean wind speed dataset is used to specify wind resource geographically. In the past, this has been a collection of wind station data, as in Diab (1995) for South Africa. Then, the estimated annual mean wind speed is used, along with assumed or estimated shape parameter/s, to represent the distribution of wind speed over time using a fitted distribution (Cavallo 1993). The Weibull distribution is most widely used (Ucar and Balo 2009; Pryor and Barthelmie 2010; Zaharim et al. 2009; Eskin et al. 2008, among others) because it fits wind speed distribution fairly well, reproducing the positive skewness, and only requires two parameters for fitting (Tuller and Brett 1984). Recently, some doubt has been raised about using the Weibull distribution as noted recently in Gunturu and Schlosser (2011). Jaramillo and Borja (2004) found that the Weibull distribution could not be generalized to two parameters for fitting

some wind regimes. Morrissey et al. (2010) also found the Weibull fitting to be inaccurate for the wind speed distribution at a particular site. The study found that the Weibull fitting underestimated lower wind speed frequencies and overestimated higher wind speed frequencies. Furthermore, buoyancy fluxes have been found by He et al. (2010) to distort typical wind behavior away from a fitted Weibull distribution. The study also found that the Weibull distribution does not reproduce the positive skewness typically observed in nighttime winds.

Once the typical behavior of wind is generalized, a reference wind turbine is typically used to estimate the power theoretically generated, applying the limitations of cut-in and cut-out wind speeds. Cut-in wind speed is the minimum speed at which wind turbines generate power, while cut-out speed is the maximum speed at which, for various reasons, power cannot be generated. An example of a typical power curve is shown in Figure 18 to illustrate the importance of cut-in and cut-out wind speed in power generation.

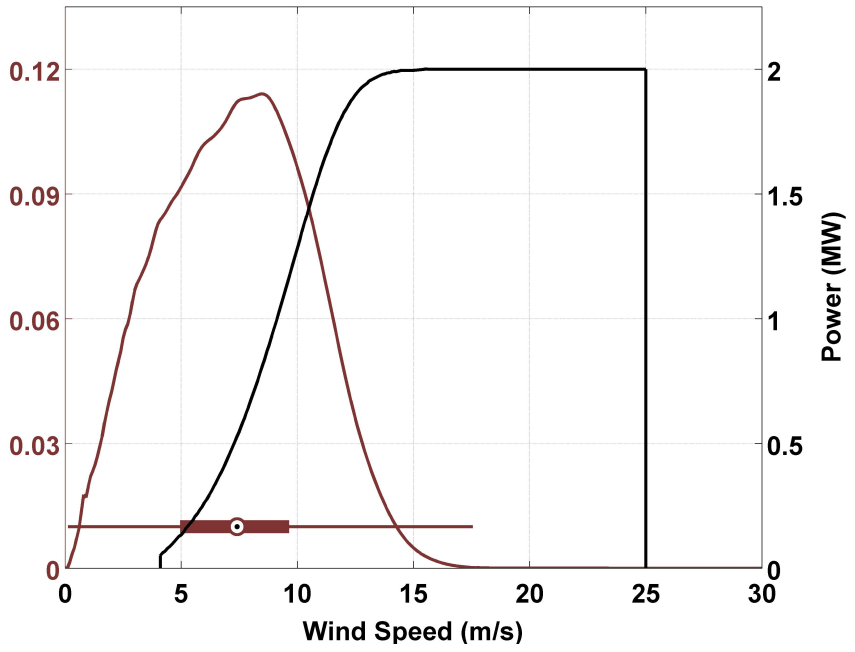

Figure 18: Power curve for a Vestas V80 2000/80 2MW turbine at 1.225km/m^3 (in black and on right axis; data from Hagemann 2008) and MERRA wind speed distribution from a location in South Africa with high potential

In order to avoid the limitations of choosing a specific wind turbine, others have described the wind resource in a more generalized form. The wind power generated by wind turbines is related to the cube of wind speed (V) and air density (ρ). A common value used to express this relationship is wind power density (WPD) using the following equation:

$$WPD = \frac{1}{2}\rho V^3 \qquad \text{(EQ-3)}$$

Due to the cubic relationship of wind power generated and wind speed, higher wind speeds are important to identify, both spatially and temporally. Due to the wind turbine mechanics as well as a means to protect the turbine itself, the efficiency of power produced by a

wind turbine decreases as wind speed increases, resulting in a relationship that is almost linear, although piecewise, with four distinct stages: no power from 0 to 4 m/s; a steep increase from 4 m/s to about 14 m/s; a flat relationship from 14 m/s to 25 m/s, independent of incremental changes in wind speed; and no power produced above the cut-out wind speed of 25 m/s. As shown in Figure 18, the majority of the power produced remains in the range between 4 m/s and 14 m/s, where small changes in wind speed result in large changes in power produced, thus resulting in highly intermittent output.

Due to recent technological advancements in wind turbines, there are more hub height options than in the past. For this reason, typical wind resource assessment requires an understanding of the changes in the potential energy generated at different hub heights. With these characterized, one can weigh calculated benefits against the marginal costs of increasing the hub height. A common approach to estimating wind speeds at different heights is to use a power law of the form:

$$\left(\frac{\overline{V_1}}{\overline{V_2}}\right)=\left(\frac{z_1}{z_2}\right)^{\alpha} \qquad \text{(EQ-4)}$$

where V_1 and V_2 are the wind speeds at the reference location and the estimated location, respectively, and z_1 and z_2 are the heights at the reference and estimated location, respectively. This relationship is also commonly used to estimate hub height wind speeds from anemometer records near the surface. In most cases, the shear exponent (α) is assumed to be 1/7 (Elliott et al. 1987, 1991; Sailor et al. 2008, among others). Schwartz and Elliot (2005) found that the actual value of the shear exponent is considerably greater than 1/7. They also found that windy sites

tend to have lower values of α than less windy sites. Using a constant value, then, might result in an overestimation of wind speed at higher altitudes for less windy sites.

Wind resource mapping of South Africa

A very important intermediate step in the typical wind characterization process is mapping the resource. So far, wind resource has not been mapped over the entire region, but there have been two completed, well-documented attempts to map wind resource over South Africa. Diab (1995) developed an initial wind resource map, effectively classifying areas of good, moderate and low wind power potential. Diab used 79 long-term weather stations of varying geographic settings with classical methods estimating mean wind speed, wind power density, and Weibull distribution parameters. She also estimates mean monthly and daily wind fluctuations over the year. Diab found that a band covering the full coast of South Africa is likely to be the area where wind potential is the highest, with some moderate potential further inland. Hagemann (2003) points out a few problems with this early work, mostly in the use of the weather station data and measurement errors in the data itself. Following Diab's work, an attempt was made by Eskom and other partners in the early 2000s to develop a more reliable wind resource map. Unfortunately, these were never made available to the public (Hagemann 2008).

Killian Hagemann produced the second wind resource map as part of his 2008 PhD dissertation. Hagemann (2008) explored the value of using the regional climate model, MM5, to develop a high-resolution wind climatology for South Africa, representing a typical year. As a result, he produced a mesoscale map of wind resource, which superseded Diab's work. This work has produced the most recent full map of wind resource in South Africa. Hagemann

estimates that South Africa has a total potential wind generation of about 80.5 TWh, 35% of total 2007 electricity sales.

Recently, it has become popular to map wind resources using a combined meso/micro-scale modeling technique imploring the Karlsruhe Atmospheric Mesoscale Model (KAMM; Adrian and Fiedler 1991; Adrian 1995) and the microscale model WAsP (Troen and Peterson 1989). WAsP makes use of the previously discussed Weibull distribution. This technique has been used in studies of Ireland, as well as Europe, Russia, and Egypt, among others (Landberg et al. 2003). A similar study began for South Africa around 2010 called the "Wind Atlas for South Africa" (WASA), coordinated by the South African National Energy Development Institute (SANERI). This work, slated to finish in June 2013, has made available some initial presentations, results, and data (Szewczuk and Prinsloo 2010). One major contribution from this work was the installation of proper wind measurement towers that record wind measurements at turbine hub heights up to 63m.

Data and Methods

With the advancement of satellite utility and measurements, global datasets are becoming more popular for areas with a limited or unreliable set of historical data. For this study, the MERRA (Modern-Era Retrospective for Research and Analysis) reanalysis dataset is used (Rienecker et al. 2011). The MERRA dataset is attractive because it attempts to represent a balance between satellite, station, and modeled climate gridded globally at an hourly time-step from 1979 to 2009. Although there are certainly limitations to the reanalysis approach, MERRA

improves on the representation of the hydrologic cycle and uses a large repository of conventional observations from various sources, as well as satellite radiance data.

Wind speed is estimated using the following logarithmic empirical relationship, taking into consideration roughness length (z0), height (z), and friction velocity (u*) (Stull 1991):

$$V_z = \left(\frac{u_*}{k}\right)\ln\left(\frac{z-d}{z_0}\right) \qquad \text{(EQ-5)}$$

The MERRA data provide the necessary variables for this calculation. In this equation, the wind is assumed to be neutrally stable, a reasonable assumption because at high wind speeds the boundary layer has high wind shear and is therefore approximately neutrally stable.

The spatial scale of MERRA is set to 1/2° by 2/3°, somewhere between mesoscale and synoptic scale, and is hourly. One of the caveats of using data aggregated over a grid is that the aggregation could cause misrepresentations of the climate. Of course, a wind farm would be subject to the wind behavior at a much smaller spatial scale, so it is important to understand the differences between gridded (i.e. aggregated) and point (i.e. as measured from a station) climate. See Appendix A for a comparison of these types of data in South Africa as a means to describe these differences.

Mapping

Using the MERRA dataset and EQ-3 to estimate wind speed at 50 m, mean wind speed is mapped to compare to Haggeman's wind atlas. Of course, Haggeman's wind atlas was produced at 10 m above ground but the logarithmic profile, in EQ-5, that is used here is not valid for

elevations this low. Figure 19 shows the mean wind speed in m/s at 50 m. These results look similar to Haggeman's in most areas in South Africa. There are higher wind speeds in the southwest and lower in the northeast. Also, South Africa has relatively high mean wind speeds compare to its neighboring countries.

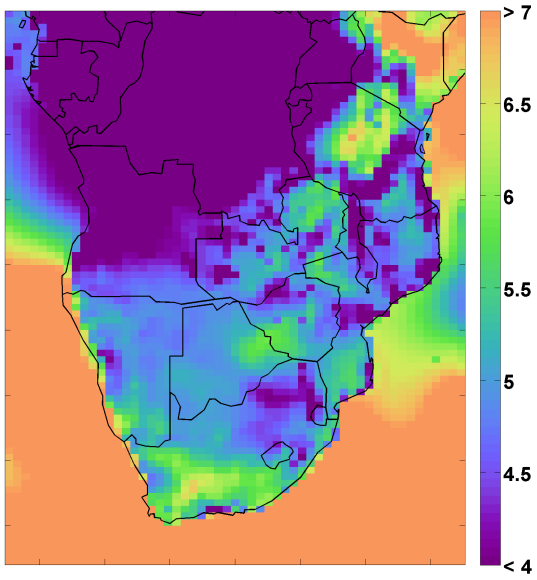

Figure 19: Mean wind speed (m/s) at 50 m for southern Africa

Wind power density and measures of central tendency

Mean and median WPD for southern Africa are shown in Figure 20. Any value below 50 W/m^2 is considered to have no wind power potential and is shown as white.

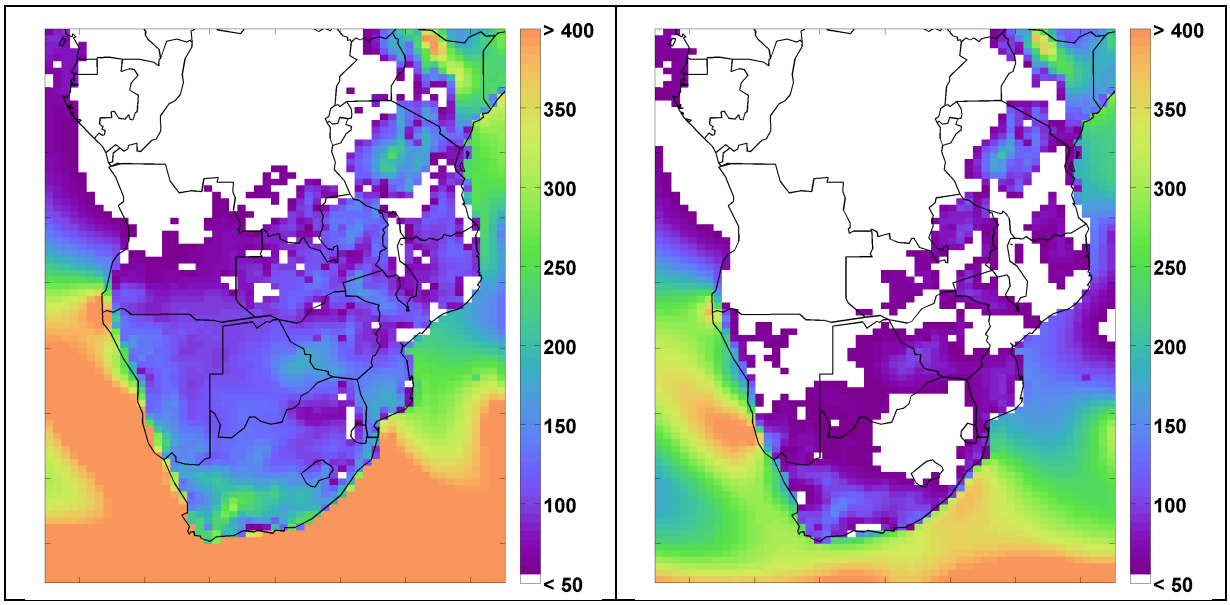

Figure 20: Mean (left) and median (right) wind power density (W/m^2)

Similar to the map of wind speed, there is a large area around central Africa (northwest in the map) where the wind power potential is poor. This area extends over the majority of the Democratic Republic of the Congo, into northern Angola, and east to the western parts of Tanzania and Uganda. The areas of good wind resource potential are in central Tanzania, the southwestern part of South Africa, and most of Kenya. There are also some smaller areas of potential along the border of Botswana and Zimbabwe, southern Mozambique, and parts of Zambia.

Typically, mean wind speed or mean WPD is used to show the central tendency of wind resource potential. Due to the skewness of the wind power density toward lower values, Gunturu and Schlosser (2012) suggest that the median is a more meaningful measure of central tendency for national grid planning. The median is especially useful because it represents what the theoretical output produced at least half of the time, providing a simplified measure of reliability. The median also provides a closer approximation of power production since the efficiency of a

typical wind turbine decreases as wind speed increases, as shown in Figure 18, i.e. the median puts less emphasis on larger values of WPD than the mean. As shown in Figure 20, the median is considerably lower than the mean. In fact, the area of poor wind resource potential in the northwest portion of the map extends south over Angola and into most of Namibia. In the past, a threshold of 220 W/m^2 was used to classify poor wind resource potential (Gustavson 1979). Although wind power technology has developed since 1979, and wind turbines are now more efficient, if a value of 220 W/m^3 was used here, the only areas of good wind resource potential would be in the east—namely the grids in central Tanzania and Kenya.

Measures of variability

Another valuable measure of wind resource is a measure of variability. Large unpredictable changes in wind speed over time are problematic for power distribution planning. Therefore, an area with lower variability is more desirable than one with higher variability, given that they have comparable central tendencies. A useful measure of variability is the coefficient of variation (CoV), which is shown for WPD for southern Africa in Figure 21. Here, a value of 1 means that the standard deviation is the same as the mean. A value above 1 indicates that the standard deviation is larger than the mean, and below 1 indicates that the mean is larger than the standard deviation. In general, the areas with a larger mean WPD have lower CoV. One exception to that would be a comparison of the central area of Tanzania with the southwestern area of South Africa. These two regions have similar mean WPD, but the southwestern part of South Africa has a significantly higher CoV suggesting that this area is less desirable for wind power harvesting. Another useful measure of variation is the robust coefficient of variation (rCoV) defined as

$$rCoV = \frac{median(|WPD - median(WPD)|)}{median(WPD)} \quad \text{(EQ-6)}$$

where WPD is a timeseries of wind power density values. The interpretation of rCoV is similar to that of CoV, except that a value of 1 means that the median absolute difference between the value and the median of the timeseries is equal to the median of the timeseries. Therefore, a rCoV of 1 means that central tendency of the absolute difference from median of the WPD timeseries is greater than twice the median or zero, since WPD cannot be negative. This map also shows the striking difference between central Tanzania and southwestern South Africa. In fact, all of South Africa appears to have a highly variant WPD, even the areas where the median value is high. In terms of variance, eastern Africa proves to exhibit the best source for wind power harvesting in this region.

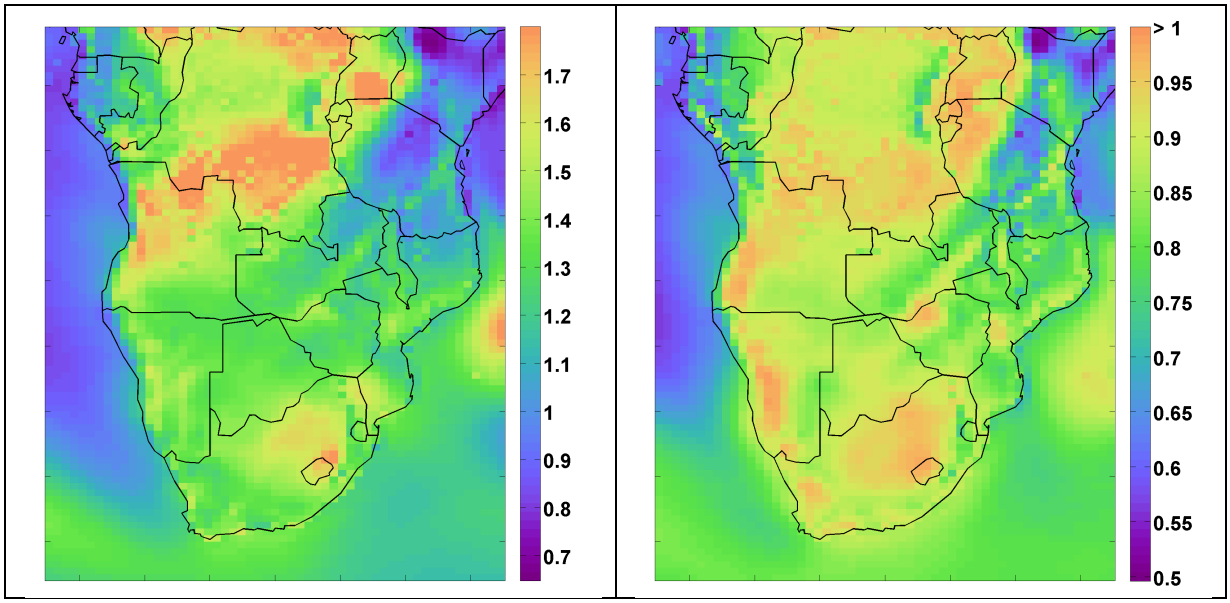

Figure 21: Coefficient of variance (left) and the robust coefficient of variance (right) of WPD

Measures of reliability

To further our understanding of the quality of wind resource in southern Africa, we have decided to map two measures of reliability. First, we must choose a threshold to classify wind power for a given grid and hour as either usable or unusable. In the past, a value of 220 W/m^2 has been demonstrated as the minimum needed for wind power generation (Gustavson 1979). For this study we have chosen to follow the US Wind Resource Atlas and use a value of 200 W/m^2 to account for advances in technology (Elliott et al., 1987), which was also used in Gunturu and Schosser (2012). The first measure we calculated is availability. Availability is the number of hours with usable WPD (i.e. WPD>=200W/m^2) divided by the number of total hours from the MERRA data. Figure 22 shows the availability fraction for southern Africa. A similar pattern emerges from this measure that we have seen before, where there is low availability in the northeastern section of the map. In fact, the majority of this region has availability close to zero, meaning that there are basically no hours with available wind power. Three regions with good availability stand out: Kenya with wind power available around half of the total time, central Tanzania with wind power available between one third and one half, and southwestern South Africa with power available between one fourth and one third of the total time.

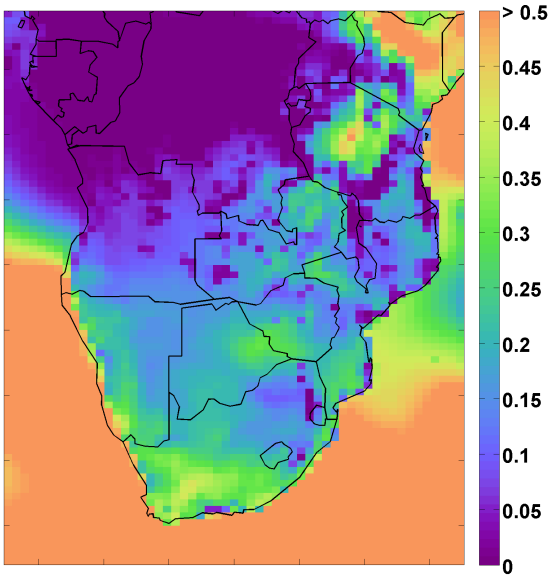

Figure 22: Availability of WPD at 50 m

The next measure of reliability we have calculated is wind power episode lengths. Here, a wind power episode is defined as a period of time where wind power is usable for consecutive hours. Each of these wind power episodes is found and the number of consecutive hours is recorded. Figure 23 shows the mean (left) and median (right) of the wind power episode lengths. We see that central Kenya has wind power episodes around 20 hours long on average, central Tanzania around 8 to 15, and southwestern South Africa around 8 to 13 hours. Unsurprisingly, the wind power episode lengths appear to be predominantly skewed towards lower values, similar to WPD, although less so. For example, the difference in the median and mean in central Tanzania is about 2 hours while in southwestern South Africa the difference is closer to 3 or 4 hours.

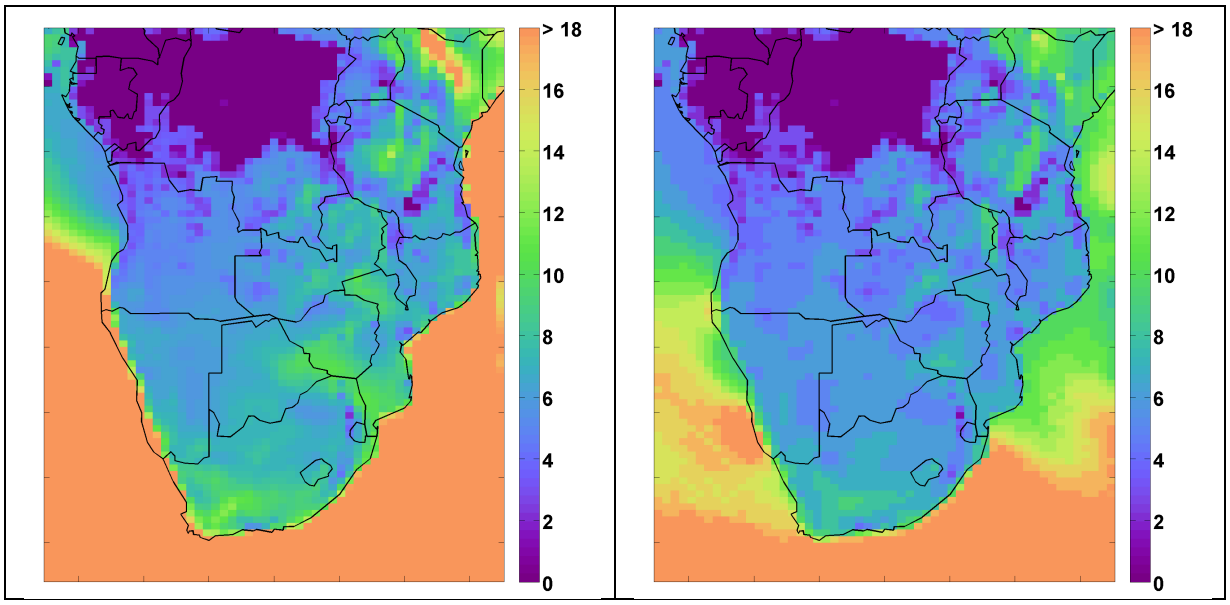

Figure 23: Mean (left) and median (right) of wind power density episode lengths at 50 m hub height

Changes over different time-scales

Since wind speed is driven largely by various climatic states, wind power potential can vary somewhat consistently over the seasonal and diurnal cycles, among others. For this part of the study, we will focus on the Republic of South Africa as an example. First, using the same WPD threshold of 200 W/m^2, we calculate a binary timeseries representing an hour with either unusable (i.d. less than the threshold) or usable (i.e. greater than the threshold) wind power. Then, we calculate the total area in South Africa with usable power and divide it by the total area in South Africa. From this calculation, we estimate the fraction of area with power, where a value of one means that all of the area has power in that hour, a value of 0.5 means half of the area has power, etc. Now, we have a single 31-year timeseries and can make claims on how the wind power potential changes over various timescales. Box and whisker plots showing the

distributions over each of the 31 years is shown in Figure 24. We again see that the distributions are skewed toward lower values with a central tendency around 0.2 and a very long tail reaching toward 1. The 75th percentile, represented by the top of the box, generally lands on 0.4 and the 25th around 0.05. Figure 25 shows the hourly mean over the 31 years in blue. Notice that the value fluctuates somewhat periodically, spanning about 0.4. This fluctuation is the diurnal cycle. For this reason, we applied a 24-hour moving average to the hourly mean, shown in red, to remove the large fluctuations. There is a clear seasonal cycle in wind power usability in South Africa, which peaks around October / November followed by a lull around April. Also notice that the mean value fluctuates from about 0.1 to 0.5 in a typical 24-hour period, meaning that the WPD in about 40% of the area drops below the threshold within the day.

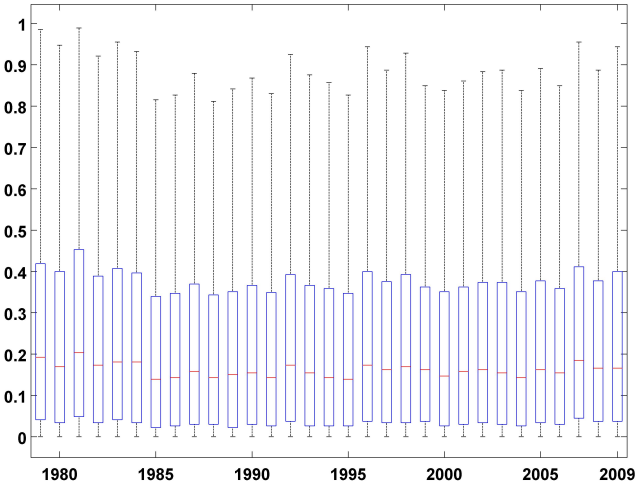

Figure 24: Distributions of the fraction of area in South Africa with usable WPD for each year of the MERRA data

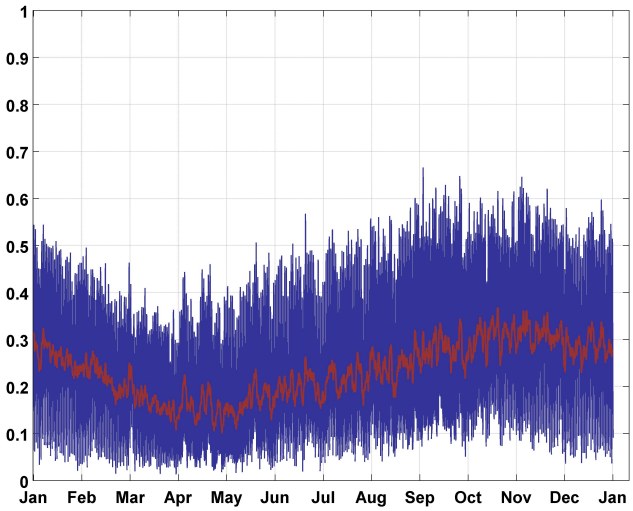

Figure 25: Hourly mean fraction of area in South Africa with usable power over the calendar year calculated over 1979-2009 in blue and with a 24-hour moving mean in red.

Since Figure 25 only shows the mean of the fraction of grids with usable power in South Africa, we wanted to get a sense of the how the seasonal pattern is distributed over all of the years. Figure 26 shows the 90th(top grey line), 50th (black), and 10th(bottom grey line) percentiles smoothed with a 168-hour (1 week) moving median. In this case, the 90th percentile represents the 1-week central tendency of the highest fraction of area with usable power that could be expected in a 10-year period. Similarly, the 10th percentile would be the lowest expected to occur in a 10-year period. The 90th percentile drops to around 0.2 in April and rises above 0.5 around October and November, while the 10th percentile hits a long peak from November to January, slightly below 0.1 and a long 6-month lull near zero from the middle of March to the middle of September. The median finds a steady peak near the beginning of October that lasts to the middle of January at around 0.5 and drops close to zero at the beginning of May. As a reference, the

electricity-demand weekly load (as a fraction of the mean) is shown to illustrate changes in demand over the seasons. Unfortunately, peak demand is in the winter months, June-July-August, when wind power availability is low.

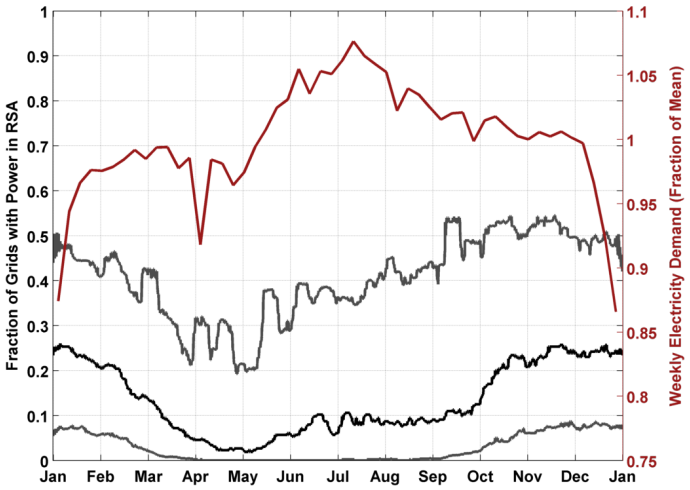

Figure 26: Median (black line), 10th percentile (bottom grey line), and 90th percentile (top grey line) of the seasonal distribution of the fraction of area in South Africa with usable WPD. Weekly electricity demand as a fraction of the mean is superimposed in red.

The availability of wind power and energy demand both fluctuate daily as well. Figure 27 shows the distribution of the fraction of area with usable power in South Africa over 24-hours using box and whisker plots, in grey. The plot starts 30 minutes after midnight and ends 30 minutes before, so the average daylight hours can be assumed to be between 6:00 and 18:00, although this does change seasonally. To avoid clutter, outliers are not shown in this plot. Outliers are assumed to be any value greater than $q_3 + 1.5\ (q_3 - q_1)$ or less than $q_1 - 1.5\ (q_3 - q_1)$, where q_1 is the 25th percentile and q_3 is the 75th percentile. The end of the grey line, top and bottom, represents these limits. The thick grey line represents q_1 at the bottom and q_3 at the top, and the black dot is the median. The red line, again, shows the mean electricity demand profile

across the day. As shown, South Africa has a much higher fraction of grids with power during the day than at night. Just after midnight, most of the grids do not have usable power, with a median around 0.03. Around 3:30, the wind starts to increase above the threshold in many of the grids, peaking around 10:00 and dropping down to around 0.1 at 15:30. The daily distribution of grids with power is ideal for matching the morning peak demand, but fails to meet the peak demand in the evening, about 20:30. Another interesting feature of this plot is the extremes. During the peak hours around 10:00, the distributions reach the full range of possible values, from zero to 1.

Wind power density at different altitudes

As wind turbine technology advances, increasing the hub height becomes more economically feasible. In a general sense, WPD increases as hub height increases because the roughness of the earth has less of an effect on the wind speed. But, as the altitude increases, the density of the air decreases at a rate of about 0.01% per meter. This means that an increase of 100 m would result in a reduction of about 1% of the WPD caused by thinner air. The intermittency could also change at different hub heights. In the following section, we will explore WPD at various heights. Using EQ-5, we can estimate wind speeds at different values of z, then convert these to WPD using EQ-3.

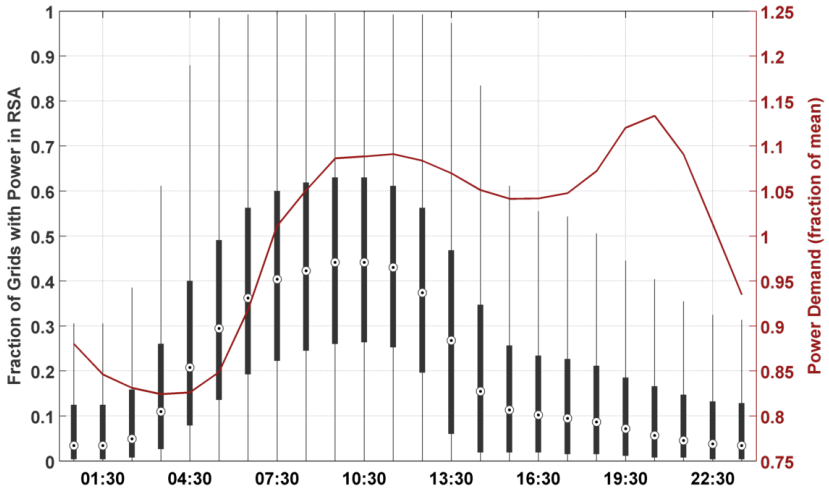

Figure 27: Diurnal distribution of the fraction of area with usable WPD in South Africa. The load is superimposed in red shown as a fraction of the mean.

Figure 28 shows the median WPD at different altitudes for 80 m and the difference between WPD at 80 m and 150 m. Generally speaking, the median WPD increases with height proportional to the central tendency.

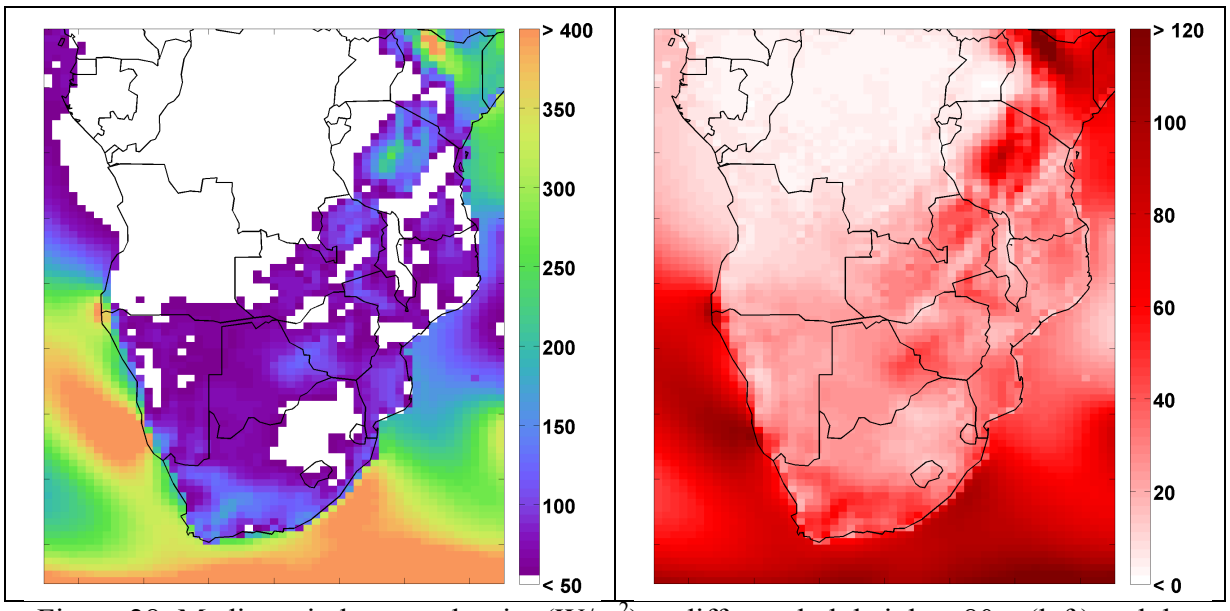

Figure 28: Median wind power density (W/m^2) at different hub heights: 80m (left) and the difference between 150m and 80m (right).

Next, we explore how the episode lengths change with altitude. Figure 29 shows the mean episode length at 80 m, then again the differences between the value at 80 m and the value at 100 m, 120 m, and 150 m. Although episode lengths are relatively high in South Africa, the length of available wind power doesn't seem to increase as much with height as the areas in Kenya or central Tanzania. In fact, the northern part of Zambia shows more promise at higher altitudes than South Africa.

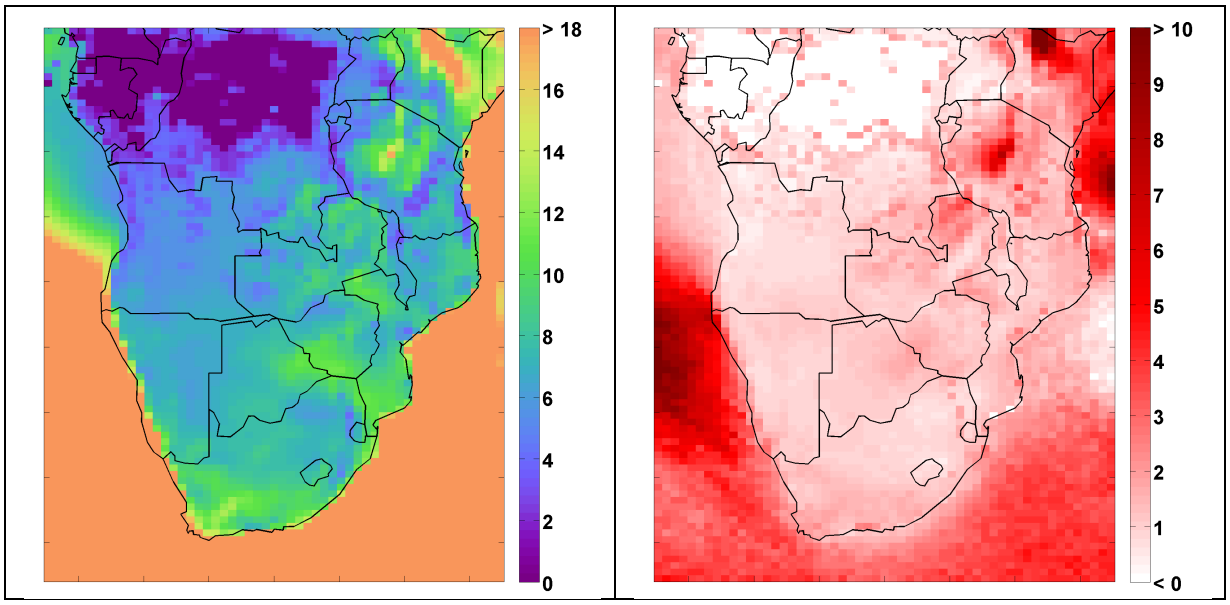

Figure 29: Mean of wind power episode length (hours) at different hub heights: 80m (left) and difference between 150m and 80m (right).

Mapping the value of interconnection

One proposed method for dealing with wind power intermittency is to connect wind farms that have negatively correlated wind speeds. Then, theoretically, when one farm does not have power, the other does, and vice versa. We wanted to investigate this potential in southern Africa using a technique developed by Gunturu and Schlosser (2012), anti-coincidence, as well as a simple rank correlation and a more complex method, principal component analysis.

Anti-coincidence

Here, we take the full hourly timeseries of WPD for every grid point in southern Africa and convert it to a binary dataset, where zeros represent unusable WPD, less than 200 W/m^2, and ones represent usable WPD, greater than 200 W/m^2. For every grid, we look at the surrounding grids in a fixed window and determine that grid's "score." This score represents a measure of

how useful it would be to interconnect wind farms with the surrounding grids. We have decided to use a window of 19 X 19 grids, as shown in Figure 31. This represents a box that is 10 grids in each direction from the point R, and is approximately 1,000 km on each side. For each grid in this box, the binary values are compared between the point of interest, R, and the surrounding grids, P. A count is made whenever there is wind power at one of the two points and not at the other. If the count is at least half of the total time series, the grid is said to be “anti-coincident” to the reference, R. The number of grids in the window that meet the anti-coincident criteria are counted and that is the score given to R.

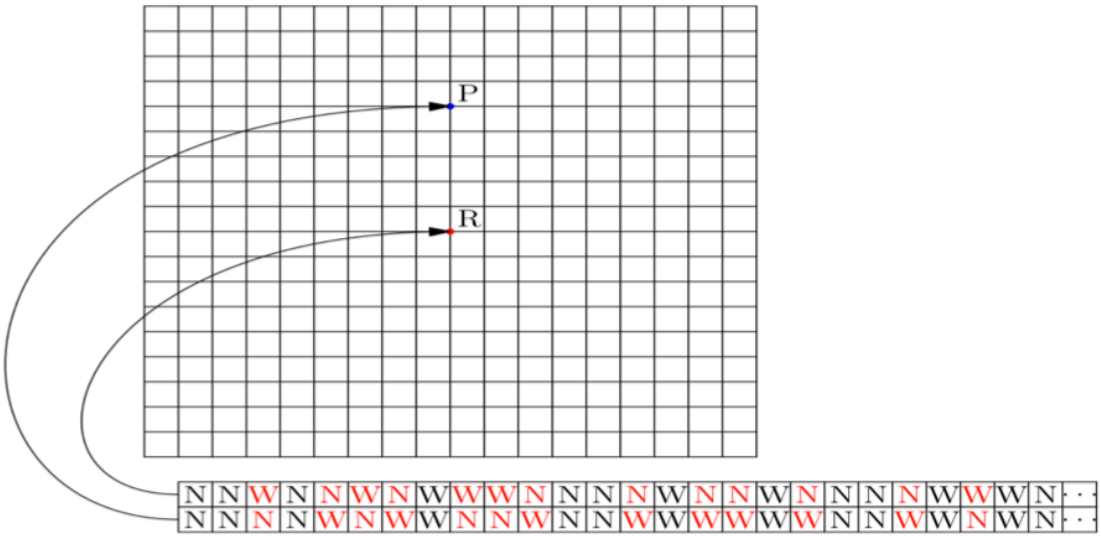

Figure 30: Anti-coincidence schematic

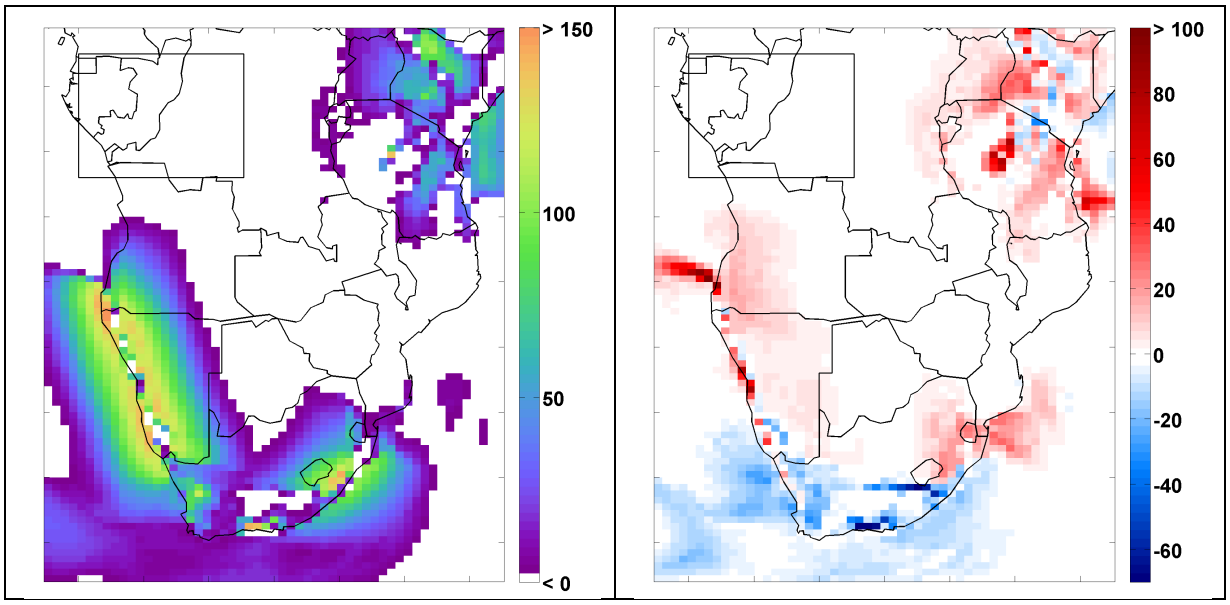

Figure 31: Anti-coincidence score at different hub heights: 80m (top left); difference between 100m and 80m (top right); difference between 120m and 80m (bottom left); difference between 150m and 80m (bottom right).

A map showing the anti-coincidence score is shown in Figure 31 for WPD at 80 m, as well as the difference between 80m and 150 m. Note for any grid that is at least 10 grids from the edge, the total number of grids in the window is 360 (19*19 - 1), so a value of 72 means that 20% of the surrounding grids are anti-coincident. The size of the grid box is shown in the northwestern area of each map in Figure 31 as reference.

For the majority of southern Africa, the anticoincidence score is zero. This is not surprising in the Congo area because the WPD is very low, but it is surprising in Zambia and Zimbabwe where there are some regions of mild potential. Also, it is surprising that central Tanzania is so low, except for a few grids of high anti-coincidence. Another interesting feature of the map at 80 m is the high score along the coast of Namibia and South Africa. This is likely caused by characteristically different wind patterns in the offshore grids compared to the wind

patterns inland. From a national planning perspective, this finding could imply that it would be a good investment to match each onshore wind farm with an offshore wind farm, even though offshore wind farms are more expensive to build. The anti-coincident score also changes considerably for different altitudes. In most of southern Africa, the score increases as height increases, especially eastern Africa and the northern coast of Namibia. But there seems to be a dividing line at the southern part of South Africa where the anti-coincidence score decreases with height, likely because the wind in the land grids starts to behave similar to the wind in the ocean grids nearby.

Null Anti-coincidence

Gunturu and Schlosser (2011) also used a relaxed criterion to characterize the value of interconnection that emphasizes the instances of unusable power at R. Like in the measure of anti-coincidence, the two binary time series that represent usable and unusable power at R and P are compared. Except, in this measure, only the instances when there is unusable power at R are considered. Every hour where there is usable power at P and unusable power at R are counted. If this count is at least greater than the total number of hours of unusable power at R, the grid, P, is considered to be “null anti-coincident” to the grid, R. These grids are counted and the total count represents the null anti-coincidence score. Figure 32 shows the schematic for null anti-coincidence.

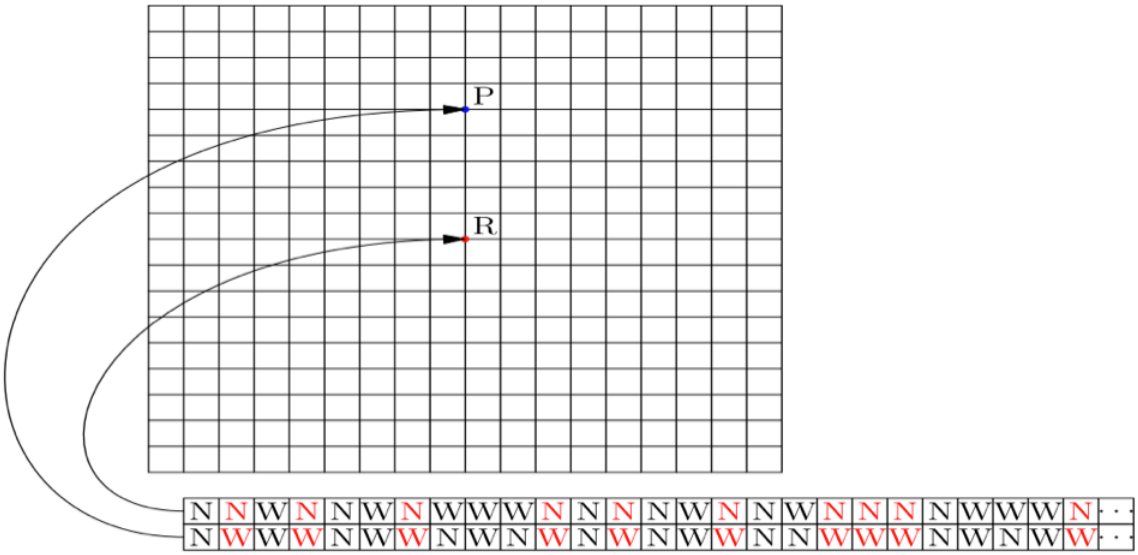

Figure 32: Null anti-coincidence schematic

Since the criteria for null anti-coincidence is somewhat relaxed as compared to the anti-coincidence criteria, we expect a higher null anti-coincidence score. Figure 33 shows the score at different hub heights. The values are highest in eastern Botswana, central Tanzania, and a large area in western Angola. South Africa shows a fairly low null anti-coincidence score, especially in the west where there is a high wind power potential. Another interesting feature of these maps is that the score never increases with hub height in southern Africa. The decreases are largest in Namibia and the cluster near the South Africa-Botswana-Zimbabwe borders.

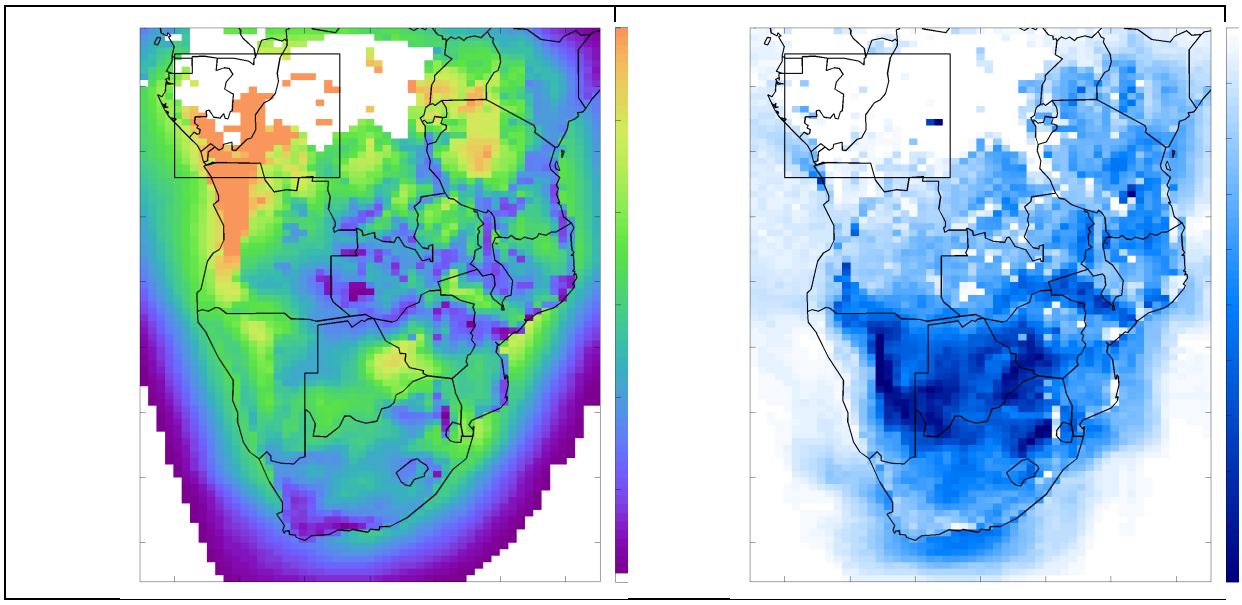

Figure 33: Null anti-coincidence score at different hub heights: 80m (top left); difference between 100m and 80m (top right); difference between 120m and 80m (bottom left); difference between 150m and 80m (bottom right).

Correlation with nearby grids

Here, we take a different approach to further our exploration of the value of interconnection in southern Africa. In the previous approach, a threshold is assumed in order to transform the dataset into a binary sequence. In order to avoid assuming a threshold, we calculate a Spearman rank correlation. Similar to the anti-coincidence score, we find the rank correlation of each point with the reference in the moving window and take an average of the rank correlations. Figure 34 shows these window-averaged rank correlations for southern Africa. In this case, a point with a negative value suggests that the timeseries at the point is negatively correlated with the points around it in the 19 by 19 window. Therefore, a negative value implies a high interconnection value, and a positive value implies low interconnection value. Here we

see a clear separation between most of South Africa, where the rank correlations are dominantly positive, and the rest of southern Africa, where the rank correlation is mostly negative.

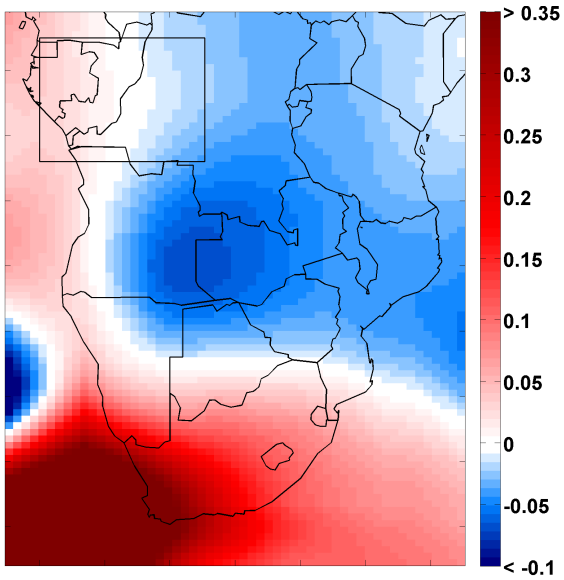

Figure 34: geographic variation of the mean rank correlation with nearby grids

Principal component analysis

Interested in the difference between the results found by these two methods, we investigate the variance of the hourly wind speeds in southern Africa using Principal Component Analysis (PCA). PCA reduces the dimensionality of a set of data into vectors of dominating variance, where the first Principal Component explains the most variance, the second explains the second-most, etc. Typically the signal, or z-score, is used rather than the raw values. The z-score is calculated by subtracting the mean and dividing by the standard deviation. We used the z-score here. Figure 35 shows the coefficients, or eigenvectors, of the first eight principal components. The first principal component explains 19% of the variance, the second explains

7%, and so on. There are 4,675 principal components total, in this case. The first eight principal components capture over half of the total variance. The areas in the maps with similar coefficient values exhibit the pattern captured in that particular principal component. Basically, the red areas in the maps are out of phase with the blue areas and the percentage value can be thought of as a measure of importance of that principal component. The first principal component shows positive values over land and some negative values in the Atlantic Ocean. This map shows that WPD onshore is negatively correlated with WPD in the Atlantic Ocean. When we look at this principal component in a timeseries, we see a strong 24-hour cycle as well as a seasonal cycle. The second principal component has captured variance that shows that South Africa is in phase with the ocean around it and out of phase with the rest of southern Africa. This second principal component is likely the variance that was captured in the rank correlation map shown previously. Principal components 3 through 7 display interesting features in the Atlantic Ocean that were likely captured in the anti-coincidence score.

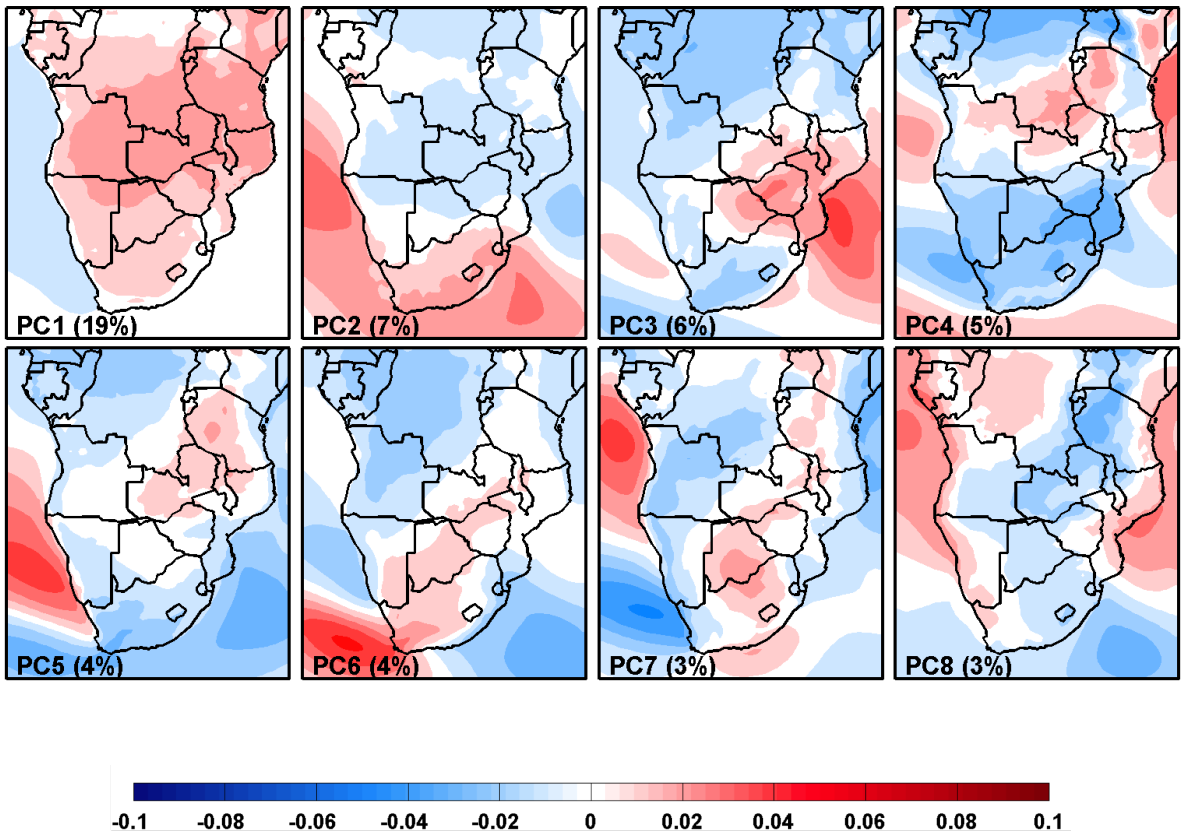

Figure 35: The first 8 Principal Component coefficients from the PCA of the signal of hourly WPD dataset over southern Africa. The values in parentheses are the percentage of variance explained by that principal component.

Since the grid domain affects the resulting PCA, we decided to narrow the domain to onshore grids in the Republic of South Africa. We also decided to use the power curve from the Vestas V80 2000/80 2MW wind turbine, shown in Figure 18, to produce capacity factor values. In this case we decided to use the raw values instead of calculating the z-score first to give more weight to higher energy production. Figure 36 shows the eigenvalues from this analysis for the first eight principal components. The percent of variance represented is shown in parenthesis. Of course, the PCA with a narrower domain is able to explain more variance in fewer principal

components. In this case, the first four principal components contain over 60% of the variance. The first principal component, which explains 38% of the capacity factor variance, is all in-phase, especially the area in the southwest where most of the wind power potential resides. This result is not ideal for interconnection. In the remaining principal components, we see distinct regions that are either in-phase or out-of-phase. Principal components 2, 4, 5, and 6 suggest that the area along the coast in the Eastern Cape province is out-of-phase with areas in the Western Cape and Northern Cape. These being out-of-phase suggest interconnection value; although, summing the variance explained by these principal components only gets us 24%—still much less than the first principal component.

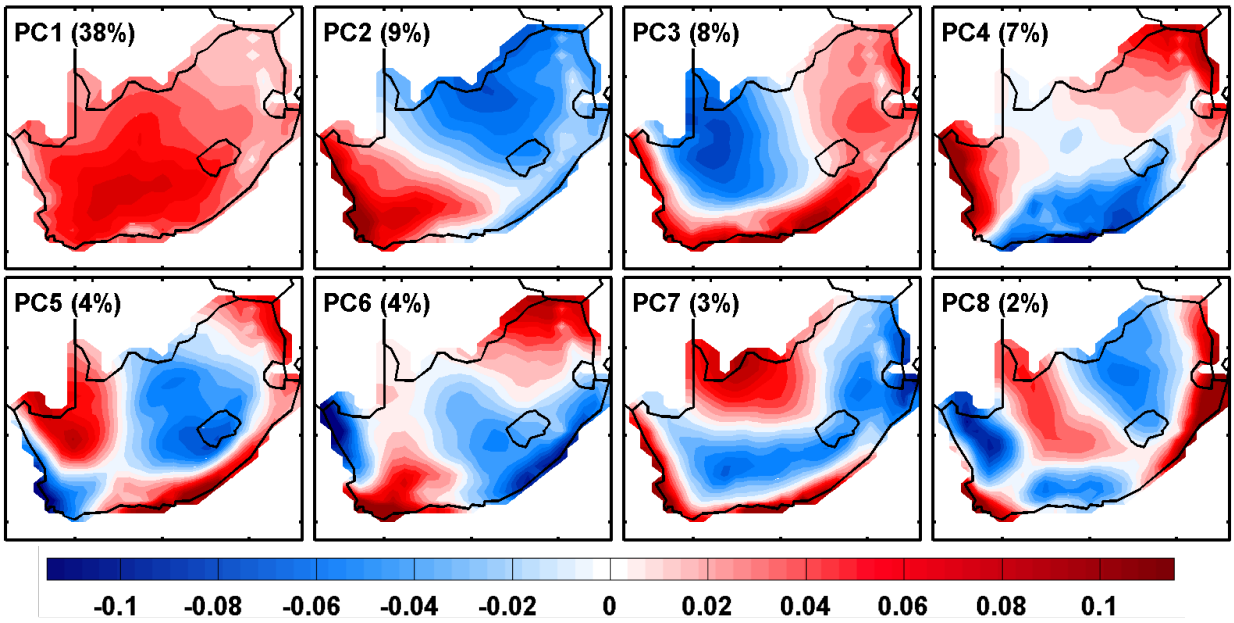

Figure 36: Geographic variation of eigenvalues from the first eight Principal Components performed on the onshore capacity factor in South Africa

Closing Remarks

Using the MERRA data, we have mapped and identified areas of high and low wind-resource potential. Based on this analysis, South Africa has moderate to high potential for wind power harvesting, especially in the west and south near the coast. Furthermore, we find that although South Africa's mean WPD is close to that of central Tanzania, wind resource in central Tanzania is more reliable. The conclusion was not obvious in the map of mean wind speed or mean WPD, but is shown clearly in other measures like median, availability, and wind-power episode lengths. In order to understand how South Africa's wind-power potential changes over various time scales, we plot the percentage of area with usable wind power based on a threshold of WPD. South Africa's potential varies over the year, with higher potential in the summer and lower potential in the winter. We also find that a larger area of South Africa has usable WPD during the day than at night. We conclude the study by presenting various measures to assess the value of interconnection, a common method suggested to reduce intermittency. Depending on the measure, different results are found. In the final measure, we show maps of dominating variances and the regions that are contributing, either positively or negatively, by use of a Principle Component Analysis.

CHAPTER 4

THE IMPACT OF CLIMATE CHANGE ON WIND AND SOLAR RESOURCES IN SOUTHERN AFRICA

Abstract: Climate change is an issue that requires global attention and cooperation. As climate science develops an understanding of changes to the future climate state, policymakers and engineering project planners beg to know what claims can be made on the subject with a reasonable level of confidence. A common and popular mitigation strategy for reducing emissions is to build away from carbon intensive electricity production to clean energy sources like the energy produced from wind and solar radiation. These sources themselves are climate dependent. In this study, we present a method to estimate the climate change impact on wind and solar resource potential which builds on previous studies that take a risk-based approach. The assessment combines climate projection output from the Integrated Global Systems Model (IGSM), which introduces emissions and climate sensitivity uncertainty, with 19 Global Circulation Models (GCMs) available from the Coupled Model Intercomparison Project phase 3 (CMIP-3). Southern Africa, specifically those in the Southern African Development Community (SADC), is used as a case study. We find little agreement between GCMs and emission scenarios, resulting in a median change close to zero by 2050 in the long-term mean of both wind speed and solar radiation (used as an indicator of change in electricity production potential). Although the extreme possibilities range from about -15% to +15% change, these are associated with low

probability. These projected results in the long-term mean wind and solar variables—and their associated probabilities—stay true to the limitations of state-of-the-art climate system models, and are apt to be useful for policy and engineering planning.

Introduction

As the threat of climate change builds, there is a push towards lower emissions. Ironically, the energy sources available without emissions are typically climate dependent, which is especially the case for wind and solar resource. As future climates begin to behave less like past climates, modeled projections of changes in the long-term future state are useful for national energy investment planning. Southern Africa provides an interesting case study for this analysis, specifically the Southern Africa Development Countries (SADC), which includes the Democratic Republic of Congo, Tanzania, and all countries south of these two. Energy demand in this region of the world is rising quickly, with an average of 6.5% per year in Mozambique and 9% per year in Angola, for example (SAPP 2012).

Of the countries in this region, South Africa has shown the most interest in wind and solar technology investment. There are currently 3 operational wind power plants in South Africa, all small-scale, although there are a few large-scale wind farms in planning. Sere Wind Farm, to be among the largest wind farms, is proposed to be built near the city of Vredendal in the Western Cape (Savannah Environmental 2007). There has also been interest in South Africa to build large-scale photovoltaic (PV) and concentrated solar power (CSP) to exploit its solar resource. Winkler et al (2007) found that CSP is the most affordable renewable energy option for decreasing emissions in South Africa. Although there are no existing large-scale CSP plants in

southern Africa, the South African electricity utility, Eskom, has recently invested in planning a 100 MW CSP plant in the Northern Cape near the city of Upington (Eskom 2012), and the South African government is promoting a 5,000 MW solar park in the Northern Cape (Zawilska et al. 2012).

The implications of possible changes in usable wind and solar potential must be well understood for future planning purposes. Some reports have noted that wind speed and cloudiness are likely to change in the future. Wind speed and cloudiness are strongly influenced by temperature differentials. Since climate change is generally characterized by changes in global temperature, one can easily make a connection between increasing emissions and these climate parameters, concluding that changes in temperature can directly affect surface wind speed and solar irradiation. These climate parameters are also influenced by physical phenomena like El Nino Southern Oscillation (ENSO) and Madden-Julian Oscillation (MJO), which could behave differently in the future (Rauthe et al 2004). Meehl et al. (2007) report that peak wind speeds will likely increase with increasing temperatures, and Hazeleger (2005) suggests that the trade winds in particular are likely to change. Land surface changes can affect local cloudiness and could be amplified in urban areas (Denman et al. 2007), but making connections between climate change and changes in solar radiation is a complicated matter (Hegerl et al. 2007). In fact, understanding the impacts of climate change on both aerosols in the atmosphere and boundary layer wind speed are problematic because of the spatial scale of current Global Circulation Models (GCMs). Studies have been done on understanding the impact of climate change on wind and solar parameters, but the subject is less studied than the impacts on biophysical sectors, e.g. agriculture.

Wind speed and solar irradiation in a Global Circulation Model

Here, we briefly address the usefulness of climate projections from GCMs. First, we must understand how wind and solar variables are understood in a GCM. Because wind is the movement of air in the atmosphere, important for tracking convective transfers of temperature and moisture, it is an essential process in the global climate system. Solar forcing is also essential, since it is the source of the majority of the energy. For these reasons, wind and solar are very common topics in climate science and much emphasis is placed on modeling these as accurately as possible. In a GCM, wind speed is modeled as an average over a large cuboid in space. The GCMs provide wind speed output at 10m, an estimation derived from the wind speed values of the atmospheric layer closest to the surface. Vertical layers in a GCM are typically defined by constant pressure, meaning that the layer heights change in space and time. These pressure layers are also unevenly distributed so that a finer resolution is achieved near the surface. In a typical GCM, the atmosphere is modeled with about 10 – 20 layers reaching to about 30km. GCMs also represent the climate at a coarse horizontal resolution of about 250 to 600 km (IPCC 2012). The problem with dividing the atmosphere into large cuboids is that many processes occur at a much smaller scale. These large cuboids are not ideal for modeling changes in small-scale wind, which is highly dependent on the effects of elevation, surface roughness, and convection. Clouds and other aerosols can also change at smaller scales than a typical GCM grid. Cloud feedbacks in particular are considered the highest uncertainty in current GCM practice (Randall et al. 2007). Cloud cover fraction output is usually estimated based on relative humidity values in each GCM cuboid. These estimations of small-scale processes on a larger scale are called “parameterization.” There are many parameterization schemes for estimating changes in wind speed and aerosols in

the various layers of the atmosphere, and the Coupled Model Intercomparison Project Phase 3 (CMIP-3) GCMs employ a variety of these schemes.

Previous attempts to characterize the future wind and solar state

In the past, climate change impact studies have typically involved one of two approaches: (i) a climate sensitivity analysis using a wide, unguided range of future climate possibilities (e.g. Kurukulasuriya 2006, Wilks 1992); or (ii) use of select climate model output, typically Global Circulation Models (GCMs) from the Coupled Model Intercomparison Project (CMIP), commonly referred to as the Intergovernmental Panel for Climate Change (IPCC) Fourth Assessment Report (AR4) models (e.g., Liu et. al 2013, Arndt et. al 2010, World Bank 2009, Immerzeel 2008). The output of these models is applied directly in a climate change impact-modeling framework to assess the impacts of climate change, resulting in a limited set of future scenarios. Research on the climate change impact on wind and solar resources follows a similar pattern, although recently there has been more activity in (ii) than (i). These studies are discussed below.

Pryor et al. (2006) attempted to estimate changes in the mean and upper percentile of wind speed in northern Europe. The authors used daily output from ten GCMs for the A2 scenario, fitting a regression model that predicts Weibull distribution parameters fitted from station data. The model was fit using mean and standard deviation of 500 hPa relative vorticity and mean of daily sea-level-reduced pressure gradients from the historical GCM runs. Then, using future outputs of the predictors, they were able to produce estimations for 10 possible futures of both the wind speed and wind power state, predicting the mean and 90^{th} percentile of each. They found that there was not much agreement between the GCMs, and no confident

conclusion could be made about changes in wind characteristics by 2050 for the wind stations used. Looking further in the future, their study suggests that mean and 90th percentile wind speeds will decrease slightly by 2100. Sailor et al. (2008) studied possible changes to wind speed and wind power produced over the northwestern United States. They used two GCMs and two Special Report on Emissions Scenarios (SRES) scenarios. They found that the historical results from the GCMs did not match weather station measurements in the area. Applying a statistical downscaling technique to the raw GCM output, they found, of course, that the agreement improved. They compared the two SRESs from each GCM and found that there wasn't much agreement, even though the same model was used. The study suggests that mean summertime winds will decrease by 5-10% in the area, and winter winds will either slightly increase or stay the same. Using typical hub heights and a common turbine power curve, they found that the power produced in the summer would decrease by about 40%. Pryor et al. (2012) used a suite of thirteen simulations from a combination of four Regional Climate Models (RCMs) nested in reanalysis data and four global climate models. These simulations were compared to independent observations and the North American Regional Reanalysis (NARR) over the contiguous United States. The RCMs were found to to reproduce historical wind patterns better than the GCMs, although the RCM architecture seems to be the primary cause of variance between models rather than the lateral boundary conditions. The study goes on to estimate changes in various wind statistics averaged over 2041-2060, finding some agreement between models in terms of sign. The simulations suggest that intense wind speeds are likely to decrease, especially in the western U.S. by 2050. Seljom et al. (2011) links 10 GCM-scenario pairs to an RCM to estimate climate change effects on the Norwegian energy sector. Changes in wind, solar irradiation, and heating

and cooling demand, among others, were estimated by interpolating the RCM results to 20 geographic locations: 7 for solar, and 13 for wind. The study found that while solar radiation and hydropower changes were significant in some of the GCM-scenario projections, changes in wind were minor, with the maximum change for all locations and months around 4.8% by 2050. Fenger et al. (2007) came to a similar conclusion of changes in wind over Norway. Pan et al. (2004) used a refined regional climate model to estimate seasonal changes in solar radiation simply by raising greenhouse gas concentrations in the regional model. A decreasing trend was found in the seasonal-mean of global solar radiation of about 0-20% over the entire United States. This trend was most noticeable in the western U.S. during fall, winter, and spring.

We have three main observations from the literature. First, there have been few studies that have looked at future changes in solar resource, likely due to the uncertainties in GCM cloud cover estimations discussed previously. Second, the studies that have estimated changes in wind speed have only found small long-term mean changes, the largest at 5-10%; although, Sailor et al. (2008) does claim that small reductions in wind speed could result in large reductions in power produced. And third, these studies did not find much agreement between historical observations and GCM output, between the different GCMs, or the SRES scenario outputs of a single GCM.

In general, research on the impacts of climate change has followed a similar pattern. The past climate state is studied briefly, and then information from climate models is applied. Next, climate change impact studies carefully apply a limited number of these scenarios to understand the future climate state. Since climate models are very computationally expensive, only a limited amount of scenarios can be effectively run to produce useful output, resulting in a scarcity of possible future scenarios. Schlosser et al. (2011) presents a method to expand the full set of

CMIP-3 GCMs to a large pool of climate predictions. The Integrated Global Systems Model (IGSM; Sokolov *et al.*, 2009 and Webster *et al*., 2011) developed near-surface temperature and precipitation projections at the zonal spatial scale for 400 scenarios representing economic and climate uncertainty. A Taylor expansion technique, described by Schlosser *et al*. (2011), was used to expand from the zonal level of detail in the longitudinal direction. This transformation requires the construction of climate-change pattern kernels, which vary through time as global temperature changes. The full ensemble of climate change projections is produced through the numerical hybridization of the IGSM zonal trends, with pattern kernels of regional climate change from 17 of the CMIP-3 models. This ensemble of future climate projections is called "hybrid frequency distributions" (HFDs). Using this framework, 6,800 climate projections are produced for each of the five CO_2 emissions policy scenarios. The HFDs, however, currently provide changes in precipitation and temperature, which are useful for biophysical impact modeling, but do not yet provide changes in other climate parameters. Also, the establishment of these HFD projections requires a selection among the SRES scenarios—namely, A2, A1b, and B1—because emission-forcing scenarios are already represented in the five policy scenarios. Fortunately, Schlosser *et* al. (2011) found strong correlations between the scenarios for precipitation and temperature, suggesting that the differences between model outputs are driven almost entirely by model choice, while SRES choice is insignificant.

Data and Method

First, a baseline needs to be established with which to compare the projected changes in climate. With the advancement of satellite utility and measurements, global datasets are

becoming more popular for areas with a limited or unreliable set of historical data. For this study, the MERRA (Modern-Era Retrospective for Research and Analysis) reanalysis dataset will be used to represent the base climate for all solar and wind characteristics (Rienecker et al. 2011). The MERRA dataset is attractive because it attempts to represent a balance between satellite, station, and modeled climate gridded globally at an hourly time-step from 1979 to 2009. MERRA improves on the representation of the hydrologic cycle and uses a large repository of conventional observations from various sources, as well as satellite radiance data. Figure 37 shows the mean wind speed over southern Africa, calculated using the log wind profile as described in Gunturu and Schlosser (2012). As shown, most of the onshore wind resource is in the southern and northeastern parts of the SADC region, with clusters of moderate wind speed in between. There is a large area of low wind speeds in the northwestern part of the map, comprised of the countries in the Congo River Basin and almost all of Angola. Figure 38 shows the mean incident solar radiation at the surface. Most of the solar resource is in the southwest, surrounding Namibia and extending out to Zimbabwe, and in the northeast in Tanzania and Kenya.

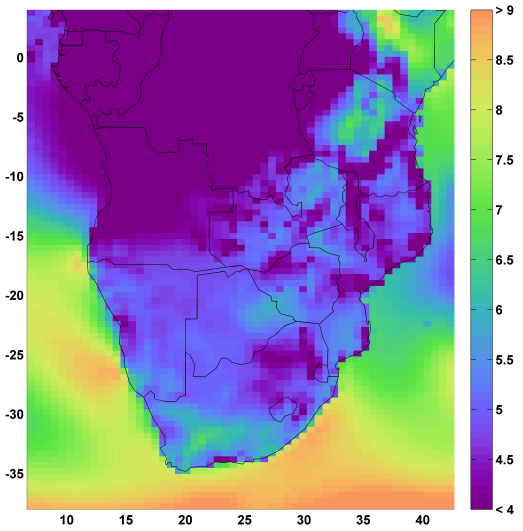

Figure 37: Geographic variation of mean wind speed (m/s) at 50m over southern Africa

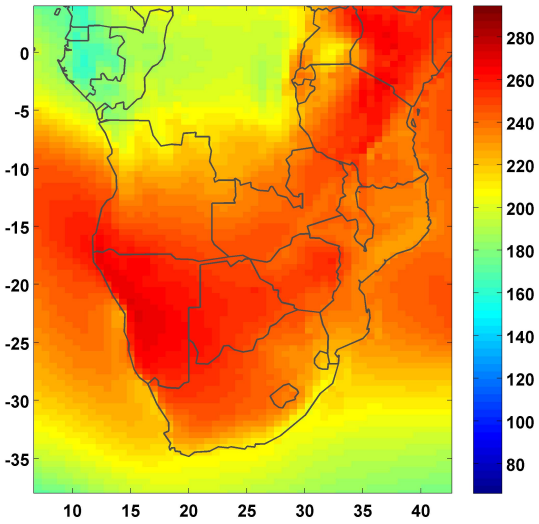

Figure 38: Geographic variation of mean incident solar radiation (W/m^2) over southern Africa

The seasonal mean wind speed and solar radiation at select grids are shown in Table 2. The grid selected for wind speed is meant to represent the proposed Sere wind farm, previously discussed. Similarly, the solar radiation values were calculated from the grid containing the site

of the proposed large CSP plant. As shown, the December-January-February (DJF) season has the potential for the most power produced, while the June-July-August (JJA) season has the least potential for both sources; although, the March-April-May (MAM) season has equally low potential for wind.

Table 2: Mean seasonal wind speed and incident solar radiation for selected wind and solar sites.

	Wind Speed (m/s)	Solar Radiation (W/m^2)
DJF	5.5	359
MAM	4.2	233
JJA	4.2	184
SON	5.1	315

Now, to understand changes in the future state of these resources, we explore the usefulness of a risk-based approach. Previous studies have used varying techniques to better understand the future state of wind and solar resource, using between 1 and 13 future scenarios. Given the recent advances in climate science provided through the HFD method, a larger pool of future scenarios can likely be generated, providing a more complete picture of the *risk* associated with climate change. Basically, a connection needs to be made between the methods presented in Schlosser et al. (2011) and changes in both wind and solar resource.

The first attempt to make these connections was to use the outputs provided by the HFD data—monthly changes in temperature and precipitation—and to relate these with wind speed changes. First, we needed to find a meaningful relationship between the predictors and the predictand in the historical data. We used the MERRA data for this investigation—monthly precipitation and temperature aggregated to the provincial level. Besides using the temperature

and precipitation data directly, we decided to use differences between onshore and offshore temperature. The final predictors were monthly temperature at the surface, precipitation, and onshore/offshore temperature gradients.

Since the intermittency of wind and solar resource is important to energy grid planning that might not be captured with mean only, we decided to count hours in each month within certain ranges of WPD, resulting in three power-potential measurements within a month. We also included mean and median WPD. In the end, we have five predictands: mean wind speed, median wind speed, hours of no power, hours of low power, and hours of high power. At first, we found that there was a fairly significant relationship between all of these predictands and at least one of the four predictors. Then, concerned that we might be finding a false relationship, we removed the seasonal mean from the predictors. After removing this mean, the predictors and predictands seem to have no significant relationship. This method was abandoned.

After finding that there is no significant relationship with the typical HFD output, we tried a new approach. A majority of the GCMs report both wind speed predictions at 10m and incident solar radiation at the surface. Using these outputs, we have related global temperature rises with the gridded wind speed and solar radiation changes for each of the GCM-SRES pairs where data are available from the CMIP-3 database. The seasonal mean was removed from each variable based on the mean of the first ten years. These differences from the mean are what we use for the model.

We first checked for a relationship by calculating a Spearman rank correlation coefficient between these two variables for four three-month periods. Figure 39 shows an example of a

global map displaying these correlation coefficients. We find that in the most extreme cases, the correlation is about 0.5 or -0.5. These values are fairly significant given that the predictor is a global parameter, and given that the findings from the previous studies, mentioned in the literature review, find only small, if any, changes to wind speed by 2050. A qualitative observation from these maps is that the correlation values appear to be showing a coherent global pattern, implying that the correlation is at least partly driven by a natural relationship.

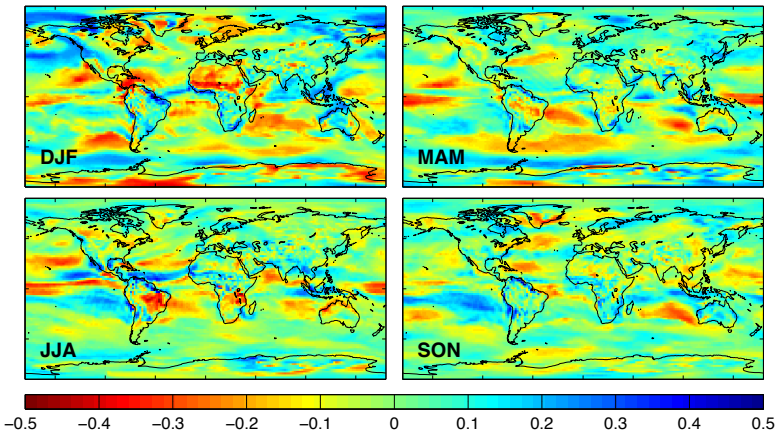

Figure 39: Correlation of wind speed cubed and global temperature rise for the CSIRO MK3.5 model running the A1b scenario for the four seasons. In the top left is the correlation with the Dec/Jan/Feb (DJF) season; in the top right is the Mar/Apr/May (MAM) season; in the bottom left is the Jun/Jul/Aug (JJA) season; and in the bottom right is the Sep/Oct/Nov (SON) season.

We then look at two locations in South Africa with characteristically different wind speed patterns. The first is near the border of the Western Cape and Northern Cape. The second location is located in the northern part of the Limpopo province. First, although the highest correlation values are close to +/-0.5, the correlations are fairly low for these two locations for the majority of the GCM-SRES pairs. The other concern is that there is not a strong agreement

between the SRESs for a given model, an important finding that drove the former HFD framework smoothly. If there was a strong agreement, we could assume that variance across model output is driven by differences in model structure. Instead, we find that the variance across model output must also be driven by the internal variability of the chaotic climate system that is modeled. This kind of uncertainty is difficult to quantify and has been left for future research.

We then move on to estimating changes in wind and solar resource potential. A locally weighted polynomial regression, as explained in Rajagopalan and Lall (1998), is used as the statistical model to represent the relationship of global mean temperature to changes in both wind speed and incident solar radiation, although other statistical models could be used. We then estimate the changes in wind speed and solar radiation based on global temperature changes produced from the 400 IGSM scenarios. Each of the CMIP-3 GCMs with wind speed output data are uniquely represented, which results in a maximum of 7,600 scenarios if the A1b scenario outputs are used. We use the CMIP-3 output data as an example because they are already well established, but the method could be applied to the CMIP-5 data. Also, since the model is set up to project changes from a modeled history, we bypass the issue of not matching the historical climate commonly found in previous studies.

Results

Results at Selected Sites

Due to the uncertainties of GCM output previously discussed, we restrict these results to projections in long-term mean seasonal changes in resource potential. Wind speed changes and

changes in solar radiation are predicted to 2050 for southern Africa by averaging results over 11 years, from 2045 to 2055. As an example, wind speed changes for the selected wind site are shown in Figure 40. Here, we present results for the Unconstrained Emissions (UE) and Level 2 Stabilization (L2S) IGSM policy cases coupled with the models derived from each SRES scenario output. As shown, the changes are relatively small, with modes close to zero and extremes from -1.5 to +1.5 m/s. In most seasons, the results tend to suggest an increase in wind speed, which would increase wind power potential; although, during the June-July-August season (JJA), there is a slight tendency toward wind speed decreases, especially in the extremes. This result is undesirable because JJA is the season with the lowest wind speeds according to the base data, and the season of highest energy demand in South Africa. Still, the results suggest that wind speed changes would be insignificant by 2050 at the selected wind site for all seasons, with a small chance of either a positive or negative change of about 20%.

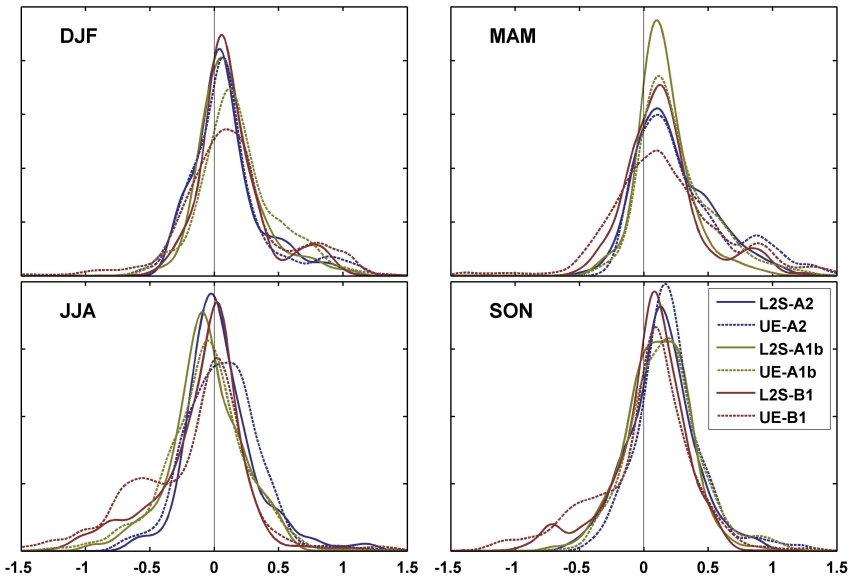

Figure 40: Density distributions of projected wind speed changes (m/s) for the selected wind site, four seasons, two policies (L2S and UE), and three SRES scenarios (A2, A1b, and B1)

Figure 41 shows the changes in solar radiation for the selected solar site. The mode for all four seasons is slightly negative in almost all scenarios, but the solar radiation changes for the selected site are likely small, if not zero. In the extreme results, changes range from about -20 to + 20 W/m^2, which equates to approximately 10% of the mean.

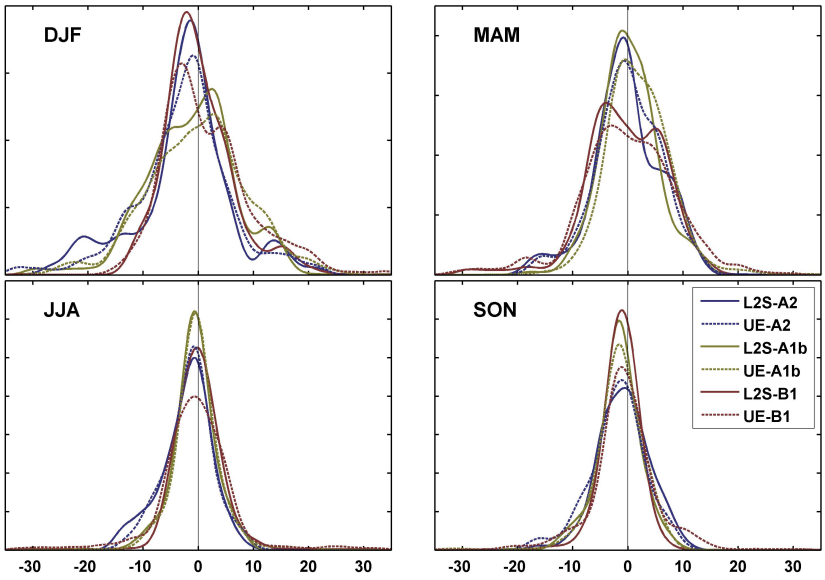

Figure 41: Density distributions of projected changes in surface solar radiation (W/m^2) for the selected CSP site, four seasons, two policies (L2S and UE), and three SRES scenarios (A2, A1b, and B1)

Notice that the results depend somewhat on the SRES scenario. This was not the case for the method used to produce precipitation and temperature change ensembles in Schlosser et al. (2011). In fact, in most cases, the differences between the results from the SRES scenario are about the same magnitude as the differences in IGSM policy cases, i.e., UE or L2S. The UE results tend to have a wider and shorter distribution than the L2S case, implying more likely extreme changes, but no obvious pattern was observed in the differences from the SRES scenario choice. Given that all of the models produce results for the A1b scenario—19 models total—and

only some produce results for the other two scenarios, the A1b model is selected for the remaining results. Also, of the three scenarios, A1b presents a medium emissions forcing case, while A2 and B1 represent the extremes.

Results over southern Africa

In the following maps, we shift focus to the JJA season because this is the season of high heat demand in South Africa. Figure 42 shows the geographic variation of changes in wind speed for the JJA season over southern Africa modeled from the A1b output. The 20th, 50th, and 80th percentiles are shown to represent the distribution of results over the 7,600 scenarios. The top row presents the L2S policy case, and the bottom row, the UE policy case. For the most part, wind speed changes are small in southern Africa. The most extreme wind speed changes occur in the ocean, where the median change ranges from about -0.5 m/s off the southern coast of South Africa to +0.4 m/s off the coast of Namibia to the west, and around the boarder of Mozambique and South Africa to the east. These same patterns emerge through all six maps. Inland, there is a cluster of increases in wind speed along the boarder of South Africa and Botswana that is especially prevalent in the UE 80th percentile. Further northwest, along the coast of the Democratic Republic of the Congo at the mouth of the Congo River and surrounding, is another area of projected increased wind speed. In general, although the differences in the results from the two policy cases are relatively small, the same pattern emerges—UE presents a wider range of possible wind speed changes, as shown in the 20th and 80th percentiles.

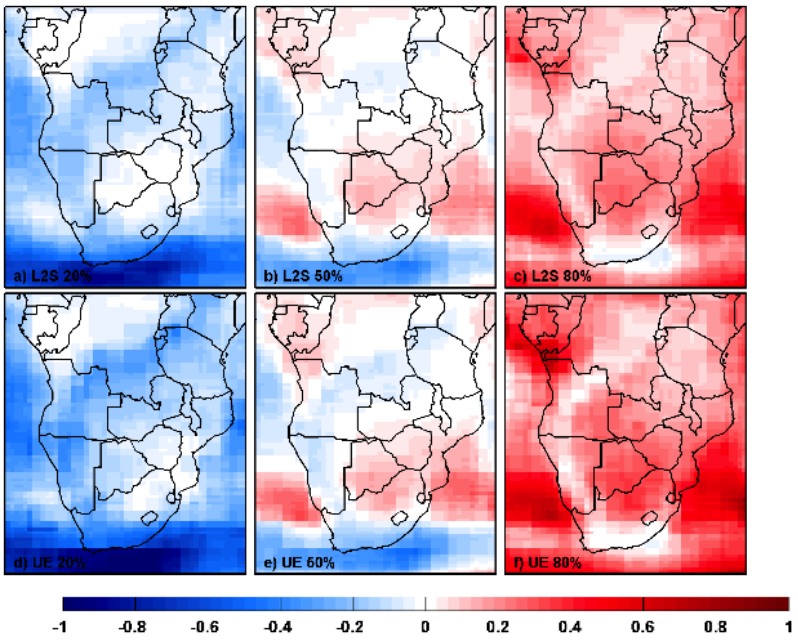

Figure 42: Geographic and scenario distribution of wind speed changes (m/s) for Jun-Jul-Aug (JJA) using the A1b model results for the statistical model. Subplots a, b, and c show the 20th, 50th, and 80th, percentiles, respectively, for the Level 2 Stabilization (L2S) policy case and d, e, and f show the same percentiles for the Unconstrained Emissions (UE) policy case.

Figure 43 shows the geographic variation of changes in solar radiation for the JJA season. This figure uses the same layout as Figure 42. Changes in solar radiation are small, even in the extremes. The median shows a decrease in solar radiation over most of the region, except an area around Malawi, west along the equator, and the southwestern tip of South Africa. The area with the strongest decrease extends from Kenya in the east and through Angola and Namibia in the west. These tendencies persist through the distribution, emerging in the 20th and 80th percentile maps. Also, we again see the extremes stronger in the UE policy case than the L2S policy case.

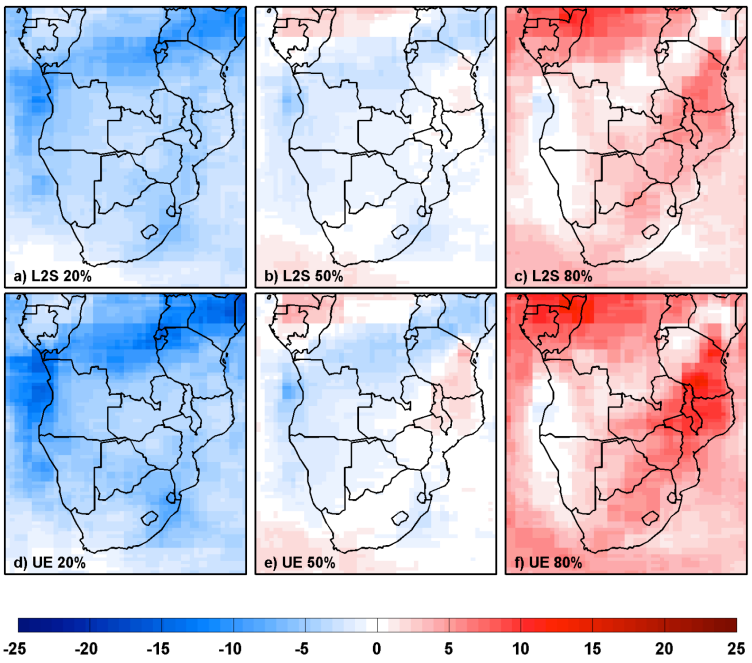

Figure 43: Geographic and scenario distribution of solar radiation (W/m^2) changes for Jun-Jul-Aug (JJA). Subplots a, b, and c show the 20^{th}, 50^{th}, and 80^{th}, percentiles, respectively, for the Level 2 Stabilization policy case and d, e, and f show the same percentiles for the Unconstrained Emissions policy case.

Although different geographic patterns emerge depending on the season modeled, changes in wind speed and solar radiation are relatively small for all seasons and regions of southern Africa. In looking at the annual mean change, some patterns do emerge. For wind, mean wind speeds are increasing offshore west of South Africa and Namibia and east of South Africa and Mozambique, but decreasing south of South Africa. These patterns persist in the extremes reaching a minimum of about -1.5 m/s, to a maximum of +1.5 m/s in the UE case, while the range for the L2S case reaches extremes of -1 m/s to +1 m/s. Onshore are smaller changes, with increasing wind clustering along the boarder of Botswana and South Africa extending to southern and central Mozambique. Decreases in wind speed extend to a larger

region—strongest in Kenya and Tanzania, but extending out to Angola, Namibia and western South Africa. The onshore changes range from about -1 m/s to +1m/s in the UE case, and -.4 m/s to +0.5 m/s in the L2S case. For annual mean changes in solar radiation, we see increases along most of the onshore area except near the coast. The areas of largest decrease in solar radiation are found along the western coast, especially near the border of Namibia and South Africa, and another area clustering around the Tanzania-Kenya-Uganda boarders. The extremes range from about -35 W/m^2 to +35 W/m^2 in the UE case, and about -18 W/m^2 to +12 W/m^2 in the L2S case.

Closing Remarks

As a response to previous studies that have tried to dissect GCM output from a select set of model results in order to understand the future state of wind and solar resource potential, we have shown a method that introduces emissions, climate sensitivity, and regional climate uncertainty. A statistical model was used to expand the HFD approach to include wind and solar parameter estimations, effectively producing a portfolio of possible outcomes. The results, even in the extremes, are consistent with previous studies, which found only small changes to wind and solar potential by 2050. We also found that the GCMs report a wide range of results. These differences in output exist across the models as well as across the emission scenarios, resulting in a central tendency close to zero change when combined. Since the emission uncertainty in the presented results exists in the different models produced from the three SRES scenario outputs as well as the IGSM scenarios, and a commonality was not found among the SRES scenario output as was found in Schosser et al. (2011), further research is required. Regardless, this study has found that either the long-term mean wind and solar resource potential will likely remain

unchanged by 2050, or that the uncertainty of the GCM models is much too large, even with state-of-the-art climate science, to make claims on the future state of these resources.

CHAPTER 5

CONCLUSIONS AND FUTURE RESEARCH

In the following chapter, I take the opportunity to discuss issues and inferences that could not be properly included in the previous chapters. In Section 1, I comment on the studies presented in the previous chapters by listing the key assumptions and limitations, as well as suggest future research. In Section 2, South Africa's options for reducing emissions are reassessed given the findings from the preceding Chapters. The prospect and current condition of regional trade and interconnection are discussed In Section 3. Section 4 presents the main areas of future research and way forward from the opinion of the author, and Section 5 presents the final conclusion.

Limitations and Key Assumptions

The following section lists the main limitations and key assumptions (i.e., what is studied and what is not) for the three studies presented in chapters 2-4. These lists are presented in a way that is meant to be concise and simple. After these lists, suggestions for future research are discussed for each study. Some of the suggestions involve relaxing or removing the key assumptions listed while other suggestions for future research involve looking into new areas.

The Impact of Climate Change on crops, irrigation demand, and hydropower in the Zambezi River Basin

In the first study, presented in Chapter 2, a suite of models is used to assess the vulnerability of the countries dependent on resources from the Zambezi River Basin to changes in climate. We find that the sectors most vulnerable to climate change are: hydropower in Zambia, irrigation in Zimbabwe and Mozambique, and flooding in Mozambique. The limitations and key assumptions from this study are as follows:

A-2.1. The study is dependent on accurately measured climate and streamflow data for the historical run as well as the future runs. For the climate data, we use observational-reanalysis data that is dependent on climate modeling, satellite measurements, as well as ground measurements. For streamflow data, we use recorded, usually hand-written data collected from various agencies and compiled in a World Bank study. While we believe these are the best available, they are subject to error.

A-2.2. The historical climate data is set to 0.5 by 0.5 degrees for monthly data and 1 by 1 degree for the daily pattern. Although we are consistent in the resolution of all subsequent modeling (e.g., lumped rainfall runoff model with large basin sizes) and result presentation (i.e., presenting impact results on a national scale), the coarseness of the historical data limits the accuracy of the results and the amount of detail considered in the modeling.

A-2.3. The future climate data is also coarse. The GCMs generally have a resolution of about 2 to 4 degrees in the latitudinal and longitudinal directions. The IGSM, which is used along with the GCMs to produce the HFDs, is 2 degrees in the latitudinal direction with no

longitudinal detail. Again, we are consistent in the presentation but this coarseness does limit the accuracy of the results.

A-2.4. In the flooding impacts analysis, we use a 40-year monthly timeseries of runoff values to fit an extreme value distribution. We then estimate return periods for the historical and future scenarios, comparing all future scenarios with the base scenario. This technique is simple, and we believe we are arriving at a reasonable conclusion, but further analysis is needed to be sure that damaging floods will increase in the future, assessing shorter time scales—hourly, daily, weekly—and considering more detailed topography and soil information. We could also look into more detail on the seasonal changes in flood events, as that would affect the agricultural specific damages, as well as other economic activities that vary with season.

A-2.5. For the water resource modeling, we use the hydropower build-out plan to 2030 including hydropower demands. These are static, not considering changes in power demand or the effects of reservoir filling.

A-2.6. We assume a static irrigated area, set to current conditions. Future irrigation infrastructure could change the stressed regions as well as hydropower production.

A-2.7. We do not consider feedback from the economy—namely, changes in food prices, energy prices, or infrastructure damaged by floods. Although these are handled by subsequent economic modeling, incremental feedback from the economy could affect investments in the hydropower and agriculture sectors in the region, in turn affecting the management of these water resources.

With a study like this one, in which the main goal is to identify sectors and regions where more detailed, project-scale studies should be directed, the list of future research suggestions is naturally quite long. Each sector study in this project could use a closer look. In general, a more extensive study of mitigation options for all sectors would be beneficial. More specifically, a more detailed study on both historical and projected flooding risk in this region could be addressed in a future research project that takes into account detailed topography and hydrology. A study like this would be difficult because of the limited data available, but is a risk worth the effort given the vulnerability of the infrastructure and people, as well as the climate and landscape. Also, we could use the modeling framework built in this study to analyze various future scenarios involving irrigated areas (A-2.6) or different hydropower build-out plans (A-2.5). In addition, as mentioned in A-2.7, building an input/output framework where the biophysical models (i.e. the models used in this study) exchange information to and from the economic models at intermediate time-scales would allow more realistic management adjustments in these sectors, especially between the water resources model, WEAP, and the economic models. Another aspect to consider is the value of cooperation between these countries, where the models could represent different levels of information exchange on food, water, and energy management reaching various levels of benefit for these economies.

Characterizing Wind Power Intermittency and Reliability in Southern Africa

In the second study, presented in Chapter 3, we use hourly reanalysis data to characterize wind power intermittency and assess the value of interconnection in southern Africa. We find that wind potential is high in Kenya, central Tanzania, and southern South Africa. With a closer look, we find that wind power resource in South Africa is unreliable (i.e., intermittent) and is

weak when power demand is highest on all relevant time-scales. The limitations and key assumptions from this study are as follows:

A-4.1. We use the MERRA data as a representation of historical hourly wind speeds, which are a combination of model, satellite, and ground measurements. This study is dependent on the accuracy, quality assurance, and compilation of these measurements by the MERRA team.

A-4.2. The spatial resolution of this data is set to 1/2 degree in the latitudinal direction and 2/3 degree in the longitudinal direction. The effects of local topography are not captured well in data at such a coarse resolution.

A-4.3. There are various spatial elements that are not considered in this analysis. These include distance to major power lines, protected areas, urban areas, ground slope, etc. These realistic limitations would impact areas that are ideal or not ideal for building wind farms.

A-4.4. Although we do consider turbines at different hub heights, we do not consider rotor diameters, turbine spacing, the variability between turbine models, etc.

A-4.5. We also do not consider wind direction. Wind turbines are large and require time and energy to turn if the wind changes direction often or too quickly.

A-4.6. We use a wind power density threshold of 200 W/m^2 for a large portion of the study to determine if the hour and location is producing power or not producing power. Although we did try most of the calculations using a threshold of 140 W/m^2, and did not see much of a change in the results, much of these calculations are dependent on the threshold value selected.

Future research suggestions for this study are extensive. For a better understanding of the variance in the wind, and for the sake of forecasting, we could investigate the effects of major physical phenomena like the El Nino Southern Oscillation, which has been shown to have effect on precipitation in the area on an inter-annual timescale, or the Maden-Julien Oscillation, which affects small time-scale intermittency patterns—on the order of days and months—of wind speed across the globe. Another area for future research would be the inclusion of differences in turbine technology, including the effects of turbine spacing, turbine models (A-4.5), and wind direction (A-4.5). Of course, we could also introduce solar power into this intermittency study, either by assessing solar power intermittency and/or the value of connecting solar parks to wind farms in various locations in southern Africa.

The Climate Change Impact on Wind and Solar Power in Southern Africa

In the third study, presented in Chapter 4, we develop a risk profile for changes in the long-term mean of wind and solar power sources. To do this, we use a statistical relationship between global mean temperature and each local gridded wind speed and solar radiation from the GCMs. We find that only small changes in wind speed and solar radiation are predicted in the median of the distributions projected to 2050. And at the extremes of the distribution, relatively significant changes are predicted in some parts of southern Africa, and are associated with low probability.

A-4.1. Again, we are dependent on future climate scenarios modeled by GCMs with coarse grid cells. We are also somewhat dependent on the 2-dimensional IGSM, which provides the risk information via global temperature changes. These are both subject to the errors in projecting future climates.

A-4.2. In the statistical model, we assume that any consistent change in either wind speed or solar radiation that correlates with changes in global temperature is a result of climate change. This assumption might not always be the case, meaning that the changes in solar radiation or wind speed could be caused by another phenomenon unrelated to climate change but, by chance, be correlated to global temperature changes.

A-4.3. We focus the study on changes in long-term mean potential because GCMs are better at projecting changes on larger time-scales. Changes in wind and solar intermittency (i.e. shorter time scales) could be significant.

A-4.4. This study projects changes in wind and solar climate parameters. Although these are the drivers of power production for these technologies, they are not perfectly correlated with energy output. Wind resource is also affected by air density and solar resource is affected by many climate parameters such as humidity, wind speed, dew point, and surface pressure.

There are many avenues where this research could be continued. GCMs tend to be better at projecting climate parameters like temperature and pressure. Since wind speed and cloud movement are influenced by pressure and temperature differentials, we might be able to represent future changes in wind and solar resource potential more accurately if we run these parameters through the statistical model instead of wind speed and solar radiation (addressing A-4.1). Using a framework like this, we could also predict changes in the reliability by modeling changes in the occurrence of low and high wind speed, e.g. 10^{th} and 90^{th} percentiles, respectively, based on the MERRA data or station data, which would address A-4.3. Additionally, we could take the study a step further by predicting changes in a distribution, like the Weibull, and run the

distribution through a power output model, directly simulating changes in power produced, addressing A-4.4.

South Africa's options for reducing emissions

As mentioned before, South Africa dominates the SAPP in terms of consumption and production, with about 80% of consumption and 81% of production. Future demands are expected to increase significantly in the future, about 38% across the entire SAPP from 2013 to 2025 (3.2% / annum on average, based on projections from SAPP [2012]). On top of this, South Africa plans to reduce emissions significantly. If South Africa is to reach its ambitious emissions reduction targets, the country has three main strategy options—assuming no significant flexibility on the demand side—which can be implemented at varying degrees: (a) remodel existing thermal plants or build new plants that are more efficient and release less emissions; (b) build wind and/or solar power in South Africa, among other renewable options; or (c) rely on imported renewable energy, likely hydropower from the Zambezi and Congo basins. Option (a) is already happening to a certain degree in South Africa, but is a long and expensive process and is not likely to meet the emission reduction targets without the help of options (b) and/or (c).

The viability of option (b) is as follows. Estimations of wind potential in South Africa have varied from 7.9 TWh (Diab 1985) to 106 TWh (Banks and Shaffer 2006, 2007). Note that the more recent studies estimate higher wind power potential than the older studies. This pattern of increased estimates persisted from 1985 to 2007. The most detailed estimate comes from Hagemann (2008), who estimated South Africa's generation potential to be: 80.54 TWh with a realistic estimation, 157.18 with an optimistic estimation, and 20.06 TWh with a pessimistic

estimation. Of course, these estimates are made by modeling the historical state of wind and do not consider climate change. Given the results found in Chapter 4 of this dissertation, wind power potential could decrease in the future in South Africa. Solar potential is estimated to be much higher than wind potential in South Africa, although there are fewer estimates in the literature. The most recent estimate found is included in Fluri (2009), who estimates CSP potential to be 547.6 GW, producing about 1,861 TWh annually. The majority of this potential is in the Northern Cape, with an estimated potential of 510.3 GW. An assessment of PV potential in South Africa was not found, but presumably would be on par with CSP potential. Additionally, considering the results found in Chapter 4 of this dissertation, solar potential is not likely to change in the regions with especially high potential currently. Basically, the limiting factors for wind and solar are not the number of sites with potential but the costs of the infrastructure and transmission, as well as dealing with power supply intermittency.

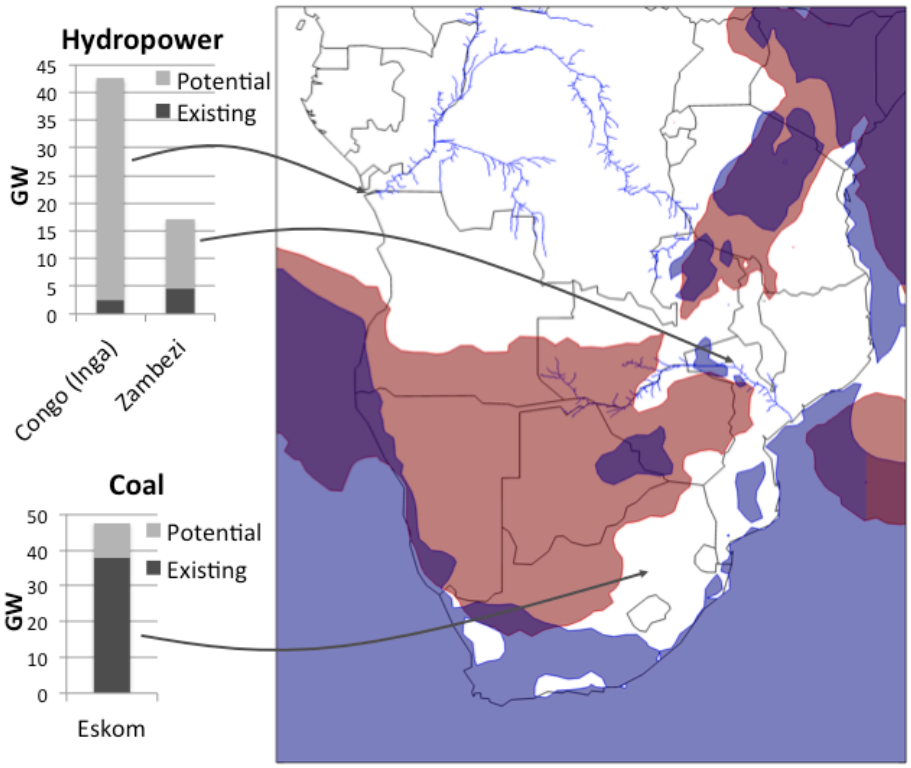

Figure 44: Map of the major sources of potential and existing power. The wind potential is the area in blue and the solar potential is the area in red. The hydropower potential is only based on large hydropower projects and the coal existing and potential capacity is based on South Africa only, where the potential includes the two large plants that are predicted to come online in 2015 and 2018.

We now take a closer look at the third option for reducing emissions, option (c). Figure 44 shows a map of the existing and potential primary sources of power in the SAPP. The area with wind power potential, shown as blue, is based on wind power density at 80m, using a median of 100 W/m^2 as the threshold. Solar power potential, shown in red, shows the areas with at least a median of 500 W/m^2 of total solar radiation. Both wind and solar data is from the MERRA, discussed in Chapter 3 of this dissertation. Hydropower potential and existing capacity is based on the largest 11 sites in the region (data from ECA [2009]). Existing and potential coal power capacity is shown for comparison purposes and is based on South Africa (i.e., Eskom)

only. The potential coal capacity is based on two large plants that will be built in South Africa by 2015 and 2018, respectively.

Solar potential exists mostly in Namibia and Botswana, with some potential in northwest South Africa, Zimbabwe, and western Zambia, as well as in the northeast of the map, around Tanzania and Kenya. Wind potential exists mostly in the southwestern part of South Africa, central Tanzania, and along the coast of Namibia. Considerable hydropower potential exists in the Zambezi and Congo basins and the majority of the planned future projects in the SAPP, about 80%, are hydropower projects (ICA 2011). Of the 11 major hydropower sites considered in Figure 44, 10 are along the Zambezi. Three of these sites have hydropower plants on them. The only hydropower site considered in the Congo is the Inga. Although this one site would provide a cheap source of renewable energy for many years (in terms of $ / GWh produced), other complications arise. First, the up-front cost is significant for the hydropower plant and the transmission. Second, planning the transmission will include difficult and possibly politically sensitive decisions, like which countries will be connected and who pays for the connections. Third, if South Africa is to be connected to the Inga, Eskom would need to agree to be dependent on a power source in the DRC. More on this prospect is discussed in the following section.

For the most part, these renewable sources in southern Africa rarely overlap. There is significant hydropower potential in the Congo basin but no potential for wind or solar. The same could be said for Mozambique. There is wind potential in southern South Africa, solar potential in the northwest, but limited hydropower potential. There are a few exceptions where these sources do overlap, most notably the potential for solar and wind power in central Tanzania and Kenya. Nonetheless, with a push towards renewable energy, and the known value of

interconnecting different-source sites to mitigate intermittency, there could be a growing need for power trade in this region.

Interconnection and Power Trade in the SAPP

In this section, the benefits, difficulties, and obstacles of power trade in the SAPP are discussed, as well as the value of interconnection on a large scale. The power trade discussed here is between power utilities. Other than Mozambique, with two power utilities, there is only one power utility per nation in the SAPP. Net imports and exports for each country are shown in Table 3. Power generation for each country is also shown for reference. Many of these countries are importing power from South Africa. In fact, Botswana, Namibia, and Swaziland import the majority of their power from South Africa. The only other country in the SAPP that exports more than it imports, besides South Africa, is the DRC (although the most recent SAPP report, as shown in Table 3, reports that Mozambique exports more than it imports and generates. Earlier studies mention that Mozambique imports more than it exports [Rosnes and Vennemo 2008; ECA 2009; ICA 2011; SAPP 2009, 2010, 2011]). Regional trade has proven to be significantly beneficial in more developed regions, such as Europe and within the USA. SAPP has already seen some of the benefits of regional trade. Spinning reserve requirements for most countries has reduced from about 20% to 15% of peak demand from 2007 to 2009 due to power trades (ECA 2009).

Currently, one of the most important issues limiting regional power trade in this area is transmission. The area with the largest congestion is the interconnection between Zambia, Zimbabwe, Botswana, and Namibia (ZIZABONA). Many of the projects underway currently in

the SAPP are transmission projects. The largest of these are the ZIZABONA project and a project to connect Tanzania to the SAPP grid. These projects are expected to cost $240 million and $330 US dollars, respectively (ICA 2011). Transmission, of course, also results in transmission losses, and increasing regional trade would result in more energy losses. Of course, power trade will likely be valuable despite these losses. Average transmission losses in the SAPP are about 6.4%, with large variations between countries, as shown in Table 3. Another concern with transmission is the possibility of the disconnection of a major transmission line. The region is prone to major floods that could take out a transmission line. Also, rebel groups in the past have destroyed major transmission as an act of war (e.g., the transmission lines of Cahora Bassa were sabotaged during the Mozambique Civil War). At extra cost, redundancies can be installed in the system that can be used in the case that transmission is disconnected. Another possibility is to build underground or underwater transmission lines, although either option would also entail extra cost as well as increased transmission losses.

Table 3: Generation, Imports, and Exports in 2011/12 (SAPP 2012)

	Generation (GWh)	Imports (GWh)	Exports (GWh)	Transmission Losses (%)
Angola	5,613	36	0	10
Botswana	372	3,180	0	3.7
DRC	7,021	440	171	10
Lesotho	486	49	7	11
Malawi	1,809	-	19	9
Mozambique	390	93	669	6.4
Namibia	1,305	2,462	294	3.2
South Africa	237,430	10,190	13,296	3.3
Swaziland	288	909	0	6
Tanzania	3,034	2,192	0	6.1
Zambia	11,381	43	66	4.6
Zimbabwe	6,951	1,531	1,025	4

Another concern in the region is cooperation among the SAPP members. Most of these countries have a long history of internal and external conflict. At present, many of these nations have weak administrations, high-risk profiles, and poor security arrangements. In spite of this, electricity trading has been rarely interrupted. The only significant interruption was the sabotage of the Cahora Bassa link to South Africa that interrupted supply for 17 years (ECA 2009). While this incident stands alone, it acts as a reminder of the security risks in the area and reinforces self-sufficiency. For example, connecting to the Mmamabula coal-fired power station in Botswana—a closer, well-managed economy—might be more attractive for South Africa than connecting to the Inga in DRC, with decades of war and instability. The Inga is about 2,800 km (about 1,700 miles) away from Johannesburg, while Cahora Basa, on the Zambezi, is about 1,300 km (about 800 miles) away.

With renewable energy as a focus of new capacity in the region, primarily hydropower, power trade might become even more valuable. We have already discussed the value of interconnecting wind farms to mitigate intermittency. Similarly, renewable energy of different sources can be interconnected. For example, in some areas, wind power generation tends to be stronger at night, while solar resource, of course, is only available during the day. Although hydropower reservoirs usually have some storage to allow flexibility of power generation, other demands for water and seasonal fluctuations in runoff interfere with power flexibility. For these reasons, interconnection and power trade in the region could offset some of these timing issues. And, as already discussed, there is little overlap between different types of renewable resources in the area. Nonetheless, power trade of this kind would need to be responsive on short time

scales and would require extensive planning and practice. Also, the findings in Chapter 3 of this dissertation, where we find that wind power in South Africa is strongest in the summer, combined with the fact that the rainy season in the Zambezi occurs in the summer, and that demand is highest in the winter, are all discouraging for the prospect of interconnection. Still, this is certainly an area for future research.

Future Research

To accompany the discussion in Section 1 of this Chapter, where future research of the individual studies is discussed, this section lists the main areas of research for the issues that this dissertation begins to address.

- Intermittency is discussed in this dissertation mostly by identifying and classifying the issue. Although we present one solution to mitigate intermittency, by interconnection, there are many other suggested solutions in the literature, such as: energy storage (or batteries) of all kinds, management options of dealing with intermittency on the supply side, like aluminum smelters or other flexible demand on the industry side, or better weather forecasting. These would all be areas of future research.
- We considered how climate change would affect hydropower in the Zambezi, and wind and solar in southern Africa, but have not yet considered how climate change would affect conventional sources (e.g., changes in water availability for cooling) or electricity demand (e.g., household heating/cooling demands, or industrial demands).

- A study of how the three renewable sources—wind, solar, and hydropower—could be interconnected to reduce intermittency would be of paramount importance. This would be especially useful for impacting the hydropower plants in planning, as it may be the case that more turbines per dam or larger reservoir storage would be valuable to allow for a more control of generation.
- Renewable energy, like wind and solar, is often in remote areas. How would this affect transmission costs and how might this be valuable for connecting remote areas to the grid?

Conclusion

With electricity demands rising quickly in southern Africa, determining the best viable options for the future infrastructure investment plan is vital for economic growth and stability. Renewable energy is a viable option for meeting future energy demands in this region. The contribution of this dissertation is an analysis of the future reliability of these energy sources, considering climate variability as well as the long-term trends caused by climate change—namely, hydropower in the Zambezi basin, characterization of wind resource intermittency, and the future state of wind and solar resources. Although the research and findings in presented here are a step forward, there is still much to learn about the power sector in southern Africa. Most of the issues facing the SAPP are not of an engineering nature, but rely on socio-economic and political circumstances. For example, some of these issues are related to questions such as: *What are the benefits of regional trade in power, and who are the main beneficiaries? How important is a stringent master plan of these renewable energy investments in southern Africa? Is a master plan, presumably administered by the SAPP, worth the costs, difficulties, or risk of failure from a*

political point of view? The need for simple yet comprehensive modeling to address the issues presented in this dissertation, as well as effective communication, is important for the many nontechnical policy-makers.

References

Adrian, G (1995) On similarity laws in regional climatology. *Archiv für Meteorologie, Geophysik und Bioklimatologie Serie A*, 55(3-4), 223–234

Adrian, G, and Fiedler, F (1991) Simulation of Unstationary Wind and Temperature Fields Over Complex Terrain and Comparison with Observations. Beitraege zur Physik der Atmosphaere, 64:27-48

Allen R, Pereira L, Raes D (1998) Crop evapotranspiration-guidelines for computing crop water requirements-FAO irrigation and drainage, Paper 56. FAO

Alton, Theresa, Arndt, Channing, Davies, Rob, Hartley, Faaiqa, Makrelov, Konstantin, Thurlow, James, Ubogu, Dumebi (2012) The Economic Implications of Introducing Carbon Taxes in South Africa, UNU-WIDER Working Paper No. 2012/46

Arndt C, Strzepeck K, Tarp F, Thurlow J, Fant C, and Wright L (2010) Adapting to climate change: an integrated biophysical and economic assessment for Mozambique. Sustain Sci, vol. 6, no. 1, pp. 7–20

Arndt C, Fant C, Robinson S, Strzepek K (2012) Informed selection of future climates. UNU-WIDER Working Paper No. 2012/60

Banks, D and Schaffler, J (2007) A Proposed Renewable Energy Plan of Action for the Western Cape. Technical report, Western Cape Department of Environmental Affairs and Development Planning

Beck L, Bernauer T (2010) Water Scenarios for the Zambezi River Basin, 2000 – 2050. ETH Zurich, Report from the Center for Comparative and International Studies, Zurich, Switzerland

Beilfuss R, Santos Dos D (2001) Patterns of hydrological change in the Zambezi Delta, Mozambique. Program for the Sustainable Management of Cahora Bassa Dam and the Lower Zambezi Valley. <http://files.gorongosa.net/filestore/348-patterns_hydrological _change_zambezi_delta.pdf>

Cavallo, AJ, Hock, SM, Smith, DR (1993) Wind energy: resources, systems, and regional strategies, in: Johansson, T. B.; Kelly, H., Reddy A.K.N., Williams R.H.: Renewable energy - Sources for fuel and electricity, Island Press

DEA (Department of Energy, Republic of South Africa) (2011) South Africa's Second National Communication under the United Nations Framework Convention on Climate Change. Department of Environmental Affairs, Republic of South Africa, Pretoria

Denman, KL, G Brasseur, A Chidthaisong, P Ciais, PM Cox, RE Dickinson, D Hauglustaine, C Heinze, E Holland, D Jacob, U Lohmann, S Ramachandran, PL da Silva Dias, SC Wofsy and X Zhang, (2007) Couplings Between Changes in the Climate System and Biogeochemistry In: *Climate Change 2007: The Physical Science Basis. Contribution of Working Group I to the Fourth Assessment Report of the Intergovernmental Panel on Climate Change* [Solomon, S,

D Qin, M Manning, Z Chen, M Marquis, KB Averyt, MTignor and HL Miller (eds)] Cambridge University Press, Cambridge, United Kingdom and New York, NY, USA

Diab, R (1985) Contributions of Wind Power to South Africa's Energy Needs South Africa Journal of Science, 81:460 463

Diab R (1995) Wind Atlas of South Africa. Department of Minerals and Energy, Pretoria

DOE (Department of Energy) (2011) Integrated Resource Plan for Electricity: 2010- 2030 (Revision 2 Final Report). Pretoria: Republic of South Africa

ECA (Economic Consulting Associates) (2009) The Potential of Regional Power Sector Integration: South African Power Pool (SAPP) Transmission & Trading Case Study. Report submitted to ESMAP

Elliott, D L, C G Holladay, W R Barchet, H P Foote and W F Sandusky (1987) Wind Energy Resource Atlas of the United States. *NASA STI/Recon Technical Report N*, 87: 24819

Elliott, D L, L L Wendell and G L Gower, (1991) An Assessment of the Available Windy Land Area and Wind Energy Potential in the Contiguous United States. Pacific Northwest Lab., Richland, WA (United States), August

Eskin, N, H Artar and S Tolun, (2008) Wind Energy Potential of Go˙kc ¸ada Island in Turkey. *Renewable and Sustainable Energy Reviews*, 12(3): 839–851

Eskom (2012) <http://www.eskom.co.za> [accessed October 2012]

Fant C, Gueneau A, Strzepek K, Awadalla S, Farmer W, Blanc E, Schlosser CA (2012) CliCrop: A crop water-stress and irrigation demand model for an integrated global assessment modeling approach. Joint Program on the Science and Policy of Global Change, Report 214. MIT. http://globalchange.mit.edu/research/publications/2264

FAO (2011) Food and Agriculture Organization profile of the Zambezi basin. <http://www.fao.org/docrep/w4347e/w4347e0o.htm> accessed 10 May 2011

Farmer W, Strzepek K, Schlosser CA, Droogers P, Gao X (2011) DSpace@MIT : A method for calculating reference evapotranspiration on daily time scales. MIT Joint Program on the Science and Policy of Global Change. MIT

Fenger, J, (2007) Impacts of Climate Change on Renewable Energy Sources: Their Role in the Nordic Energy System: A Comprehensive Report Resulting from a Nordic Energy Research Project. Nordisk Ministerrad (København)

Fluri, TP, (2009) The Potential of Concentrating Solar Power in South Africa. Energy Policy 2009;37: 5075-5080

Gunturu, U B & Schlosser, C A (2012) Characterization of wind power resource in the United States. Atmospheric Chemistry and Physics Discussions

Gunturu, Udaya Bhaskar, and Schlosser, C Adam, (2011) "Characterization of Wind Power Resource in the United States and its Intermittency." *MIT Joint Program on the Science and Policy of Global Change*, Cambridge, 24(14), 3624–3648

Gupta V, Sorooshian S (1983) Uniqueness and observability of conceptual rainfall-runoff model parameters: the percolation process examined. Water Resour. Res., 19(1):269-276 doi:10.1029/WR019i001p00269

Gupta V, Sorooshian S (1985) The relationship between data and the precision of parameter estimates of hydrologic models. J Hydrol 81:57–77

Gustavson, M R (1979) Limits to Wind Power Utilization. *Science*, 204(4388): 13

Hagemann, K (2003) Validation of Mesoscale Modeling Data for Wind Resource Assessments. BSc Honours Thesis. Department of Environmental and Geographical Science, University of Cape Town

Hagemann, K (2008) Mesoscale Wind Atlas of South Africa. PhD dissertation, University of Cape Town

Hargreaves G, Allen R (2003) History and evaluation of Hargreaves evapotranspiration equation. J Irrig Drain E-Asce 129:53–63

Hazeleger, W (2005) Can global warming affect tropical ocean heat transport? *Geophys. Res. Lett.*, **32**, L22701, doi:10.1029/2005GL023450

He, Y, A H Monahan, C G Jones, A Dai, S Biner, D Caya and K Winger, 2010: Probability Distributions of Land Surface Wind Speeds over North America. *Journal of Geophysical Research*, 115(D4): D04103

Hegerl, GC, F W Zwiers, P Braconnot, NP Gillett, Y Luo, JA Marengo Orsini, N Nicholls, JE Penner and PA Stott, (2007) Under- standing and Attributing Climate Change. In: *Climate Change 2007: The Physical Science Basis. Contribution of Working Group I to the Fourth Assessment Report of the Intergovernmental Panel on Climate Change* [Solomon, S, D Qin, M Manning, Z Chen, M Marquis, KB Averyt, M Tignor and HL Miller (eds.)]. Cambridge University Press, Cambridge, United Kingdom and New York, NY, USA

ICA (International Consortium for Africa) (2011) Regional Power Status in African Power Pools. Report

Immerzeel W (2008) Historical trends and future predictions of climate variability in the Brahmaputra basin. International Journal of Climatology, vol. 28, no. 2, pp. 243–254

Intpow (Norwegian Renewable Energy Partners) (2010) World Hydro Potential and Development. available online <http://www.intpow.com/index.php?id=487&download=1> accessed June 2013

IPCC (Intergovernmental Panel on Climate Change) Data Distribution Centre (2012). <http://www.ipcc-data.org> [accessed September 2012]

Jaramillo, O A and M A Borja, (2004) Wind Speed Analysis in La Ventosa, Mexico: A Bimodal Probability Distribution Case. *Renewable Energy*, 29(10): 1613–1630

Kaczmarek Z, (1993) Water balance model for climate impact analysis. ACTA Geophysica Polonica 41(4):1-16

Kashaigili J, McCartney M, Mahoo H (2006) Modeling the hydrology of the Usangu Plains Wetlands for environmental management, IWMI Research Report 104. Water Management

Kurukulasuriya P, Mendelsohn R, Hassan R, Benhin J, Deressa T, Diop M, Eid HM, Fosu KY, Gbetibouo G, Jain S, Mahamadou A, Mano R, Kabubo-Mariara J, El-Marsafawy S, Molua E, Ouda S, Ouedraogo M, Sene I, Maddison D, Seo SN, Dinar A (2006) Will African Agriculture Survive Climate Change?. The World Bank Economic Review, vol. 20, no. 3, pp. 367–388

Landberg, L, Myllerup, L, Rathmann, O, Petersen, E L, J rgensen, B H, Badger, J, and Mortensen, N G (2003) "Wind Resource Estimation?An Overview." *Wind Energy*, 6(3), 261–271

Liu JJ, Folberth CC, Yang HH, Röckström JJ, Abbaspour KK, Zehnder AJBA (2013) A global and spatially explicit assessment of climate change impacts on crop production and consumptive water use. PLoS One, vol. 8, no. 2, pp. e57750–e57750

Meehl, GA, TF Stocker, WD Collins, P Friedlingstein, AT Gaye, JM Gregory, A Kitoh, R Knutti, JM Murphy, A Noda, SCB Raper, IG Watterson, AJ Weaver and Z-C Zhao, (2007) Global Climate Projections. In: *Climate Change 2007: The Physical Science Basis. Contribution of Working Group I to the Fourth Assessment Report of the Intergovernmental Panel on Climate Change* [Solomon, S, D Qin, M Manning, Z Chen, M Marquis, KB Averyt, M Tignor and HL Miller (eds.)]. Cambridge University Press, Cambridge, United Kingdom and New York, NY, USA

Mitchell T, Jones P (2005) An improved method of constructing a database of monthly climate observations and associated high-resolution grids. Int J Climatol 25:693–712

Morrissey, M, W Cook and J Greene, (2010) An Improved Method for Estimating the Wind Power Density Distribution Function. *Journal of Atmospheric and Oceanic Technology*, 27(7): 1153–1164

Neitsch S, Arnold J, Kiniry J (2005) Soil and water assessment tool theoretical documentation: version 2005. Model Description. Soil and Water Research Laboratory

Pan, Z, Segal, M, Arritt, R W, and Takle, E S (2004) "On the potential change in solar radiation over the US due to increases of atmospheric greenhouse gases." *Renewable Energy*, 29(11), 1923–1928

Peterson, Erik L, Mortensen, Niels G, Landberg, Lars, Hojstrup, Jorgen, and Frank, Helmut P, (1997) Wind Power Meteorology. Riso National Laboratory, Roskilde, Denmark

Pryor, S C, Schoof, J T & Barthelmie, R J (2006) Winds of change?: Projections of near-surface winds under climate change scenarios. Geophys. Res. Lett. 33

Pryor, S C and R J Barthelmie, (2010) Climate Change Impacts on Wind Energy: A Review. *Renewable and Sustainable Energy Reviews*, 14(1): 430–437

Pryor, S C, R J Barthelmie, and J T Schoof, (2012) Past and future wind climates over the contiguous USA based on the North American Regional Climate Change Assessment Program model suite, J. Geophys. Res., 117, D19119, doi:10.1029/2012JD017449

Rajagopalan, B & Lall, U, (1998) Locally weighted polynomial estimation of spatial precipitation. Journal of Geographic Information and Decision Analysis

Randall, DA, RA Wood, S Bony, R Colman, T Fichefet, J Fyfe, V Kattsov, A Pitman, J Shukla, J Srinivasan, RJ Stouffer, A Sumi and KE Taylor, (2007) Cilmate Models and Their Evaluation. In: Climate Change 2007: The Physical Science Basis. Contribution of Working Group I to the Fourth Assessment Report of the Intergovernmental Panel on Climate Change [Solomon, S, D Qin, M Manning, Z Chen, M Marquis, KB Averyt, M Tignor and HL Miller (eds.)]. Cambridge University Press, Cambridge, United Kingdom and New York, NY, USA

Rao N, Sarma P (1988) A simple dated water-production function for use in irrigated agriculture. Ag Water Manage 13:25-32

Rauthe, M, Hense, A, and Paeth, H (2004) A model intercomparison study of climate change-signals in extratropical circulation. *International Journal of Climatology*, 24(5), 643–662

Reilly, J, S Paltsev, K Strzepek, NE Selin, Y Cai, K-M Nam, E Monier, S Dutkiewicz, J Scott, M Webster and A Sokolov (2012) Valuing Climate Impacts in Integrated Assessment Models: The MIT IGSM. MIT Joint Program Report Series, Report 219

Rienecker, M M, Suarez, M J, Gelaro, R, Todling, R, Bacmeister, J, Liu, E, Bosilovich, M G, Schubert, S D, Takacs, L, Kim, G-K, Bloom, S, Chen, J, Collins, D, Conaty, A, da Silva, A, Gu, W, Joiner, J, Koster, R D, Lucchesi, R, Molod, A, Owens, T, Pawson, S, Pegion, P, Redder, C R, Reichle, R, Robertson, F R, Ruddick, A G, Sienkiewicz, M, and Woollen, J (2011) MERRA: NASA's Modern-Era Retrospective Analysis for Research and Applications. *Journal of Climate*, 24(14), 3624–3648. Sailor, D J, Smith, M & Hart, M, (2008) Climate change implications for wind power resources in the Northwest United States. *Renewable Energy* 33, 2393–2406

Rosenzweig C, Iglesias A (1998) The use of crop models for international climate change impact assessment. In: Tsuji, GY, Hoogenboom, G Thornton, PK (eds) Understanding options for agricultural production. Kluwer Academic Publishers, Dordrecht, The Netherlands, pp: 267-292

Rosnes, Orvika and Vennemo, Haakon (2008) Africa Infrastructure Country Diagnostics (AICD) - Powering Up: Costing Power Infrastructure Investment Needs in Southern and Eastern Africa.

RSA (Republic of South Africa) (2010) *Reducing Greenhouse Gas Emissions: The Carbon Tax Option.* Pretoria, South Africa: National Treasury, Government of the Republic of South Africa

Sailor, D J, Smith, M & Hart, M (2008) Climate change implications for wind power resources in the Northwest United States. Renew Energ 33, 2393–2406

SAPP (Southern Africa Power Pool) (2010) Annual Report 2010. <http://www.sapp.co.zw/docs/R9%20-%20SAPP%20Statistics%20-%202010.pdf>

SAPP (Southern Africa Power Pool) (2011) Annual Report 2011. <http://www.sapp.co.zw/docs/2010%20Annual%20report.pdf>.

SAPP (Southern Africa Power Pool) (2012) Annual Report 2012. <http://www.sapp.co.zw/docs/SAPP%202012%20annual%20report.pdf>

SAPP (Southern Africa Power Pool) (2013) Overview of the SAPP, presentation by Eng. Musara Beta, available on <http://www.usea.org/sites/default/files/event-/SAPP%20Overview.pdf>

Savannah Environmental (2007) Final Scoping Report: Proposed Wind Energy Facility and Associated Infrastructure, Western Cape Province. Report prepared for Eskom Holdings Limited

Schlosser CA, Gao X, Strzepek K, Sokolov A, Forest CE, Awadalla S, Farmer W (2011) Quantifying the Likelihood of Regional Climate Change: A Hybridized Approach. *MIT Joint PRogram on the Science and Policy of Global Change*, <http://globalchange.mit.edu/pubs/abstract.php?publication_id=2212.> (Feb. 1, 2012)

Schwartz, M and D Elliot, (2005) Towards a Wind Energy Climatology at Advanced Turbine Hub-Heights. *Preprint, 15th Conference on Applied Climatology, Savannah, GA, American Meteorological Society*

Seljom, P, Rosenberg, E, Fidje, A, Haugen, J E, Meir, M, Rekstad, J, and Jarlset, T (2011) Modelling the effects of climate change on the energy system—A case study of Norway *Energy Policy*, Elsevier

Sheffield J, Goteti G, Wood EF (2006) Development of a 50-year high-resolution global dataset of meteorological forcings for land surface modeling. J Climate 19:3088–3111

Showers, Kate B (2009) Congo River's Gand Inga Hydroelectric scheme: linking environmental history, policy and impact. Water History, 1:31-58

Sieber J, Purkey D (2007) User Guide for WEAP21. Stockholm Environment Institute

Sokolov AP, Stone PH, Forest CE, Prinn R, Sarofim MC, Webster M, Paltsev S, Schlosser CA, Kicklighter D, Dutkiewicz S, Reilly J, Wang C, Felzer B, Melillo JM, Jacoby HD (2009) Probabilistic forecast for twenty-first-century climate based on uncertainties in emissions (without policy) and climate parameters. J Climate 22:5175–5204

Stull, R B, (1991) *An Introduction to Boundary Layer Meteorology*, volume 13. Kluwer Academic Publishers: Dodrecht, The Netherlands, first edition, 666 p.

Sutcliffe JV, Parks, YP (1987) Hydrological modelling of the Sudd and Jonglei Canal. Hydrolog Sci J 32:143–159

Szewczuk, S, and Prinsloo, E (2010) Wind Atlas for South Africa (WASA). *Quaternary Real and Relevant Conference*, <http://www.sawea.org.za/images/stories/SAWEA%20docs/WASA_SAWEP_2010.pdf> (May. 2, 2012)

Tilmant A, Beevers L, Muyunda B (2010) Restoring a flow regime through the coordinated operation of a multireservoir system: the case of the Zambezi River basin. Water Resources Research 46 W07533

Troen, I, and Petersen, E, (1987) European Wind Atlas. Riso National Laboratory, Roskilde

Tshombe, L M, Ferreira, I W, Uken, E (2007) NEPAD vision and the INGA hydro-electric scheme. Journal of Energy in Southern Africa, Vol 8 No 3 pg 19-25

Tuller, S E and A C Brett, (1984): The Characteristics of Wind Velocity That Favor the Fitting of a Weibull Distribution in Wind Speed Analysis. *Journal of Applied Meteorology*, 23: 124–134

Ucar, A and F Balo (2009): Investigation of Wind Characteristics and Assessment of Wind-Generation Potentiality in Uludag-Bursa, Turkey. *Applied Energy*, 86(3): 333–339

USBR (US Department of the Interior, Bureau of Reclamation) (1993) Drainage manual: a Water Resources Technical Publication. US Department of the Interior, Washington DC

Wahaj R, Maraux F (2007) Actual crop water use in project countries: a synthesis at the regional level. World Bank, Washington DC

WASA (Wind Atlas for South Africa) (2012) < http://www.wasaproject.info> [accessed May 2012]

Webster, M, A P Sokolov, J M Reilly, C E Forest, S Paltsev, C A Schlosser, C Wang, D Kicklighter, M Sarofim, J Melillo, R G Prinn and H D Jacoby (2011): Analysis of climate policy targets under uncertainty. Climatic Change, 112(3-4), 569-583

Wilks DS (1992) Adapting stochastic weather generation algorithms for climate change studies. Climatic Change, vol. 22, no. 1, pp. 67–84

Wilson, Duncan, and Adams, Ivan (2006) Review of Security of Supply in South Africa: A Report to the Department of Public Enterprise.

Winkler (ed) (2007). Long Term Mitigation Scenarios: Technical Report. Prepared by the Energy Research Centre for Department of Environment Affairs and Tourism, Pretoria, October 2007. http://www.erc.uct.ac.za/Research/publications/07-Winkler-LTMS-Technical%20Report.pdf

World Bank (2009) The cost to developing countries of adapting to climate change: new methods and estimates. The Global Report of the Economics of Adaption to Climate Change Study, World Bank, Washington, DC http://siteresources.worldbank.org/EXTCC/Resources/EACC-june2010.pdf

World Bank (2010) The Zambezi River Basin: a multi-sector investment opportunities analysis, Volume 1, Summary Report. World Bank, Washington DC. http://siteresources.worldbank.org/INTAFRICA/Resources/Zambezi_MSIOA_-_Vol_1_-_Summary_Report.pdf

Yates DN, Strzepek KM (1998) Modeling the Nile Basin under climatic change. J Hydrologic Engrg 3:98–108

Zaharim, A, A M Razali, R Z Abidin and K Sopian, (2009) Fitting of Statistical Distributions to Wind Speed Data in Malaysia. *European Journal of Scientific Research*, 26(1): 6–12

Zawilska, E, Brooks, MJ, Meyer, AJ, (2012) A Review of Solar Resource Assessment Initiatives in South Africa: The Case for a National Network. American Solar Energy Society

APPENDIX A

COMPARISON OF MERRA GRIDDED DATA TO WASA STATION DATA

Here, the MERRA data are compared to recently taken wind station data from the ongoing Wind Atlas for South Africa (WASA) project. Data from the 10 wind masts are freely available from the WASA website (WASA 2012). These stations have wind speed data at a 10-minute aggregation usually starting in the middle of 2010 to the present. Since 2011 was the only consecutive full year of data available at the time this paper was written, this year is used to compare to the MERRA data. Also, the WASA data was aggregated to an hourly time-step to match the MERRA data.

There are many fundamental differences between station data recorded at a point and gridded data aggregated over a large region. First, wind masts are generally installed near where wind farms are likely to be built. This means that they are in areas of high wind potential and usually placed away from obstructions that might interfere with the anemometer. Therefore, we expect that the wind station data will represent one of the highest wind potential points in the MERRA grid. Keep in mind that the MERRA data represent an area roughly greater than 3,600 km^2. Also note that the MERRA data represents wind speeds from 1979 to 2009, while the WASA data represents 2011. Figure 45 shows the mean as a bar superimposed by box and whisker plots of both the WASA station data and the MERRA data at the grid where the station resides for the 8 stations with a full 2011 record.

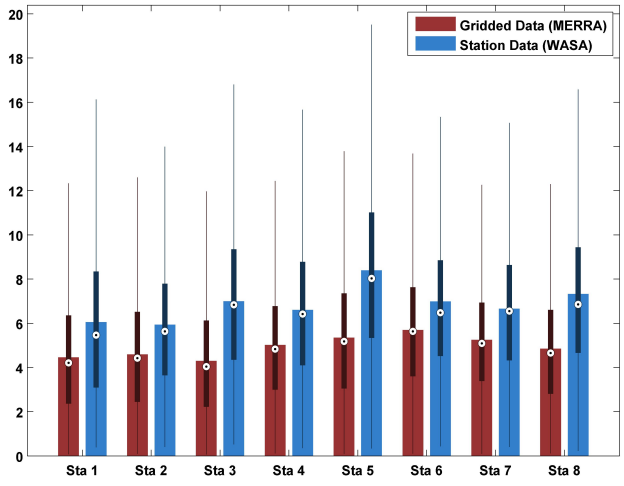

Figure 45: Mean, shown as bar plots, and distributions, shown as box and whisker plots, for WASA (blue) and MERRA (red) for 8 stations

As expected, the station data are always higher than the gridded data. The station data means are about 2 m/s higher, and the 75th percentile is about 3 m/s higher. Since the station data only represent 1 year and the MERRA data represent 31 years, we wanted to compare these using the same length of record. As an example, Figure 47 shows the 31 years, 1979-2009, from the gridded data compared to the station data from 2011 for the first station, labeled "Sta 1." This figure clearly shows that the station data are characteristically different for station 1. In fact, the station data appear to have a considerably larger central tendency and variance for all stations. Another interesting characteristic is that the station data tend to be more skewed towards lower values than the gridded data. The skewness for each station is shown in Figure 46. Except for two stations, which are close, the skewness in the station data is considerably higher than the gridded data.

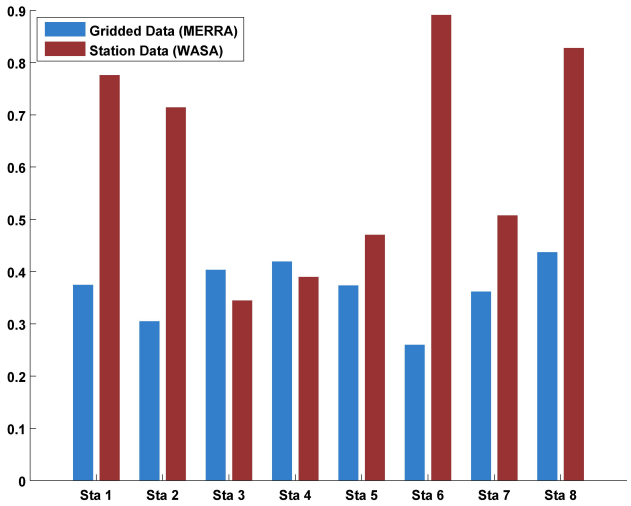

Figure 46: Skewness of MERRA (blue) compared to WASA (red) for 8 stations

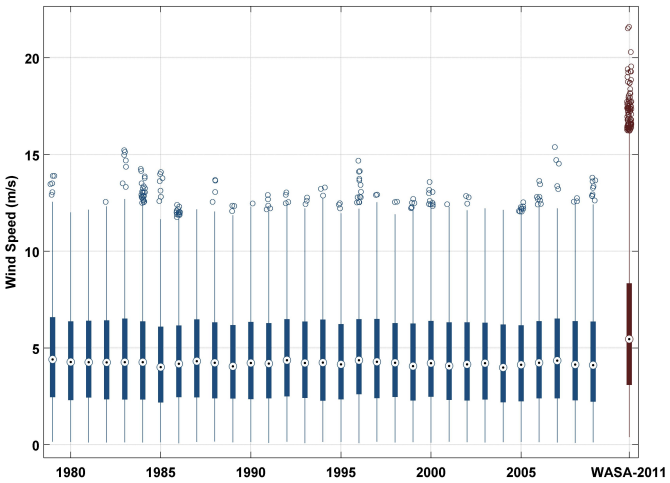

Figure 47: Box and whisker plots of wind speed distributions for the 31 years of MERRA (blue) and WASA for 2011 (brown)

Another important characteristic of wind for the national power grid is the distribution of wind over various time scales. Figure 48 shows the distribution of wind speed over the year for station 1, as an example. For this figure, the 10th, 50th (median), and 90th percentiles were calculated from the 31 years of the MERRA data, and then smoothed using a 24-hour moving average in order to remove the daily cycle. In this case, the 10th percentile represents the lowest daily mean in a 10-year period, and the 90th percentile, the highest in a 10-year period. Again we see that the station data is typically much higher than the gridded data, but in this figure, the difference in the variance is more apparent. We also found that the seasonal cycle (i.e. higher in DJF and lower in JJA for station 1) is fairly close between the two datasets.

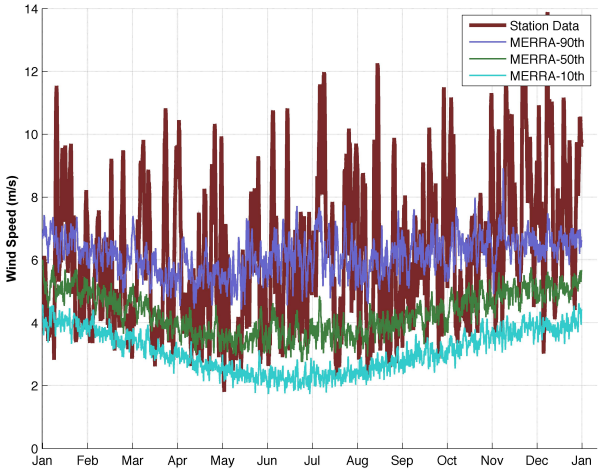

Figure 48: Seasonal cycle of wind speed for the station (WASA) in brown and MERRA in blue, green, and cyan for station 1

The distribution of wind speed over the daily time-scale is also important for national energy planning. Figure 49 shows the daily distribution using box and whisker plots for each

hour for station 1 as an example. Using these plots, we were able to conclude that the two datasets show a similar daily distribution for all stations.

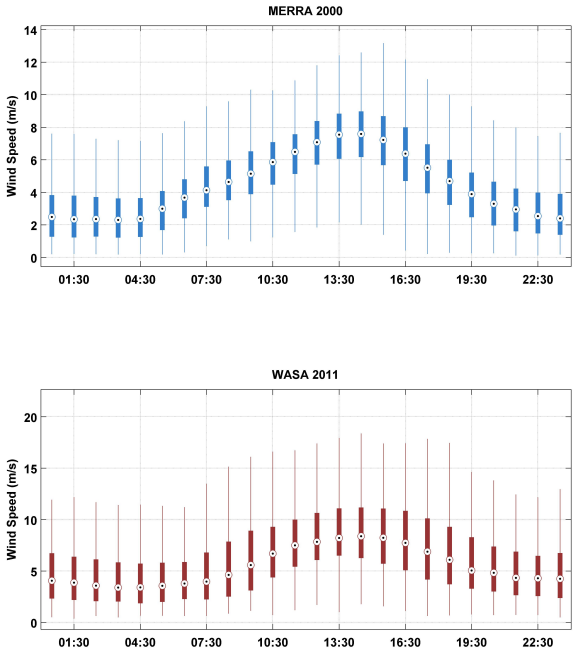

Figure 49: Diurnal Cycle of wind speed for MERRA (top) and WASA for station 1

This exercise illustrates some of the fundamental differences between gridded and station data in South Africa. First, the station data have a considerably higher central tendency than the gridded data. With the gridded data representing an aggregate of possible wind farm cites, some cites could have higher and lower wind resource potential. Second, the station data have a much higher variance than the gridded data (this is especially apparent in Figure 48). And third, the station data are more skewed toward lower values than the gridded data. Local wind is subject to small-scale turbulence and terrain inhomogeneities that can cause large changes in the spectra.

Some of these characteristics are dampened or removed in the grid aggregation. These findings are important to consider when estimating wind resource potential using gridded data.